MUNGASAJI MAHARAJ MAHAVIDYALAYA, DARWHA

3.3.2.1. Number of research papers in the Journals notified on UGC website during the last five years

Year	2020-21
Number	09

	Title of paper	Name of the author/s	Department of the teacher	Name of journal	Year of publication	ISSN number
1	Kaluza – Klein Cosmological Model for Barotropic Fluid Distribution with Varying (t) in Creation Field theory of Gravitation (11)	Dr. Vilas B Raut	Mathmatics	Indo Asian Philosopher	Oct 20-March 2021	2348-5825 Impact Factor 6.1
2	Johannes Kelper : An Astronomer who changed vision of the Universe (47)	Dr. Vilas B Raut	Mathmatics	Interlink research Analysis	Jan-Jun 2021	0976 – 0377 Impact Factor 6.2
3	Cyclo-condensation of substituted thiosemicarbazides: synthesis of 2,5-disubstituted 1,2,4-triazolidin- 3-thione	Dr. N. A. Rashidi	Chemistry	International Journal of Current Advanced Research (Vol 9, Issue 08(A), pp 22890-22893,)	August 2020	2319-6475, Impact factor 6.614

4	Titled Universe with big rip singularity inLyra Geometry	Dr.Y.S.Solanke	Mathematics	Modern Physics letter A Scopus Indexed	June 2020	0217-7323 Print 1793-6632 Web Impact Factor 2.066
5	Anisotropic Plane Symmetric Model with Massless Scalar field	Dr.Y.S.Solanke	Mathematics	Indian Journal of Physics Scopus Indexed	July 2020	0973-1458 Print 0974-9845 web Impact Factor 1.407
6	Accelerating Dark Energy Universe with LRS Bianchi type-I Space- Time.	Dr.Y.S.Solanke	Mathmatics	International Journal of Geometric Methods in Modern Physics (World Scientific). Scopus Indexed	2021	Online 1793-6977 Impact Factor 1.28
7	Comparison of free length thermodynamically and acoustically of alpha Alumina (Alpha-Al2O3) nano suspension in Ethanol base fluid.	Dr.P.D.Bageshwar	Physics	International Journal of Scientific Research in Science and Technology	Jan-Feb 2021	Online ISSN: 2395-602X ISSN:-2395-6011- UGC Approved. Vol.8, Issue1
8	Effect of COVID-19 on Indian Economy	Dr. K. V. Dhawle	Commerce	Galaxy Link	May 2021	2319-8508 I.F. 6.7
9	Place of Agriculture in National Economy	Dr. K. V. Dhawle	Commerce	ROYAL	June 2021	2278-8158 I.F. 5.7
	Total 09					

IMPACT FACTOR 6.10
ISSN 2348-5825
Indo Asian Philosopher (IAP)
Issue : XVI, Vol. V
Oct. 2020 To Mar. 2021
www.irasg.com

Research Paper 3 Mathematics

N Kaluza-Klein Cosmological Model for Barotropic Fluid Distribution with Varying Ë(t) in Creation Field theory of Gravitation

V. B. Raut
Dept. of Mathematics,
MungsajiMaharajMahavidyalaya,
Darwha, Dist. Yavatmal

ABSTRACT

We have studiedthe Hoyle-NarlikarC-field cosmology for Kaluza-Klein space-times with varying cosmological constant $\Lambda(t)$, when the universe is filled with barotropic fluid distribution. To get deterministic solution, we assumed that $\Lambda = \frac{1}{a^2}$ as considered by as in Chen & Wu (Phys. Rev. D, 41:695, 1990), where a is a scale factor. The various special cases of the model (30) viz. Dust filled universe $(p=0)$, Stiff fluid universe $(\rho = p)$ and Radiation dominated era $(\rho = 3p)$ are also discussed. The physical aspects for these models are also studied.

Keywords : *C*-Field cosmology, Barotropic fluid, Varying cosmological constant $\Lambda(t)$.

Introduction :

The model of the universe used for the investigations dealing with physical process called as a big-bang model. The big-bang model has various problems To overcome the problems in the big-bang model, alternative theories were proposed from time to time. The most popular theory was put forward by Bondi&Gold [1] called steady state theory.The theory fails for not giving any physical justification for continuous creation of matter and the principle of conservation of matter was iolated in this formalism. To overcome this difficulty, Hoyle &Narlikar [2] adopt a field theoretical approach by introducing a massless and chargeless scalar-field C in the Einstein-Hilbert action to account for matter creation. The theory proposed by Hoyle and Narlikar called as*C*-field theory which has no big-bang type singularity as in

Bondi& Gold steady state theory. It is pointed out by Narlikar [3] that matter creation is accomplished at the expense of negative energy *C*-field. Narlikar&Padmanabhan [4] have obtained solution of Einstein field equations admitting radiation with negative energy massless scalar field *C*. Chatterjee& Banerjee [5] have extended the study of Hoyle-Narlikar theory [6, 7, 8] in higher dimensional space times. Like this many other researches Singh &Chaubey [9], Adhav*et al*.[10] , Bali &Kumawat [11],Katore [12], Tyagi& Parikh [13], Malekolkalami [14] have investigated*C*-field cosmological model .

Recently, large numbers of cosmological models have been studied by the inclusion of cosmological constant Λ and studied the role of Λ at very early and later stages of the evolution of the universe. Bergmann [15] has interpreted the cosmological constant Λ in terms of Higgs scalar field. In quantum field theory, the cosmological constant is considered as the vacuum energy density. Dolgov [16, 17] shows that cosmological constant remains constant in the absence of any interaction with matter and radiation.Bertolami [18] considered cosmological models with a variable cosmological constant of the form $\Lambda \sim t^{-2}$. Chen &Wu [19] have also solved the problem by considering $\Lambda \sim R^{-2}$, where R is the scale factor in the Robertson-Walker space time. Krause &Turner [20] have suggested that universe possess a non-zero cosmological constant. Recently, the value of cosmological constant $\Lambda = 1.934 \times 10^{-35} s^{-2}$ was predicted by the cosmological relativistic theory of Carmeli&Kuzmenko [21]. This value of cosmological constant matches with measurements obtained by High-Z Supernovae Team and Supernovae Cosmological Project [22-25]. Number of cosmological models in which Λ decays with time have been investigated by number of authors *viz.* Singh & Singh [26], Lui&Wesson [27], Pradhan&Pande [28], Adhav*et al*.[29], Singh & Kumar [30], Ram &Verma [31]. Bali &Saraf [34] have investigated*C*-field cosmological model for Barotropic fluid distribution with varying Λ in FRW space-time.Ghate& Salve [35, 36] have studied some cosmological model with varying $\Lambda(t)$ in creation field theory of gravitation.

In this paper, we have investigated Kaluza-Klein space-times for barotropic fluid distribution with varying cosmological constant $\Lambda(t)$ in the creation field theory of gravitation. The solution of the field equations are obtained by assuming a relation $\Lambda = \frac{1}{a^2}$ (Chen & Wu [19]), where a is a scale factor. This work is organized as follows. In Section 2, the model and field equations have been presented. The solution of field equations has been discussed in Section 3. Then in Section 4, the physical aspects of the model have been discussed. In the last Section 5 concluding remarks have been expressed.

Metric and Field Equations:

We consider the Kaluza-Klein metric in the form

$$ds^2 = dt^2 - A^2\left(dx^2 + dy^2 + dz^2\right) - B^2 d\psi^2, \quad (1)$$

where A, B are scale factors which are functions of time t only and $\sqrt{-g} = A^3 B$.

The Einstein's field equations by introduction of *C*-field is modified by Hoyle and Narlikar[6, 7, 8] with varying Λ is given by

$$R_i^j - \frac{1}{2} R g_i^j = -8\pi G\left[\underset{(m)}{T_i^j} + \underset{(c)}{T_i^j}\right] - \Lambda(t) g_i^j. \quad (2)$$

The energy momentum tensor $\underset{(m)}{T_i^j}$ for perfect fluid and creation field $\underset{(c)}{T_i^j}$ are given by

$$\underset{(m)}{T_i^j} = (\rho + p) v_i v^j - p g_i^j \quad (3)$$

and

$$\underset{(c)}{T_i^j} = -f\left(C_i C^j - \frac{1}{2} g_i^j C^\alpha C_\alpha\right), \quad (4)$$

Here ρ is the energy density of massive particles and p is the pressure. v_i are co-moving four velocities which obeys the relation $v_i v^j = 1, v_\alpha = 0, \alpha = 1, 2, 3$. The coupling constant between matter and creation field is greater than zero. It is assumed that creation field C is a function of time only i.e. $C(x,t) = C(t)$.

The Hoyle-Narlikar field equations (2) for the metric (1) with the help of equations (3) and (4) given by

$$3\frac{\dot{a}^2}{a^2} + 3\frac{\dot{a}\dot{b}}{ab} = 8\pi G\left(\rho - \tfrac{1}{2} f\dot{C}^2\right) + \Lambda \quad (5)$$

$$2\frac{\ddot{a}}{a} + \frac{\ddot{b}}{b} + \frac{\dot{a}^2}{a^2} + 2\frac{\dot{a}\dot{b}}{ab} = 8\pi G\left(-p + \tfrac{1}{2} f\dot{C}^2\right) + \Lambda \quad (6)$$

$$3\frac{\ddot{a}}{a} + 3\frac{\dot{a}^2}{a^2} = 8\pi G\left(-p + \tfrac{1}{2} f\dot{C}^2\right) + \Lambda \quad (7)$$

where overhead dot $(\dot{})$ denotes differentiation with respect to time t.

The conservation equation

$$\left(8\pi G T_i^j + \Lambda g_i^j\right)_{;j} = 0, \quad (8)$$

leads to

$$8\pi\dot{G}\left[\rho - \tfrac{1}{2} f\dot{C}^2\right] + 8\pi G\left[\dot{\rho} - f\dot{C}\ddot{C} + \left(3\frac{\dot{a}}{a} + \frac{\dot{b}}{b}\right)(\rho + p) - \left(3\frac{\dot{a}}{a} + \frac{\dot{b}}{b}\right) f\dot{C}^2\right] + \dot{\Lambda} = 0 \quad (9)$$

using $\dot{G} =$ constant

$$\dot{\rho} + \left(3\frac{\dot{a}}{a} + \frac{\dot{b}}{b}\right)(\rho + p) = f\dot{C}\left(\ddot{C} + \left(3\frac{\dot{a}}{a} + \frac{\dot{b}}{b}\right)\right) f\dot{C}^2\Big] + \dot{\Lambda} = 0 \quad (10)$$

Now using $\dot{C} = 1$ and barotropic equation $p = \gamma\rho$, equation (7) reduce to

$$-8\pi\gamma\rho = 3\frac{\ddot{a}}{a} + 3\frac{\dot{a}^2}{a^2} - 4\pi G f - \Lambda \quad (11)$$

Equation (5) leads to

$$8\pi G\rho = 3\frac{\dot{a}^2}{a^2} + 3\frac{\dot{a}\dot{b}}{ab} + 4\pi G f - \Lambda \quad (12)$$

Solving equations (11) and (12) gives

$$3\frac{\ddot{a}}{a}+(3+3\gamma)\frac{\dot{a}^2}{a^2}+3\gamma\frac{\dot{a}\dot{b}}{ab}=(1-\gamma)4\pi Gf+(1+\gamma)\Lambda \quad (13)$$

Now to obtained the exact solution one extra condition needed we assume a relation between metric condition given by

$$a=b^n \quad (14)$$

Where *n* is arbitrary constant and a,b are metric potential.Without loss of generality we assume *n=1* with this eq. (13) gives

$$3\frac{\ddot{a}}{a}+(3+3\gamma)\frac{\dot{a}^2}{a^2}+3\gamma\frac{\dot{a}^2}{a^2}=(1-\gamma)4\pi Gf+(1+\gamma)\Lambda \quad (15)$$

To get deterministic solution in terms of cosmic time t, we assume that $\Lambda=\frac{1}{a^2}$, where a is scale factor. {Chen & Wu (*Phys. Rev. D* 41:695,1990)} in equation (15) which leads to

$$2\ddot{a}+(2+4\gamma)\frac{\dot{a}^2}{a}=\frac{2}{3}(1-\gamma)4\pi Gfa+\frac{2}{3a}(1+\gamma) \quad (16)$$

Substitute $\dot{a}=F(a),\ddot{a}=FF'withF'=\frac{dF}{da}$ in equation (16) which gives

$$\frac{dF^2}{da}+\frac{(2+4\gamma)}{a}F^2=\frac{2}{3}(1-\gamma)4\pi Gfa+\frac{2}{3a}(\gamma+1) \quad (17)$$

on solving equation (16) reduces to

$$\frac{da}{\sqrt{\alpha a^2+\beta}}=dt \quad (18)$$

which on simplification gives

$$a=\sqrt{\frac{\beta}{\alpha}}\sinh\sqrt{\alpha}t \quad (19)$$

$$\Lambda=\frac{1}{a^2}=\frac{\alpha}{\beta}\text{cosech}^2\sqrt{\alpha}t \quad (20)$$

where

$$\alpha=\frac{4\pi Gf(1-\gamma)}{2(1+\gamma)} \quad (21)$$

$$\beta=\frac{1+\gamma}{3(1+2\gamma)} \quad (22)$$

From equation (14), (19), (20) equation (12) gives

$$8\pi G\rho=\text{cosech}^2\sqrt{\alpha}t\left(6\propto-\frac{\alpha}{\beta}\right)+\frac{8\pi Gf}{1+\gamma} \quad (23)$$

3.Solution of the Field Equations:

Merticequation (1) after using Equation (14), (19) becomes

$$ds^2=dt^2-\left(\frac{\alpha}{\beta}\sinh^2\sqrt{\alpha}t\right)[dx^2+dy^2+dz^2+d\varphi^2] \quad (24)$$

Using barotropic condition $p=\gamma\rho$ and equation (14) ,equation (10) leads to

$$2\dot{c}\ddot{c}+8\dot{c}^2\frac{\dot{a}}{a}=\frac{2\dot{\rho}}{f}+\frac{8(1+\gamma)\rho}{f}\frac{\dot{a}}{a}+\frac{2\Lambda}{8\pi Gf}$$

substituting equations (19), (20)and (22) we get

$$\frac{d\dot{C}^2}{dt}+8\sqrt{\alpha}\coth\sqrt{\alpha}t\dot{C}^2=8\sqrt{\alpha}\coth\sqrt{\alpha}t\left(\frac{1+\gamma}{8\pi Gf}\right)\left[\left(6\alpha-\frac{\alpha}{\beta}\right)\left(-2\sqrt{\alpha}\coth\sqrt{\alpha}t\,\text{cosech}^2\sqrt{\alpha}t\right)\right]-\frac{2\alpha\sqrt{\alpha}}{4\pi Gf\beta}\coth\sqrt{\alpha}t\,\text{cosech}^2\sqrt{\alpha}t \quad (25)$$

To get deterministic value of, we assume $\alpha=1$. Equation (25) leads to

$$\frac{d\dot{C}^2}{dt}+(8\coth t)C^2=8\coth t \quad (26)$$

From equation (25), we get

$$\dot{C}^2(sinht)^8 = 8\int coth t(sinht)^8 dt \qquad (27)$$

On simplification equation (27) reduces to

$$\dot{C}^2 = 1, \qquad (28)$$

whichagain leads to

$$C = t\,. \qquad (29)$$

We find $\dot{C} = 1$, which agrees with the value used in source equation. Thus creation field C is proportional to time t and the metric (1) for constraints mentioned above, leads to

$$ds^2 = dt^2 - (\beta sinh^2 t)[dx^2 + dy^2 + dz^2 + d\varphi^2] \qquad (30)$$

I Special Cases:

From equations (21),(22) we have

$$\alpha = \frac{4\pi Gf\ (1-\gamma)}{6(1+\gamma)} \text{ and } \quad \beta = \frac{1+\gamma}{3(1+2\gamma)}$$

Case I: Dust Filled Universe $(\gamma = 0)$: then

$$\alpha = \frac{4\pi Gf}{6} \text{ and } \alpha = \frac{1}{3}$$

Equation (18) leads to

$$\frac{da}{\sqrt{u^2a^2+\frac{1}{3}}} = dt \text{ for } u^2 = \frac{4\pi Gf}{6}$$

whichagain reduces to

$$a = \frac{1}{\sqrt{3}u} sinh[u(t+t_0)] \qquad (31)$$

$$\Lambda = \frac{1}{a^2} = \frac{3u^2}{sinh^2[u(t+t_0)]} \qquad (32)$$

$$q = -\frac{a\ddot{a}}{\dot{a}^2} = -tanh^2[u(t+t_0)] \qquad (33)$$

Case II: Stiff Fluid Universe $(\gamma = 1)$: then

$$\alpha = 0 \text{ and } \beta = \frac{2}{9}$$

Equation (18) leads to

$$da = \frac{\sqrt{2}}{3} dt,$$

whichgives

$$a = \frac{\sqrt{2}}{3}(t + t_0) \quad (34)$$

$$\Lambda = \frac{9}{2((t+t_0))^2} \quad (35)$$

$$q = 0 \quad (36)$$

Case III: Radiation Dominated Universe $\left(\gamma = \frac{1}{3}\right)$: then we get

$$\alpha = \frac{u^2}{2} \text{and} \beta = \frac{4}{15}$$

Equation (18) leads to

$$\frac{da}{\sqrt{a^2 + \frac{8}{15u^2}}} = dt$$

whichon simplification gives

$$a = \frac{2\sqrt{2}}{\sqrt{15}u} sinh\left[\frac{u}{\sqrt{2}}(t + t_0)\right] \quad (37)$$

$$\Lambda = \frac{15u^2}{8\sinh^2\left[\frac{u}{\sqrt{2}}(t+t_0)\right]} \quad (38)$$

$$q = -tanh^2\left[\frac{u}{\sqrt{2}}(t + t_0)\right] \quad (39)$$

4. Physical Aspects of the Model:

The homogeneous mass density (ρ), the cosmological constant (Λ), the scale factor (a) and deceleration parameter (q) for the model (30) given by

$$8\pi G\rho = \left\{6 - \frac{1}{\beta}\right\} cosech^2 t + 4\pi Gf + 6 \quad (40)$$

$$a = \sqrt{\beta} sinht \quad (41)$$

$$\Lambda = \frac{1}{\beta}\text{cosech}^2\, t \quad (42)$$

$$q = -tanh^2\, t \quad (43)$$

The reality condition $\rho > 0$ leads to

$$(6\beta - 1) + \beta(4\pi Gf + 6)sinh^2 t > 0$$

We find $\Lambda \sim \frac{1}{t^2}$, C increases with time, the scale factor (a) increases with time representing inflationary phase. Since $q < 0$, hence the model (30) represents accelerating universe which matches with the result as obtained by Riess*et al.*[23] and Perlmutter*et al.*[25].

Conclusion :

1. For dust universe, the scale factor increases with time representing inflationary universe. The cosmological constant decreases as time increases. The deceleration parameter, which indicates that the universe is accelerating. Hence the model (30) represents accelerating universe which matches with the result as obtained by Riess*et al.* [23] and Perlmutter*et al.*[25].
2. For stiff fluid the scale factor increases with time and decreases as time increases. The deceleration parameter indicating the universe is in uniform motion.
3. For radiation dominated universe the model behaves exactly same as for dust and stiff fluid case. The deceleration parameter which indicates that universe is accelerating. Hence the model (30) represents accelerating universe which matches with the results as obtained by Riess*et al.*[23] and Perlmutter*et al.*[25].

References :-

1) Bondi, H., Gold, T., "The steady state theory of the expanding universe", *Mon. Not. R. Astron. Soc.*, 108, 252,(1948).
2) Hoyle, F., Narlikar, J. V., "A Conformal theory of gravitation", *Proc. Roy. Soc.A, Mathe. Phys. Sci.*, Vol. 294, Issue 1437, pp 138-148 (1966). Doi:10.1098/rspa.1966.0199.
3) Narlikar, J. V., "Singularity and Matter Creation in Cosmological Models", *Nat. Phys. Sci.*, Vol. 242, pp135-136, (1973).
4) Narlikar, J. V., Padmanabhan, T., "Creation-field cosmology: A possible solution to singularity, horizon, and flatness problems", *The Ame. Phys. Soc., Phys. Rev. D*, Vol. 32, pp 1928-1934, (1985).
5) Chatterjee, S., Banerjee, A., "C-field cosmology in higher dimensions", *Gen. Rel. Grav.*, Vol. 36, No. 2, pp 303-313,(2004).
6) Hoyle, F., Narlikar, J. V., "On the avoidance of Singularities in C-field Cosmology", *Proc. Roy. Soc.A, Math. Phys. Sci.*, Vol. 278, Issue 1375, pp 465-478, (1964).
7) Hoyle, F., Narlikar, J. V., "The C- Field as a Direct Particle Field", *Proc. Roy. Soc. of Lon., A, Math. Phys. Sci.*, Vol. 282, Issue 1389, pp 178-183, (1964).
8) Hoyle, F., Narlikar, J. V., "A new theory of gravitation", *Proc. Roy. Soc.A Math. Phys. Sci.*, Vol. 282, Issue 1389, pp 191-207, (1964).
9) Singh, T., Chaubey, R., "Bianchi type I, III, V, VI0 and Kantowski-Sachs universes in creation field cosmology", *Astro. Spa. Sci.*, 321, pp 5-18,(2009).

10) Adhav, K. S., Dawande, M. V., Raut, R. B., Desale, M. S., "LRS Bianchi type-I universe in Creation-field Cosmology", *Bulg. J. Phys*., 37, pp 184-194, (2010).

11) Bali, R., Kumawat, M., "C-field Barotropic Fluid cosmological model with variable G in FRW Space -Time", *Elec. J. Theor. Phys*, Vol. 8, No. 25, pp 311-318,(2011).

12) Katore, S. D., "Plane Symmetric Universe in Creation Field Cosmology", *The Afr. Rev. Phys*., 8:0024. (2013).

13) Tyagi A., Parikh S., "Bianchi Type-VI0 Cosmological Model with Barotropic Perfect Fluid in Creation Field Theory with Time Dependent L", Prespacetime Journal| April 2017 | Volume 8 | Issue 4 | pp. 841-851,(2017).

14) Malekolkalami, B, "LRS Bianchi Type I in C-Field Cosmology with Varying Ë(t)", bjp2018,4,374-384.(2018).

15) Bergman, P. G. "Comments on the scalar-tensor theory", *Int. J. Theo. Phys.*, Vol. 1, No. 1, pp 25-36 (1968). Doi:10.1007/BF00668828.

16) Dolgov, A, D., "In the very early universe", (eds. Gibbons, G. W., Hawking, S. W. and Siklos, S. T. C.), *Cambridge University Press*, Cambridge, (1983).

17) Dolgov, A. D., Sazhin, M. V., Zeldovich, Ya, B., "Basics of modern cosmology", *Editions Frontiers*, (1990).

18) Bertolami, O., "Time dependent cosmological term", *NuovoCimento B*, Series 11, Vol 93, Issue 1, pp 36-42, (1986).

19) Chen, W., Wu, Y. S., "Implications of a cosmological constant varying as *R2*", *Phys. Rev. D*, Vol. 41, pp 695-698,(1990).

20) Krause, L. M., Turner, M. S., "The cosmological constant is back", *Gen. Relat. Grav.*, Vol. 27, Issue 11, pp 1137-1144 (1995). Doi:10.1007/BF02108229.

21) Carmeli, M., Kuzmenko, T., "*Value* of the *Cosmological Constant* in the*Cosmological Relativity Theory*",*Int. J. Theor. Phys.*, 41, 1, pp 131-135,(2002).

22) Garnavich, P. M. *et al.*, "Constraints on cosmological models from Hubble Space Telescope observations of High-Z supernovae", *Astrophys. J.*, Vol. 493, No. 2, pp L53-L57, (1998).

23) Riess, A. G. *et al*., "Observational Evidence from Supernovae for an Accelerating Universe and a Cosmological Constant", *Astronomy. J.*, Vol. 116, Issue 3, pp 1009-1038, (1998).

24) Schmidt *et al.*, "The High-Z Supernova Search: Measuring cosmic Deceleration and Global curvature of the universe using Type Ia Supernovae", *Astophys. J.*, 46,(1998).

25) Perlmutter, S. *et al*., "Measurements of and from 42 high red-shift supernovae", *Astrophys. J*., 517, pp 565-586,(1999).

26) Singh, T., Singh, G. P., "Some cosmological model with constant deceleration parameter", *NuovoCimento B*., Vol. 106, No. 6, pp617-622, (1991).

27) Liu, H., Wesson, P.S., "Universe model with a variable Cosmological Constant and a Big Bounce", *The Astrophysical J.*, 562, pp 1-6, (2001).

28) Pradhan, A., Pandey, P., "Some Bianchi type I viscous fluid cosmological models with a variable cosmological constant", *Astrophys. Spa. Sci*., Vol. 301, No. 1-4, pp 127-134,(2006).

29) Adhav, K. S., Ugale, M. R., Kale, C. B., Bhende, M. P.,"Bianchi Type III Anisotropic Cosmological Models with Varying Ë ", *Bulg. J. Phys*., 34, pp 260-272, (2007).

30) Singh, C. P., Suresh Kumar, "Bianchi type-I space time with variable cosmological constant", *Int. J. Theor. Phys*., 47, pp 3171-3179,(2008).

31) Ram, S., Verma M. K., "Bulk viscous fluid hypersurface-homogenuous cosmological models with time varying G and Ë", *Astrophys. Spa.Sci*., Vol. 330, Issue 1, pp.151-156,(2010).

32) Bali, R., Saraf, S., "C Field Cosmological model for barotropic fluid distribution with varying Ë in FRW space time", Int. J. Theor. Phys. 52: pp 1645-1653, (2013). DOI 10.1007/s10773-013-1486-6.

33) Ghate, H. R., Salve, S. A., "Kaluza–Klein dust filled universe with time dependent in creation field cosmology", *Res. J. of Rec. Sci.*, Vol. 3, (ISC-2013), pp 53-57, (2014).

34) Ghate, H. R., Salve, S. A., "LRS Bianchi Type-V Cosmological Model for Barotropic Fluid Distribution with Bulk Viscosity & Decaying Vacuum Energy Ë (t) in Creation Field Theory of Gravitation", *PrespacetimeJ.*, Vol.7, Issue 8, (2016).

RNI. MAHMUL02805/2010/33461

IMPACT FACTOR 6.20

ISSN 0976-0377

International Registered & Recognized
Research Journal Related to Higher Education for all Subjects

INTERLINK RESEARCH ANALYSIS

UGC APPROVED, REFEREED & PEER REVIEWED RESEARCH JOURNAL

Issue : XXIII, Vol. VI
Year - 12 (Half Yearly)
(Jan. 2021 To June 2021)

Editorial Office :
'Gyandeep',
R-9/139/6-A-1,
Near Vishal School,
LIC Colony,
Pragati Nagar, Latur
Dist. Latur - 413531.
(Maharashtra), India.

Contact : 02382 - 241913
09423346913,09637935252,
09503814000,07276301000

Website
www.irasg.com

E-mail :
interlinkresearch@rediffmail.com
visiongroup1994@gmail.com
mbkamble2010@gmail.com
drkamblebg@rediffmail.com

Publisher :
Jyotichandra Publication,
Latur, Dist. Latur.-415331
(M.S.) India

Price: ₹ 200/-

RNI. MAHMUL02805/2010/33461
Interlink Research Analysis
IMPACT FACTOR 6.20
ISSN 0976-0377
Issue:XXIII,Vol.VI, Jan.2021 To June 2021

I N D E X

RNI. MAHMUL02805/2010/33461
Interlink Research Analysis
IMPACT FACTOR 6.20
ISSN 0976-0377
Issue : XXIII, Vol. VI, Jan. 2021 To June 2021

Johannes Kepler : An Astronomer Who Changed Vision of the Universe

V. B. Raut
Dept. of Mathematics,
Mungsaji Maharaj Mahavidyalaya,
Darwha, Dist. Yavatmal

6 **Research Paper - Mathematics**

ABSTRACT

This article is devoted to the life and works of Johannes Kepler (1571-1630) a German Astronomer, Mathematician and Philosopher. He is considered as founder of physical astronomy. He is famous for the three Laws of planetary motion. The first law is that the planets move in ellipses with the Sun in one focus. Before this law it was assumed the planets move in circles. Despite his physical weakness, harassment of not getting arrears of salary, living in poverty and other domestic troubles, this genius astronomer worked hard and discovered great astronomical facts.

Key words: Johannes Kepler ,Tycho Brahe, Laws of planetary motion.

Johannes Kepler (1571-1630)

Childhood and Education:

Johannes Kepler was born on 27th December 1571 in longitude 290 7' , latitude 480 54' in the city of Weil der Stet , Württemberg , Holy Roman Empire , Germany. His parents were in good condition but by some reason, the father lost all his slender income. His father left home when Johannes was five years old and never returned. His mother was the daughter of an innkeeper. Johannes was employed in inn as a pot-boy between the ages of nine and twelve. He was sickly lad and suffered violent illness which affected his life .Childhood small-pox made his vision weak.

At his childhood he developed love for astronomy. At the age of six he observed the Great Comet of 1577. At the age of nine he observed Lunar Eclipse in 1580. After completing school education he went to the University of Tubingen, where he graduated second on the list.

His connection with astronomy was through Copernican theory heard in University lectures. Johannes had been offered an astronomical lectureship at Graz. Astronomy in those days was supposed to be a minor science and had little of the special dignity.

Early Work:

Kepler struggled hard in different ways to find law governing orbits of planets and their distances from the sun. One of his ideas was based on inscribing a large number of equilateral triangles in a circle. They envelop another circle bearing a definite ratio to the first. This does for the orbit of two planets (see figure:1). Then he tried inscribing and circumscribing squares, hexagons and examined if the circles thus defined would correspond to the several planetary orbits. But they would not give any satisfactory result.

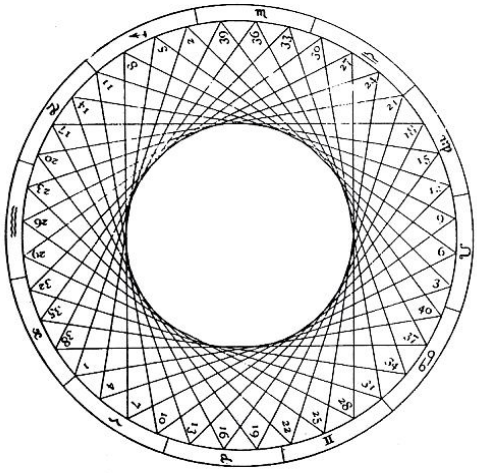

Figure 1 : Number of equilateral triangles inscribed in a circle

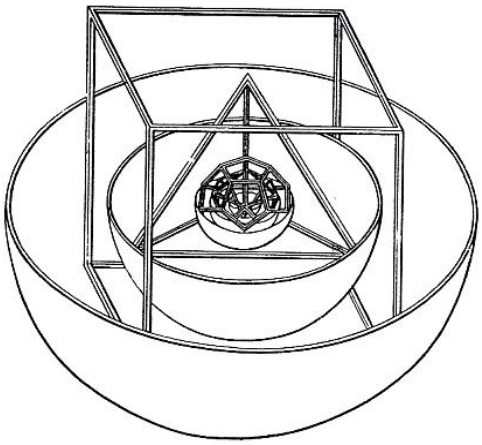

Figure 2: Framework with inscribed and circumscribed spheres and other regular solids

Kepler thought plane figures will not do with the celestial orbits. He suddenly got a brilliant idea of inscribing the regular solids (see figure: 2). He represented the earth's orbit by a sphere as the norm and measured of all six planets known at that time. Around earth he circumscribed a dodecahedron and puts another sphere round that which is approximately the orbit of Mars, round that a tetrahedron which marked the sphere of the orbit of Jupiter, round that sphere he placed a cube which roughly gives the orbit of Saturn. On the other hand he inscribed in the sphere of the earth's orbit an icosahedrons and inside the sphere determined by that an octahedron which figures he takes to enclose the sphere of Venus and Mercury respectively.

This discovery was purely fictitious and accidental. First of all, eight planets are known and secondly their real distances agree only very approximately with hypothesis. But this idea gave him great delight.

Kepler then worked on to predict the cause of the planet's motion. He thought of some propelling force originated from the Sun, like the spokes of a windmill.

Work with Tycho Brah:

When Kepler's first book was published he get introduced Tycho and Galileo. Tycho Bray (1546 – 1601) was well-known Danish astronomer. He was at Prague and he had best planetary observations at that time.

Tycho Brahe (1546 – 1601:

Tycho invited Kepler and offered him the post of mathematical assistant.Kepler accepted it. Kepler says "for observations his sight was dull , for mechanical operations his hand was weak". But in mathematical skills he was superior to Tycho. Because of physical and financial weaknesses, Kepler sought help from Tycho and Tycho helped him with kindness.

The Emperor Rudolph did a good work in maintaining these two eminent astronomers Tycho Brahe and Kepler.

Tycho Brahe (1546 - 1601)

Tycho prepared tables of passages of planets know as Rudolphine tables. It was main work of his life but he died in 1601 before completing them. On his death-bed he intrusted the completion of them to Kepler, who undertook their charge. But the Imperial funds stopped by wars and other difficulties. Kepler could get even his own salary. The work slowed too much.

Kepler then proceeded to study optics. He gave a Very accurate explanation of working of human eye. He made many hypothesis, some of them are close to the law of refraction of light in dense media.

Main Work of Kepler's Life:

All the time in his stay at Prague (1600 – 16120) Kepler made a severe study of

the motion of the planet Mars. In order to find true theory of motion of Mars, he carefully analysed Tycho's books of observations. At that time Aristotle had taught that circular motion was the only perfect and natural motion for heavenly bodies. Afterwords Hipparchus and others found that planets did not revolve in simple circle but in combinations of circles. The small circle carried by a bigger one was called an Epicycle. But this failed to represent speeds of the planets.

Kepler had the accurate planetary observations of Tycho for reference but he found immense difficulty in obtaining the true position of the planets for long together on any such theory considered above. He specially studied motion of the planet Mars because that was sufficiently rapid in its changes for a considerable collection of data. He tried all manner of circular orbits for the Earth and for the Mars, placing them in all sort of aspects with respect to the Sun. The aim was to find such an orbitand such a law of speed, for both the Mars and Earth that a line joining them produced out to the Sun should always mark correctly the apparent position of Mars as seen from the Earth.

Kepler introduced the idea of an Equant i.e. an arbitrary point about which the speed might be uniform. Kepler tried all sorts of combinations, the relative position of the earth and Mars were worked out. He compared it with Tycho's recorded observations. But this agreed for a short time and lateron a discrepancy showed itself.

Kepler did this enormous labour and attempts groping in the dark. At length he got a point that seemed nearly right . But before long the posiyion of the planet as calculated and recorded by Tycho, differed by eight minutes of arc, or one-eight of a degree. There was a possible way of thinking that Tycho's observations might be wrong by this small amount. But Kepler had known Tycho and he thought Tycho was never wrong eight minutes in an observation.

Kepler set out the whole way again and said that with those eight minutes he would yet find out the law of the universe. He gave up the idea of uniform motion and tried varying circular motion, inversely as its distance from the Sun. To simplify calculation, he divided the orbit the orbit into triangles and tried if making the triangles equal would do (see Figure:3).

Surprisingly this worked beautifully! The rate of description of areas is uniform.

Kepler greatly rejoices. He thought he won the war. But long fresh little errors appeared and grew in importance. Still a part of truth had been gained.

He fixed the law of speed, which is now known as Kepler's **second law of planetary motion**: ***'the radius vector describes equal areas in equal times'.***

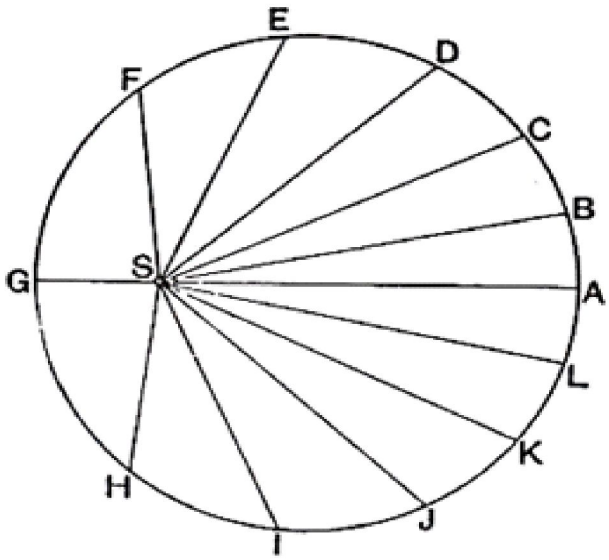

Figure 3 : Eccentric circle divided into equal areas. Around the sun S a planet moves from A to B, From B to C , and so on in equal times.

But what about the shape of the orbits? Now he tried an oval. He tried several varieties of ovals. They were better than a circle but still were not right. The geometrical and mathematical difficulties of calculations were becoming tedious, overwhelming. Kepler's six years continuous labour were leading deeper and deeper into complications.

An accidental ray of light broke upon him in a way. Half the extreme breadth intercepted between yhe circle and oval broke upon him in a way. Half the extreme breadth intercepted between the circle and the oval was 429/100000 of the radius, and he remembered that the "optical inequality" of Mars was also about 429/100000. This coincidence in his own words, woke him out of sleep and impelled him instantly to try making the planet 'oscillate in the diameter of its epicycle instead of revolve around it '. A long course of day and night of calculations arrived him to hit the motion . Finally he obtained the curve described by the planet. It is a special kind oval-the ***ellipse.***

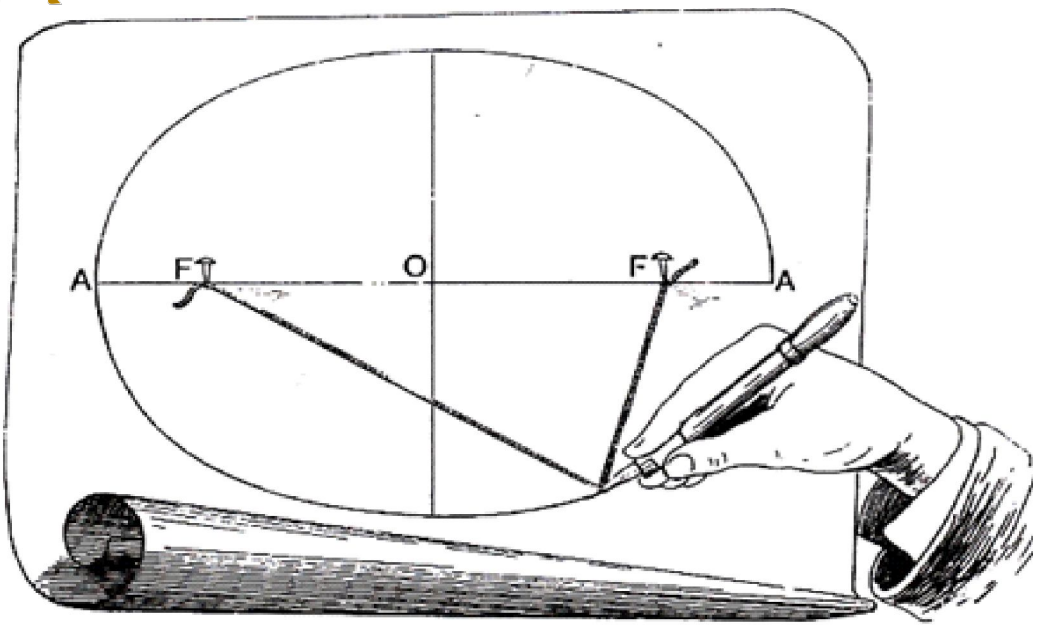

Figure 4 : – Mode of drawing an ellipse. The two pins F are fixed and are the foci.

This gave birth of his **first law of planetary motion:**

"Planets move in ellipses with the Sun at one focus"

Kepler's both the laws agreed with Tycho's planetary observations.

Financial and Domestic Troubles:

After conquering Mars Kepler wanted to study Jupiter, Mercury and rest of the planets. But the death of the patron Emperor in 1612 put an end to all these schemes. At Prague his salary was not regularly paid and remained always in arrears. He lived in poverty and his family suffered a lot. One of his sons died of small-pox, and he lost his wife after eleven days. He could not get any money at Prague. He decided to leave Prague and move to Linz. He accepted a professorship at Linz. Meanwhile his old mother was charged with witchcraft. She was sent to prison. Kepler had to hurry from Linz to interpose. He succeeded in saving her from the torture but she remained in prison for a year.

Third Law:

In spite of domestic troubles, harassing and unsuccessful attempts to get his rights,

he still studied his old problem of finding some possible connection between the distances of the planets from the Sun and their times of revolution i.e. the length of their years.

He found that the cube of the distances of a planet from the Sun is proportional to the square of the time taken by the planet to revolve round the Sun.

Kepler stated his third law as :

"***the ratio of r3 to T2 for every planet is the same".*** His rapture on detecting the law was unbounded and he breaks out : *" The die is cast, the book is written, to be read either now or by posterity, I care not which; it may well wait a century for a reader , as God has waited six thousand years for an observer "*.

Kepler's Books

1. *Astronomia Nova* : He published it in 1609. His first two laws appeared in this book.
2. *Hormonics Mundi* : He published it in 1619.He described his 'third law ' in this book.
3. *Epitome Astronomiae :* Published in 1621. It was a summary of Copernican theory, a clear and popular exposition of it . But it was banned by the Church and it gave Kepler no satisfaction.
4. *Astronomia Pars Optica :* His optical studies appeared in this book. He was founder of modern optics.He explained the process of vision by refraction within the eye.
5. *Dioptrice :* In this book he described real , virtual, upright and inverted images and magnification. He explained the working of a telescope .
6. *Stereometrica Doliorum :* This book formed the basis of Integral Calculus.

Last Years:

In his last years kepler still worked on Rudolphine tables of Tycho and with small help from Vienna, completed them. But he could not get financial support to print them. He applied to the Court though he was sick for applying. They delayed four years with no relief. Finally any how with a great trouble he had to pay himself for printing it. The book contains first really accurate tables which navigators ever possessed. This great publication marks an era in Astronomy.

Almost all time in his life Kepler and his family had to live in bitter poverty. Once more he made determined attempt to get his arrears of salary paid to rescue himself from poverty. For this purpose he travelled to Prague . He pleaded his own case in the imperial meeting. But it was all fruitless.

Exhausted by the journey, weakened by over-study, and disheartened by the failure to get arrears of salary, he caught a fever. He died on 15th November, 1630 at the age of 59, at Regensburg and was buried there. His burial site was lost after the Swedish army destroyed the Churchyard and not even a single stone aroused of his memory.

Brewster says of him :- "Ardent, restless, burning to distinguish himself by discovery, he attempted everything ; and once having obtained a glimpse of a clue , no labour was too hard in following or verifying it. A few of his attempts succeeded - a multitude failed. Those which failed seem to us now fanciful, those which succeeded appear to us sublime. But his methods were the same".

A life of such a labour, crowned by three brilliant discoveries, the world owes to the harshly treated German genius , Johannes Kepler.

References :-

1) James R. Newman : The World of Mathematics , Volume-1 .Simon and Schuster, New York .
2) Max Casper : Kepler, Doer Publications.
3) Robert S. Westman : Johannes Kepler : Short Biography, Encyclopedia Britannica.
4) http://en.wikipedia.org/wiki/Johannes_Kepler.
5) http://www-history.mcs.st-and.ac.uk/Printonly/Kepler.html.

IJCAR

CURRENT ADVANCED RESEARCH

crossref

International Journal of Current Advanced Research

INDEX COPERNICUS IC VALUE: ICV-2016: 83.75 NEW

MEDICAL COUNCIL OF INDIA (MCI) VALID PUBLICATION NEW

'Thomson Reuters' Researcher ID:V-3274-2017 NEW

SJIF Scientific Journal Impact Factor 2017: 6.614 NEW

Journal DOI: 10.24327/IJCAR NEW

RESEARCHERID THOMSON REUTERS | NCBI PubMed | THOMSON REUTERS ENDNOTE | ICMJE INTERNATIONAL COMMITTEE of MEDICAL JOURNAL EDITORS

The International Journal of Current Advanced Research (IJCAR) (SJIF Impact Factor 2017: 6.614) is one of the leading open access publisher, with hundreds of papers published each year related to different areas ranging from **Life Sciences, Physical Sciences and Engineering, Social Science and Humanities and Health Science.** The core vision of IJCAR is to promote knowledge and technology advancement for the benefit of academia, professional research communities and industry practitioners. The aim is to support you to achieve success in your research and scholarly experience.

Researchers, PhD scholars and professionals from academia and industry are solicited to submit completed research and developments in the listed areas below. With a large research community of authors, readers, editors and reviewers bounded together by their talent and integrity, IJCAR publications are available online freely for everyone worldwide. All published papers undergo high-quality peer review and rigorous editorial processes.

The International Journal of Current Advanced Research is an Open Access journal since 2012 with high citations in Google Scholar. This journal is indexed in ESCI - IP & Science - Thomson Reuters - Web of Science.

Multidisciplinary Journal covers all Subjects:

Life sciences : Agricultural, Biological Sciences, Biotechnology, Biochemistry, Genetics, Molecular Biology, Environmental Science, Ecology, Arachnology, Biodiversity and Conservation, Entomology, Limnology, Ichthyology, Malacology, Immunology and Microbiology, Neuroscience, Marine Biology.

Health Sciences: Medicine and Dentistry, Nursing and Health Professions, Pharmacology and Toxicology, Pharmaceutical Science, Veterinary Science, Veterinary Medicine, the Journal invites original papers, review

International Journal of Current Advanced Research
ISSN: O: 2319-6475, ISSN: P: 2319-6505, Impact Factor: 6.614
Available Online at www.journalijcar.org
Volume 9; Issue 08(A); August 2020; Page No.22890-22893
DOI: http://dx.doi.org/10.24327/ijcar.2020.22893.4526

Research Article

CYCLO-CONDENSATION OF SUBSTITUTED THIOSEMICARBAZIDES: SYNTHESIS OF 2,5- DISUBSTITUTED 1,2,4-TRIAZOLIDIN- 3-THIONE

Nazia .A. Rashidi

Department of Chemistry, Mungasaji Maharaj College, Darwha, Dist:Yavatmal, MS, India

ARTICLE INFO

Article History:
Received 6th May, 2020
Received in revised form 15th June, 2020
Accepted 12th July, 2020
Published online 28th August, 2020

Key words:
thiosemicarbazides, cyclo-condesation reaction, 1,3,4-thiadiazolidine, de-tert-butylation.

ABSTRACT

2-N-t-butylimino-3-γ-picolinoyl-5-arylimino-1,3,4-thiadiazoles (IVa-f) have been synthesized following the interaction of 1-γ-picolinoyl-4-aryl-3-thiosemicarbazides (IIIa-f) and t-butyl imino isocyanodichloride. The former (IIIa-f) in turn have been prepared by the condensation of aryl isothiocyanates (Ia-f) and isoniazide. The intermediate products (IVa-f) have been first isomerized into 2-γ-picolinoyl-4-N-t-butyl-5-arylimino-1,2,4-triazolidine-3-thiones (Va-f). The product (Va-f) have been successfully de-t-butylated into respective 2- γ-picolinoyl-5-arylimino-1,2,4-triazolidine-3-thiones (VIa-f). The structures of these compounds were established on the basis of elemental analysis and IR, PMR, Mass spectral data.

INTRODUCTION

From a last decade a lot of work is going on, on the triazole ring, scientists develop a lot of new compounds related to this moiety and screened them for their different pharmacological activities to get a molecule which have good pharmacological activity and lesser side effect. Synthesis of various substituted 1,3,4-thiadiazole and 1,2,4-triazole are reported in the literature. 1,2,4-Triazoles show various biological activities (Singh R. J. and Singh D. K. 2009; Upmanyu N. 2006) and have been synthesized from different compounds (Bhaskar C.S.2002; Buscemi S.1996; Yoo B. R. 1998). Most of them possess good pharmacological activity. Isoniazide is itself a potent drug; therefore we incorporated some part of it as a substituent in the synthesis of some new derivative of triazole. The current work describes the synthesis of 2-γ-picolinoyl-4-N-t-butyl-5-arylimino-1,2,4-triazolidine-3-thiones (Va-f) and their de-t-butylation into respective 1,2,4-triazolidine-3-thiones (VIa-f).

Experimental

All melting points were measured using electro-thermal apparatus are uncorrected. IR spectra were measured using KBr disc plate technique on a Bruker FT-IR spectrophotometer. ^{1}HNMR spectra (DMSO-d_6 and $CDCl_3$) were carried out on a Bruker Advance 400 MHz spectrometer using TMS as internal reference (chemical shifts in ó, ppm). The reagent required for the synthesis of 1,3,4-thiadiazolidines are Isoniazide, aryl isothiocyanates (Vogel A. I. 1958) and tert-butyl isothiocyanate (Striewsky W. 1960). The tert-butylimino isocyanodichloride was prepared following earlier reported method (Dyson G. M. and Harington. 1940). The 1-γ-picolinoyl-4-aryl-3-thiosemicarbazides (IIa-f) were prepared by the reaction of Isoniazide and aryl isothiocyanate (Ia-f) in chloroform medium as below

Corresponding author:* **Nazia .A. Rashidi
Department of Chemistry, Mungasaji Maharaj College, Darwha, Dist:Yavatmal, MS, India

Preparation of 1-γ-picolinoyl-4-p-tolyl-3-thiosemicarbazides (II)

Isoniazide and p-tolyl isothiocyanate (Ia) was reacted in chloroform medium for 1.5 h. On removal of chloroform by vacuum distillation a colourless solid (IIa) was separated. It was washed with petroleum ether (60-80^0) and crystallized from ethanol, m.p 164^{0}C having molecular formula $C_{14}H_{14}N_4OS$.

(IIIa): IR spectra: (KBr) cm-1: 3271,3232 (N-H), 1668 (C=O), 1310 (C-N), 1254 (C=S); 1H-NMR (DMSOd6) ppm: 2.2 (3H, s, Ar-CH3), 3.66 (1H, s, N-H), 8.6-8.62 (1H,d, NH-NH), 8.65-8.67 (1H,d, NH-NH), 7.04-7.07 (2H, d, Ar-H), 7.2-7.3(2H, d, Ar-H), 7.6-7.7 (2H, d, Pyridyl-H), 7.8-7.81 (2H, d, Pyridyl-H).

On the basis of above chemical properties and IR and NMR spectral data (Singh. T., Bhattacharya A. and Verma V.K. 1992; Dyer J. R.1974; Colthup N. B., Daly L. H. and Wiberly S. E.1964), the compound (IIa) has been assigned the structure, 1-γ-picolinoyl-4-p-Tolyl-3-thiosemicarbazide (IIa). The reaction of isoniazide was capable of extension to different aryl isothiocyanates (Ib-f), and the related products have been isolated in good yield. (Table -1)

Interaction of 1-γ-picolinoyl-4-aryl-3-thiosemicarbazides (II) and N-t-butyl imino isocyanodichloride:

Synthesis of 2-N-t-butylimino-3-γ-picolinoyl-5-arylimino-1,3,4-thiadiazoles (IV):

Experiment No. 1

Preparation of 2-N-t-butylimino-3-γ-picolinoyl-5-p-tolylimino-1,3,4-thiadiazoles (IVa).

1-γ-picolinoyl-4-p-tolyl-3-thiosemicarbazide (IIa) (0.01 mole) was suspended in chloroform (15.0 ml). To this a solution of N-t-butyl imino isocyanodichloride (0.01 mole) in chloroform was added. The reaction mixture was refluxed over water bath for 3.0 hr. The evolution of hydrogen chloride gas was observed. After completion of reaction, the reaction mixture was cooled and chloroform was distilled off, when a sticky mass was obtained. It was repeatedly washed with petroleum ether (60-80°C) followed by addition of ethanol; a solid acidic to litmus was isolated. It was crystallised from ethanol, and identified as monohydrochloride of 2-N-t-butylimino-3-γ-picolinoyl-5-p-tolylimino-1,3,4-thiadiazole (IIIa), yield 85%, m.p. 178°C. On basification with dilute ammonium hydroxide solution afforded a free base (IVa). It was crystallised from ethanol, m.p. 218°C having molecular formula C19H21N5OS. The compound gave positive test for N and S elements and found to be non-desulphurizable when boiled wit alkaline plumbite solution.

(IIIa): IR spectra: (KBr) cm-1: 3313 (N-H), 1618 (C=O), 1573 (C=N), 1298 (C-N), 697 (C=S); **1H-NMR** ($DMSOd^6$) ppm: 1.2 (9H, s, t-Bu-H), 2.2 (3H, s, Ar-CH3), 7.0 (2H, d, Ar-H), 7.5 (2H, d, Ar-H), 7.7 (2H, d, Pyridyl-H), 7.9 (2H, d, Pyridyl-H), 8.7 (1H, s, N-H).

On the basis of above chemical properties and spectral data, the compound (IVa) has been assigned the structure, 2-N-t-butylimino-3-γ-picolinoyl-5-p-tolylimino-1,3,4-thiadiazoles (IVa). The other compounds (IVb-f) were prepared by extending the above reaction to other, 1-γ-picolinoyl-4-aryl-3-thiosemicarbazides (IIb-f) and the related products were isolated in good yield. (Table-2.2)

Preparation of 2-γ-picolinoyl-4-N-t-butyl-5-p-tolyl imino-1,2,4-triazolidin-3-thione (Va) (Isomerization)

The 2-N-t-butylimino-3-γ-picolinoyl-5-p-tolylimino-1,3,4-thiadiazoles (IVa) (0.01 mole) was refluxed with 5% ethanolic NaOH (15 ml) for 1.5 hr. After completion of reaction, the reaction mixture was cooled and poured in ice crushed water. The greenish yellow solid was obtained. It was crystallized from ethanol, yield 83%, m.p 226-228°C having molecular formula $C_{19}H_{21}N_5OS$.

(IIIa): IR spectra: (KBr) cm-1: 3232 (N-H), 1619 (C=O), 1546 (C=N), 1297 (C=S);

1H-NMR ($DMSOd^6$) ppm: 1.2 (9H, s, t-Bu-H), 2.4 (3H, s, Ar-CH3), 7.1-7.3 (4H, m, Ar-H), 7.7-7.8 (4H, m, Pyridyl-H), 8.4 (1H, s, N-H). **MS (m/z)** :[M^+] peak at m/z 367 and 366 [M^+-1], 351, 275, 223 and 106 which confirmed its molecular weight and possible fragmentation.

On the basis of above chemical properties and spectral [illegible] the compound (Va) has been assigned the structure, [illegible] picolinoyl-4-N-t-butyl-5-p-tolyl imino-1,2,4-triazolidin-3-thione (Va). The other compounds (Vb-f) were prepared by extending the above reaction to other, 2-N-t-butylimino-picolinoyl-5-p-tolylimino-1,3,4-thiadiazoles (IVb-f) and related products were isolated in good yield. (Table-2)

De-t-butylation of 2-γ-picolinoyl -4-N-t- butyl-5-imino-1,2,4-triazolidin-3-thiones (V).

Preparation of 2- γ-picolinoyl-5-p-tolylimino-1,2,4-triazolidin-3-thione (VIa).

The 2-γ-picolinoyl-4-N-t-butyl-5-p-tolyl imino-1,2,4-triazolidin-3-thione (Va) (2 gm) was hydrolyzed by boiling with 30% sulphuric acid (10 ml) under reflux for [illegible] underwent de-tert-butylation (Lacey R. N.1960). The [illegible] gradually went into solution and a clear solution was obtained. After completion of reaction, the product (VIa) poured into crushed water. It was crystallized, m.p 142°C [illegible] molecular formula $C_{15}H_{13}N_5OS$.

1H-NMR ($DMSOd^6$) ppm: 2.4 (3H, s, Ar-CH3), 7.1-7.3 (4H, m, Ar-H), 7.7-7.8 (4H, m, Pyridyl-H), 8.4 (1H, s, N-H), 12.4 (1H, s, N-H).

The absence of signal for t-Bu proton in PMR spectra of compound (VIa) proved that compound (Va) has successfully de-tert-butylated. On the basis of above chemical properties and spectral data, the compound (VIa) has been assigned the structure, 2-γ-picolinoyl-5-p-tolyl imino-1,2,4-triazolidine-3-thione (VIa). The other compounds (VIb-f) were prepared by extending the above reaction to other, 1-γ-picolinoyl-4-N-t-butyl-5-aryl imino-1,2,4-triazolidin-3-thiones (Vb-f) and the related products were isolated in good yield. (Table-2).

Table 1 Formation of 1-γ-picolinoyl-4-aryl-3-thiosemicarbazides (II)

Reagents : Isoniazide and Aryl isothiocyanates (I)

Aryl Isothiocyanate (I)	1-γ-picolinoyl-4-Aryl-3-thiosemicarbazides (II)	Yield %	M.P °C	Found (Calculated) % C%	H%	N%
	1-γ-picolinoyl-4-p-tolyl-3-thiosemicarbazide (IIa)					
p-tolyl isothiocyanate (Ia)	1-γ-picolinoyl-4-o-tolyl-3-thiosemicarbazide (IIb)	87	164	58.73 (58.74)	4.62 (4.89)	19.46 (19.57)
o-tolyl isothiocyanate(Ib)	1-γ-picolinoyl-4-m-tolyl-thiosemicarbazide (IIc)	91	170	58.65 (58.74)	4.80 (4.89)	19.40 (19.57)
m-tolyl isothiocyanate(Ic)	1-γ-picolinoyl-4-pheayl-3-thiosemicarbazide (IId)	91	184	58.60 (58.74)	4.82 (4.89)	19.50 (19.57)
phenyl isothiocyanate(Id)	1-γ-picolinoyl-4-p-chlorophenyl-3-thiosemicarbazide (IIe)	85	194	57.15 (57.35)	4.39 (4.41)	20.40 (20.38)
o-chlorophenyl isothiocyanate(Ie)	1-γ-picolinoyl-4-o-chlorophenyl-3-thiosemicarbazide (IIe)	75	162	50.72 (50.90)	3.39 (3.59)	18.00 (18.27)
p-chlorophenyl isothiocyanate(If)	1-γ-picolinoyl-4-p-chlorophenyl-3-thiosemicarbazide (IIf)	83	186	50.70 (50.90)	3.46 (3.59)	18.05 (18.27)

Table 2 Synthesis of 2-N-t-butylimino-3-γ-picolinoyl-5-Arylimino-1,3,4-thiadiazoles (IV):Isomerisation of (IV) & De-tert-bultylation into 2-γ-picolinoyl-5-arylimino-1,2,4-triazolidin-3-thione (VI)

Reagents : 1-γ-picolinoyl-4-Aryl-3-thiosemicarbazides (II) and t-butyl isocyanodichloride

1-γ-picolinoyl-4-aryl-3-thiosemicarbazides (II)	2-N-t-butylimino-3-γ-picolinoyl-5-arylimino-1,3,4-thiadiazoles(IV)	M.P °C	2-γ-picolinoyl-4-N-t-butyl-5-arylimino-1,2,4-triazolidine-3-thione (V)	Yield %	M.P °C	2-γ-picolinoyl-5-arylimino-1,2,4-triazolidine-3-thione (VI)	M.P °C	Mol. formula
(IIa)	(VIa)	218	(Va)		226-228	(VIa)	123	
(IIb)	(VIb)	263	(Vb)	87 91	152-154	(VIb)	106	
(IIc)	(VIc)	251	(Vc)	93	201-203	(VIc)	118	$C_{19}H_{18}N_5OS$ $C_{19}H_{18}N_5OS$ $C_{19}H_{18}N_5OS$
(IIId)	(VId)	224	(Vd)	83 78	210-212	(VId)	124	$C_{19}H_{18}N_5OS$ $C_{19}H_{17}ClN_5OS$ $C_{19}H_{17}ClN_5OS$
(IIIe)	(VIe)	242	(Ve)	81	158-160	(VIe)	178	
(IIIf)	(VIf)	231	(Vf)		262-264	(VIf)	132	

RESULTS AND DISCUSSION

The 1-γ-picolinoyl-4-p-tolyl-3-thiosemicarbazides (IIa) were prepared by the reaction between Isoniazide and different p-tolyl isothiocyanate (Ia) in chloroform medium. Further the cyclo-condensation of 1-γ-picolinoyl-4-p-tolyl-3-thiosemicarbazides (IIa) with t-butyl imino isocyanodichloride in chloroform lead to the light yellow coloured solid with the evolution of hydrogen chloride gas. The product was acid to litmus. On determination of equivalent weight it was found to be mono hydrochloride (IIIa-f) yield 85%, m.p. 178°C.On basification with ammonium hydroxide, afforded a free base (IVa)) crystallized from aqueous ethanol, m.p. 218°C. On the basis of spectral data IR and 1H NMR and above facts the compound (IVa) has been assigned the structure as 2-N-t-butylimino-3-γ-picolinoyl-5-p-tolylimino-1,3,4-thiadiazoles (IVa).

The other compounds (IVb-f) were prepared by extending the above reaction to other, 1-γ-picolinoyl-4-aryl-3-thiosemicarbazides (IIb-f) and the related products were isolated in good yield. (Table-2). Isomerisation of product (IVa) was carried out by refluxing with 5% ethanolic NaOH for 1.5 hr.On the basis of elemental data and spectral analysis the structure of isomerised product (Va) was found to be 2-γ-picolinoyl-4-N-t-butyl-5-p-tolyl imino-1,2,4-triazolidine-3-thione. The other compounds (Vb-f) were prepared by extending the above reaction to other, 2-N-t-butylimino-3-γ-picolinoyl-5-p-tolylimino-1,3,4-thiadiazoles (IVb-f) and the related products were isolated in good yield. (Table-2).

The 2-γ-picolinoyl-4-N-t-butyl-5-p-tolyl imino-1,2,4-triazolidin-3-thione (Va) was hydrolyzed by boiling with 30% sulphuric acid under reflux for 3.0 h. underwent de-t-butylation. The structure of 2 -γ-picolinoyl-5-p-tolyl imino-1,2,4-triazolidine-3-thione (VIa) was confirmed from it's ^{1}H NMR spectral data. The absence of signals due to C-H of t-butyl group in 1H NMR spectra of product (VIa) confirmed that compound (Va) was successfully de-tertbutylated into 2-γ-picolinoyl-5-p-tolyl imino-1,2,4-triazolidine-3-thione (VIa). The above reaction was extended to synthesize compounds (VIb-f) (Table 2). The elemental analysis and spectral data IR, 1H-NMR and Mass of all the synthesized compounds was in full agreement with the proposed structures. The formation of compounds II, III, IV, V and VI can be explained by the following ***reaction schemel.***

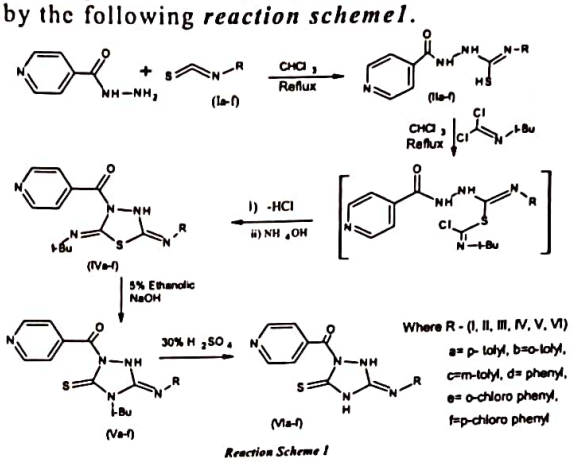

Reaction Scheme I

CONCLUSION

The present work attempt to synthesize some new derivatives of triazole moiety by incorporating isoniazide in it's structure in view of having more promising pharmacological and pathological activities and confirmation of structures were successfully carried out with elaborate characterization by spectral data. Obtained spectral data has prompted to further evaluate the possible information from the spectra to understand synthetic approach and the dynamic property of molecules synthesized. These synthesized compounds are expected to possess biological activities.

Acknowledgement

The author is grateful to the Principal, Shri Mungasaji Maharaj Mahavidyalaya, Darwha for allowing to carry out research work. The authors is thankful to The Director , RSIC, Punjab University , Chandigarh for providing elemental analysis and IR,PMR, Mass Spectral data.

References

1. Singh R. J. and Singh D. K. 2009. Syntheses, characterization and biological activity of some 1, 2, 4-triazole derivatives. *E-J.Chem.* **6(3)**, 796-800.
2. Singh R. J. and Singh D. K. 2009. Syntheses, characterization and biological screening of some novel 1, 2, 4-triazoles. *Asian J. Research Chem,* **2(4)**, 536-538.
3. Upmanyu N. 2006. Triazoles. As A Promising Medicinal Agents, **4(3)**.
4. Bhaskar C.S., Vidhale N.N. and Berad B.N. 2002. *Asian J.Chem*, 14,162.
5. Buscemi S., Vivona N. and Caronna T. 1996. *J. Org. Chem.*, **61**, 8379.
6. Yoo B. R., Suk M. Y.., Y-Man. Yu, S-Gyn. Hong and Jung I. N.1998. *Bull. Korean Chem. Soc.*, **19(3)**, 358.
7. Paulvannan K., Chen T. and Hale R.2000. *Tetrahedron*, **56**, 8071.
8. Vogel A. I. 1958. A Text Book of Practical Organic Chemistry, Including Qualitative Analysis, *Longmans*, **IIIrd** Ed,.
9. Striewsky W., Schmidte, Sectender M. and Hitzler F. 1960. *Leibig's Ann*, 192, 568.

10. Dyson G. M. and Harington. 1940. *J. Chem. Soc.*,191.
11. Singh. T., Bhattacharya A. and Verma V.K. 1992. *J. Indian Chem. Soc.*, **69**,153-156.
12. Dyer J. R.1974. Application of Absorption Spectroscopy of Organic Compound, *Prentice-Hall.*
13. Colthup N. B., Daly L. H. and Wiberly S. E.1964. "Introduction to Infraredand Raman Spectroscopy", Academic Press, NewYork.
14. Silverstein R. M., Bassler G. C. and Morrill T. C. "Spectrometric Identification of Organic Compo 4th Edn.", John Wiley & Sons, New York 1981.
15. 15. Lacey R. N.1960. Structure and Mechanis Organic Chemistry, *J. Chem. Soc.*,163.

How to cite this article:

Nazia .A. Rashidi (2020) ' Cyclo-Condensation of Substituted Thiosemicarbazides: Synthesis of 2,5- Disubstituted 1,2,4-Triazolidin- 3-Thione', *International Journal of Current Advanced Research,* 09(08), pp. 22890-22893.
DOI: http://dx.doi.org/10.24327/ijcar.2020.22893.4526

****

Modern Physics Letters A
2050196 (20 pages)

DOI: 10.1142/S0217732320501965

Tilted universe with big rip singularity in Lyra geometry

V. J. Dagwal[*,¶], D. D. Pawar[†,‖], Y. S. Solanke[‡,**] and H. R. Shaikh[§,††]

[*]*Department of Mathematics, Government College of Engineering, Nagpur 441108, India*
[†]*School of Mathematical Sciences, Swami Ramanand Teerth Marathwada University, Vishnupuri Nanded 431606, India*
[‡]*Mungsaji Maharaj Mahavidyalaya, Darwha, Yavatmal 445202, India*
[§]*Department of Physics, Government Polytechnic, Murtizapur, India*
[¶]*vdagwal@gmail.com*
[‖]*dypawar@yahoo.com*
[**]*yadaosolanke@gmail.com*
[††]*hrshaikh001@gmail.com*

Received 9 November 2019
Accepted 22 April 2020
Published 23 June 2020

We have examined tilted cosmological models by using conformally flat space-time with wet dark fluid in Lyra geometry. In order to solve the field equations we have considered a power law. In this paper we have discussed tilted universe with time-dependent displacement field vector, heat conduction vectors and also discussed big rip singularity. Some physical and geometrical properties are also investigated. We have also extended our work to investigate the consistency of the derived model with observational parameter from the point of astrophysical phenomenon such as look-back time-redshift, proper distance, luminosity distance, angular-diameter distance and distance modulus.

Keywords: Tilted models; conformally flat space-time; wet dark fluid; Lyra geometry.

1. Introduction

In a tilted cosmology the tilt can become extreme in a limited time as measured along the fluid congruence, with the result that the group orbits become time-like. This means that the models are no longer spatially homogeneous. A spatially homogeneous universe is said to be non-comoving if the fluid velocity vector is not orthogonal to the group orbits, otherwise the model is said to be co-moving. Dynamical tilted universe is explored by King and Ellis;[1] Ellis and King;[2] Goliath and Ellis.[3] Larena[4] has studied cosmological matter fluid in tilted universe and discussed the effect of peculiar velocity. Herrera *et al.*[5] constructed the Szekeres

[¶]Corresponding author.

space-time tilted model. Dunn and Tupper[6] analyzed the physical properties of tilted universe for perfect fluid.

Herrera *et al.*[5] derived tilted observer for thermodynamics and hydrodynamics properties. Sharif and Tahir[7] constructed the physical properties of tilted model for different space-time. Sahu *et al.*[8] and Sahu and Kumar[9] discussed spatially homogeneous universe for various space-time in different gravitation theory and geometry. Dagwal and Pawar;[10,11] Pawar and Dagwal[12,13] analyzed tilted dark energy models, tilted two fluid models and tilted scalar field for solving cosmological problem. Sandin[14] and Verma[15] (2009) examined the effect of two fluid models on tilted universe and solved the exact solutions.

The importance of wet dark fluid is derived from the fact that it is a good calculation for various fluids, including water, in which the internal attraction of the molecules makes negative pressure possible. One of the virtues of this model is that the square of the sound speed, c_s^2 which depends on $\partial p/\partial\rho$, can be positive, which still gives rise to the cosmic acceleration in the current epoch.

Homogeneous and isotropic wet dark fluid model is analyzed by Holman and Naidu.[16] Higher-dimensional space-time with wet dark fluid in modified theory of gravity has been expressed by Sahoo and Mishra.[17] Chaubey[18] and Singh and Chaubey[19] investigated physical and geometrical properties of wet dark fluid. Samanta *et al.*[20] considered negative pressure with wet dark fluid. Physical implications of wet dark fluid in biometric theory of gravitation have been studied by Jain *et al.*[21]

We have inspired to use the wet dark fluid (WDF) as a model for dark energy which stems from an experiential equation of state investigated by Hayward[22] to treat water and aqueous solution.

The equation of state for Wet Dark Fluid is

$$p_{\mathrm{WDF}} = \gamma(\rho_{\mathrm{WDF}} - \rho^*)$$

and motivated by the fact that it is good approximation for various fluids, including water, in which the internal attraction of the molecules makes negative pressure possible.

We use the energy conservation equation

$$\dot{\rho}_{\mathrm{WDF}} + 3H(p_{\mathrm{WDF}} + \rho_{\mathrm{WDF}}) = 0$$

From equation of state and using $3H = \frac{\dot{v}}{v}$ in the above equation, we get

$$\rho_{\mathrm{WDF}} = \frac{\gamma}{1+\gamma}\rho + \frac{s}{v^{(1+\gamma)}}$$

where s is the constant of integration and v is the volume expansion.

Wet dark fluid naturally comprises two components: a piece that behaves as a cosmological constant as well as a standard fluid with an equation of state $p = \gamma\rho$. We can show that if we take $s > 0$, this fluid will not violate the strong energy

condition $p + \rho \geq 0$

$$p_{\mathrm{WDF}} + \rho_{\mathrm{WDF}} = (1+\gamma)\rho_{\mathrm{WDF}} - \gamma\rho^{*} = (1+\gamma)\frac{s}{v^{(1+\gamma)}} \geq 0.$$

Lyra[23] has expressed a modification of Riemannian geometry by presenting a gauge function into the structure less manifold, which bears a close resemblance to Weyl's geometry. A static universe has been obtained by Sen.[24] Thermodynamic equilibrium property in Lyra's geometry has been calculated by Karade and Borikar.[25] Sen and Dunn[26] explored Einstein field equations constructed on Lyra's manifold. Halford[27] considered the vector field ϕ_i in Lyra's manifold which plays a parallel role of cosmological constant Λ in general theory of relativity. Cosmological solution in Lyra's geometry has been constructed by Bhamra.[28] Vacuum cosmological universe in Lyra's geometry has evaluated by Beesham.[29] Mohanty *et al.*[30] obtained non-existence cosmological model for Perfect Fluid in Lyra's geometry. Pawar *et al.*;[31] Dagwal and Pawar[32] developed tilted universe in Brans–Dicke theory of gravitation and general relativity, respectively. The behaviors of dark energy, mesonic scalar field, magnetic field and anisotropy parameter in gravitation theories are developed by Aktaş *et al.*[33,34] Yousaf[53,54] investigated different tilted and non-tilted model in modified gravity. Non-comoving models with wet dark fluid in scalar theory of gravitation are formulated by Sahu *et al.*[35] Aktaş,[36] Aygün *et al.*,[37] Yılmaz *et al.*[38] and Dagwal and Pawar[39,40] have studied Lyra geometry and other alternative theories.

LRS Bianchi type-I metric is the spatially homogeneous and anisotropic flat universe. FRW universe has the equivalent scale factor for each of the three spatial directions where as LRS Bianchi type-I metric has dissimilar scale factors. The singularity of LRS Bianchi type-I metric behaves like Kasnser metric. It has been studied that a metric filled with matter, the early anisotropy in LRS Bianchi type-I metric speedily expires away and evolves into a FRW universe. It has simple mathematical form and motivating because of the capability to clarify the cosmic evolution of the early universe. Due to its prominence, several authors have explored LRS Bianchi type-I metric from different aspects.

Abdussattar and Prajapati[41] investigated LRS Bianchi type-I with modified Chaplygin gas equation of state. Bishi *et al.*[42] developed LRS Bianchi type-I in $f(R,T)$ gravity. Solanke *et al.*[43] presented LRS Bianchi type-I metric in the presence dark energy.

Motivated by the above work, we have examined tilted cosmological models by using conformally flat space-time with wet dark fluid in Lyra geometry. In this paper, we have discussed tilted universe with time-dependent displacement field vector, heat conduction vectors and also discussed big rip singularity. We have investigated distances in cosmology. This paper is organized as follows. Section 2 deals with metric and field equations, Sec. 3 deals with physical and geometrical property, Sec. 4 deals with distances in cosmology, Sec. 4.1 deals with look-back time-redshift, Sec. 4.2 deals with proper distance, Sec. 4.3 deals with luminosity distance, Sec. 4.4 deals with angular-diameter distance, Sec. 4.5 deals with distance

modulus, Sec. 5 deals with results and discussion. The conclusion was provided in Sec. 6.

2. Metric and Field Equations

We consider the metric in the form

$$ds^2 = -dt^2 + e^{2\alpha}\,dx^2 + e^{2\beta}(dy^2 + dz^2) \tag{1}$$

where α and β are the functions of t alone.

The field equations of wet dark fluid in Lyra geometry are given by

$$R_i^j - \frac{1}{2}g_i^j R + \frac{3}{2}\phi_i\phi^j - \frac{3}{4}g_i^j\phi_k\phi^k = T_i^j, \tag{2}$$

where ϕ is a time-dependent displacement field vector, defined by

$$\phi_i = (0, 0, 0, \gamma(t)). \tag{3}$$

The energy–momentum tensor given by

$$T_i^j = (p_{\mathrm{WDF}} + \rho_{\mathrm{WDF}})u_i u^j + p_{\mathrm{WDF}}g_i^j + q_i u^j + u_i q^j, \tag{4}$$

together with

$$g_{ij}u^i u^j = -1, \quad q_i q^i > 0, \quad q_i u^j = 0, \tag{5}$$

where p_{WDF} is the pressure and ρ_{WDF} is the energy density of wet dark fluid, q_i is the heat conduction vector orthogonal to u^i. The fluid vector u^i has the components $\left(\frac{\sinh\lambda}{e^\alpha}, 0, 0, \cosh\lambda\right)$ satisfying Eq. (5) and λ is the tilt angle.

The field equation (2) for metric (1) reduces to

$$2\beta_{44} + 3\beta_4^2 + \frac{3}{4}\gamma^2 = (\rho_{\mathrm{WDF}} + p_{\mathrm{WDF}})\sinh^2\lambda + p_{\mathrm{WDF}} + 2q_1\frac{\sinh\lambda}{e^\alpha}, \tag{6}$$

$$\alpha_{44} + \beta_{44} + \alpha_4\beta_4 + \alpha_4^2 + \beta_4^2 + \frac{3}{4}\gamma^2 = p_{\mathrm{WDF}}, \tag{7}$$

$$\beta_4^2 + 2\alpha_4\beta_4 - \frac{3}{4}\gamma^2 = -(\rho_{\mathrm{WDF}} + p_{\mathrm{WDF}})\cosh^2\lambda + p_{\mathrm{WDF}} - 2q_1\frac{\sinh\lambda}{e^\alpha}, \tag{8}$$

$$(\rho_{\mathrm{WDF}} + p_{\mathrm{WDF}})e^\alpha\sinh\lambda\cosh\lambda + q_1\cosh\lambda + q_1\frac{\sinh^2\lambda}{\cosh\lambda} = 0. \tag{9}$$

Here the index 4 after a field variable denotes the differentiation with respect to cosmic time t.

The set (6)–(9) are four field equations containing seven unknown α, β, γ, p_{WDF}, ρ_{WDF}, λ, q_1. To obtain a determinate solution we have to consider three additional constraints.

First, we consider that the space-time is conformally flat, which gives

$$C_{2323} = \frac{e^{4\beta}}{3}[\alpha_{44} + \alpha_4^2 - \beta_{44} - \beta_4\alpha_4]. \tag{10}$$

Second, the shear scalar is proportional to the expansion scalar α and β (Ref. 20)

$$\alpha = m\beta, \tag{11}$$

where m is constant.

The motive behind considering this condition is described with reference to Thorne,[44] the observations of the velocity-red-shift relation for extragalactic sources suggest that Hubble expansion of the universe is isotropic today within $\approx 30\%$ (1996). To put more precisely, red-shift studies place the limit $\frac{\sigma}{H} \leq 0.3$ on the ratio of shear σ to Hubble constant H in the neighborhood of our galaxy today. Collins *et al.*[45] pointed out that for spatially homogeneous metric, the normal congruence to the homogeneous expansion satisfies that the condition $\frac{\sigma}{H}$ is constant.

Solving Eqs. (10) and (11) we get

$$\alpha = \log(n_2^m T) \quad \text{and} \quad \beta = \log(n_2 T^{1/m}), \tag{12}$$

where $T = mt - n_1$, n_1, n_2 are integration constants.

Equation (12) can be rewritten as

$$e^{\alpha} = n_2^m T \quad \text{and} \quad e^{\beta} = n_2 T^{1/m}. \tag{13}$$

Hence the line element (1) is reduced to

$$ds^2 = -\frac{dT^2}{m^2} + n_2^{2m} T^2\, dx^2 + n_2^2 T^{2/m}(dy^2 + dz^2), \tag{14}$$

3. Some Physical and Geometrical Properties

Finally, in order to obtain the solution of the equation we consider the following equation of state:

$$\rho_{\text{WDF}} = -2p_{\text{WDF}}. \tag{15}$$

From Eqs. (6), (8) and (15) we get

$$\rho_{\text{WDF}} = -2p_{\text{WDF}} = \frac{4(n_2 - m + 2)}{3n_2^2 T^2}, \tag{16}$$

where $T = mt - n_1$, n_1, n_2 are integration constants.

The energy density of wet dark fluid is presented by 3D and 2D graphs in Figs. 1 and 2, respectively. The energy density of wet dark fluid approaches toward infinity when cosmic time is at the initial stage. For large value of cosmic time, the energy density of wet dark fluid is zero. The energy density of wet dark fluid has big rip singularity at $T = \left(t = \frac{n_1}{m}\right)$. It has big bang singularity at big value of t. The intermediate phase is between big bang and big rip singularity.

Using Eqs. (7) and (16) we get

$$\gamma^2 = \frac{4(n_2 + 3n_2 m - m - 3m^2 + 1)}{3n_2^2 T^2}. \tag{17}$$

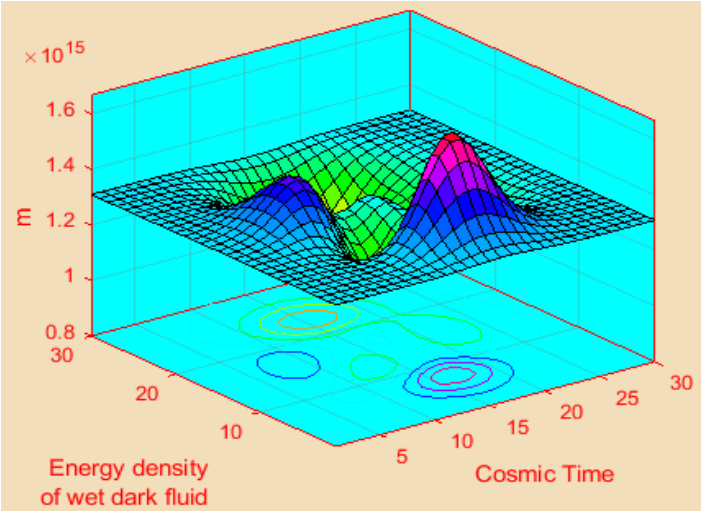

Fig. 1. Behavior of energy density of wet dark fluid vs. cosmic time t (1 unit = 1 billion years) and m with different n_2.

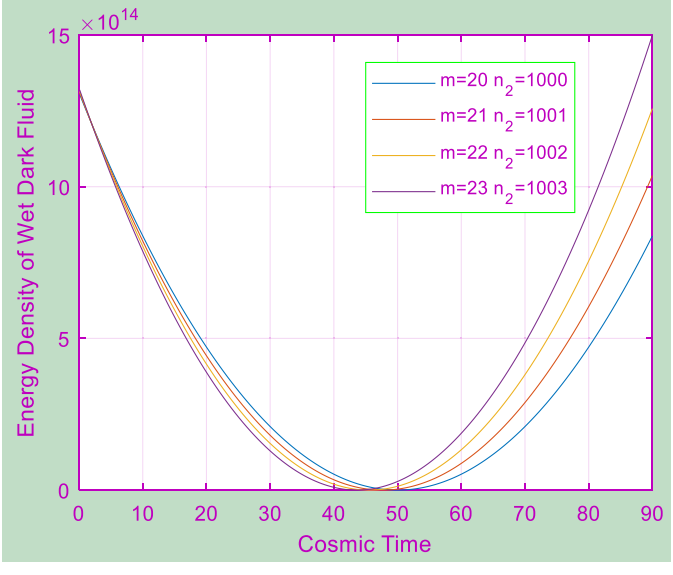

Fig. 2. Energy density of wet dark fluid against cosmic time t (1 unit = 1 billion years).

The variation of γ against cosmic time is shown in Fig. 3. When cosmic time is large, $\gamma \to 0$ but when $T \to 0$, the value of γ is diverging. The model has big rip singularity at $T = \left(t = \frac{n_1}{m}\right)$. The model is vanishing at big bang and diverges at big rip i.e. the model is beginning at big bang and finishes with big rip singularity. When $T = \left(t = \frac{n_1}{m}\right)$, the value of $\gamma \to \infty$.

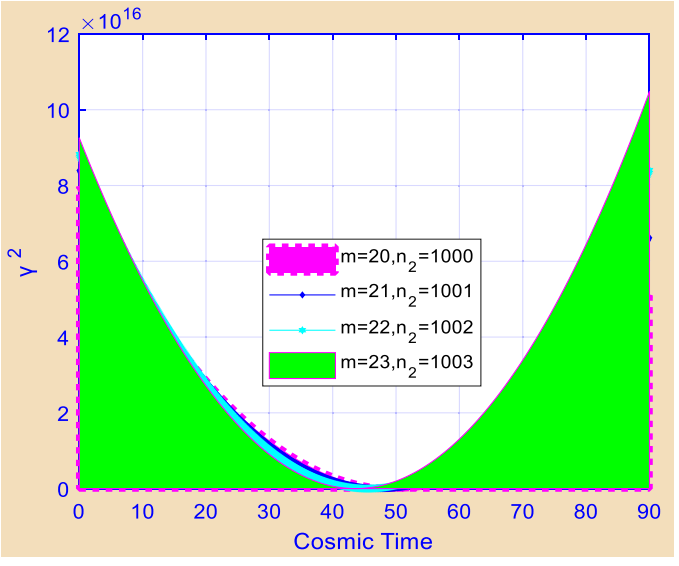

Fig. 3. Variation of γ against cosmic time t (1 unit = 1 billion years).

The tilt angle λ, flow vectors $u^i$and heat conduction vectors q_i for the model (14) are given by

$$\cosh\lambda = M^{1/2}, \quad \sinh\lambda = (M-1)^{1/2}, \tag{18}$$

where $M = \frac{4n_2+9n_2m-9m^2-7m-2}{6(n_2+3n_2m+1-2m-3m^2)}$.

$$u^1 = \frac{(M-1)^{1/2}}{n_2^m T}, \quad u^4 = M^{1/2}. \tag{19}$$

The variations of flow vectors versus cosmic time are represented in Fig. 4 by locating the value $n_2 = (1000, 1001, 1002, 1003)$ and $m = (20, 21, 22, 23)$. The flow vectors increase with increase in cosmic time. The flow vectors diverge when $T = \left(t = \frac{n_1}{m}\right)$. The flow vectors approach to zero for large value of cosmic time. The flow vectors start with big bang when$T \to \infty$.

$$q_1 = \frac{N_1}{T}, \quad q_4 = \frac{N_2}{T}, \tag{20}$$

where

$$N_1 = \frac{2Mn_2^m(M-1)^{1/2}(2m+3m^2-n_2-3n_2m-1)}{n_2^2}$$

and

$$N_2 = \frac{2(M-1)M^{1/2}(n_2+3n_2m+1-2m-3m^2)}{n_2^2}.$$

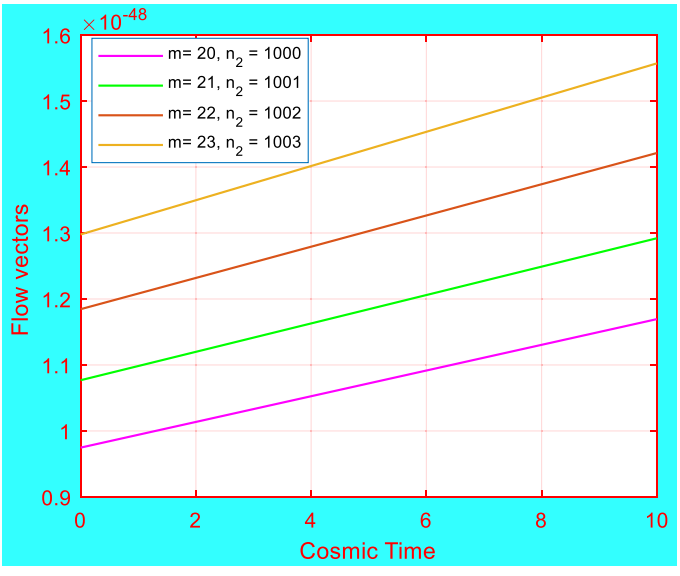

Fig. 4. Variation of flow vectors against cosmic time (1 unit = 1 billion years).

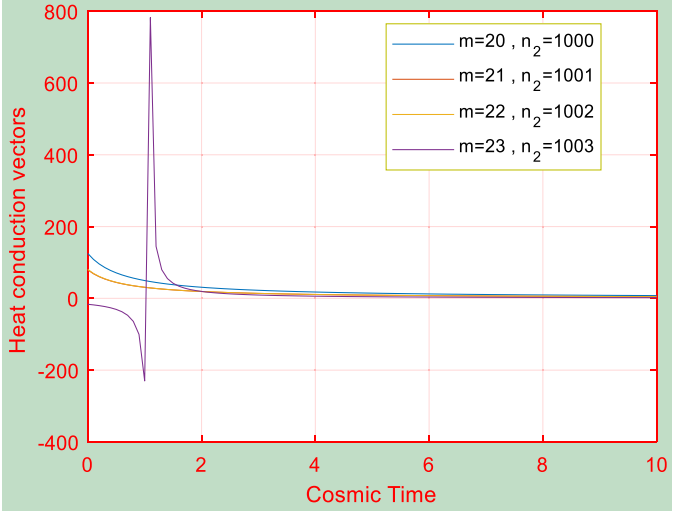

Fig. 5. Variation of heat conduction vectors against cosmic time t (1 unit = 1 billion years).

The profiles of heat conduction vectors are represented by 2D and 3D graphs in Figs. 5 and 6. The heat conduction vectors start at $T \to \infty$ and end with $T = \left(t = \frac{n_1}{m}\right)$. The heat conduction vectors approach to infinite at trivial value of cosmic time.

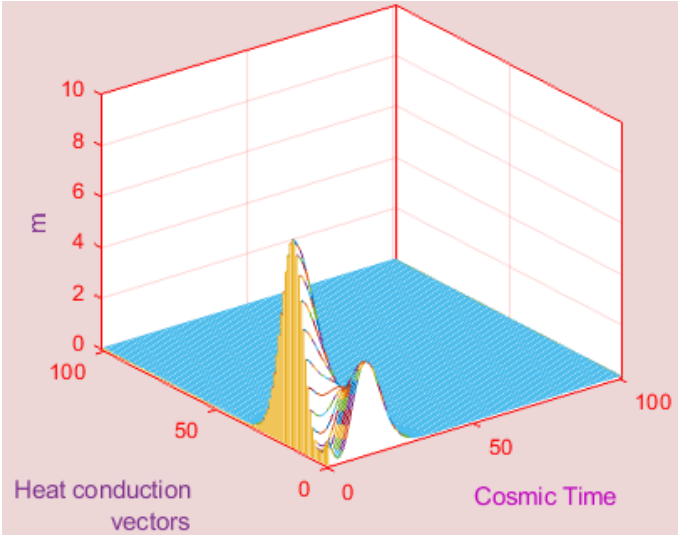

Fig. 6. Variation of heat conduction vectors against cosmic time t (1 unit = 1 billion years) and m.

The scalar expansion and shear scalar are

$$\theta = \frac{(m+2)M^{1/2}}{n_2 T}, \tag{21}$$

$$\sigma^2 = \frac{2(m-1)^2}{3n_2^2 T^2}, \tag{22}$$

The variations of the scalar expansion against cosmic time are represented in Fig. 7 by locating the values $n_2 = (1000, 1001, 1002, 1003)$ and $m = (20, 21, 22, 23)$. The scalar expansion increases with trivial value of cosmic time. When $T \to 0$, scalar expansion expanded the universe. The scalar expansion initiates at big bang and stops with big rip.

The profile of shear scalar against cosmic time is shown in Fig. 8 by setting the values $n_2 = (1000, 1001, 1002, 1003)$ and $m = (20, 21, 22, 23)$. When $T \to \left(t = \frac{n_1}{m}\right)$, the shear scalar is expanding. The shear scalar is in between the values of initial and large cosmic time. The shear scalar starts at $T \to \infty$ and ends at $T \to 0$. The shear scalar has big rip singularity at $T \to \left(t = \frac{n_1}{m}\right)$. The shear scalar begins at big bang and finishes with big rip singularity. The shear scalar has same singularity like energy density of wet dark fluid and time dependent displacement field vector.

The spatial volume and the rate of expansion H_i in the direction of x, y, z-axis, are respectively, given as

$$\begin{aligned} V &= n_2^m n_2^2 T^{\frac{2+m}{m}}, \\ H_1 &= \frac{2m}{n_2 T}, \quad H_2 = H_3 = \frac{2}{n_2 T}. \end{aligned} \tag{23}$$

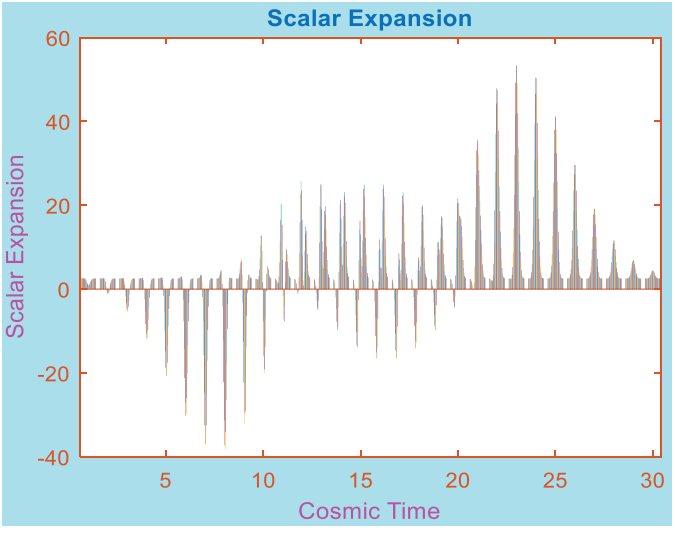

Fig. 7. Variations of scalar expansion against cosmic time t (1 unit = 1 billion years).

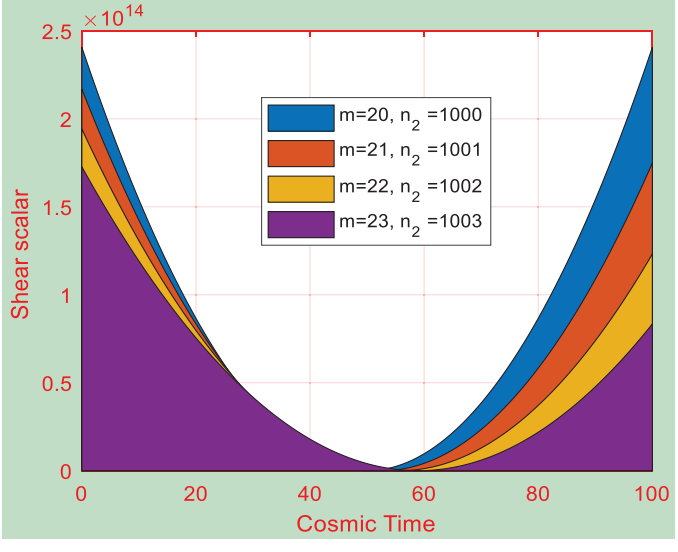

Fig. 8. Variation of shear scalar against cosmic time$t$ (1 unit = 1 billion years).

The variations of spatial volume against cosmic time are represent in Fig. 9 by setting the values of $n_2 = (1000, 1001, 1002, 1003)$, $m = (20, 21, 22, 23)$ and $n_1 = -0.3$. The spatial volume has same singularity like energy density of wet dark fluid, time dependent displacement field vector and shear scalar.

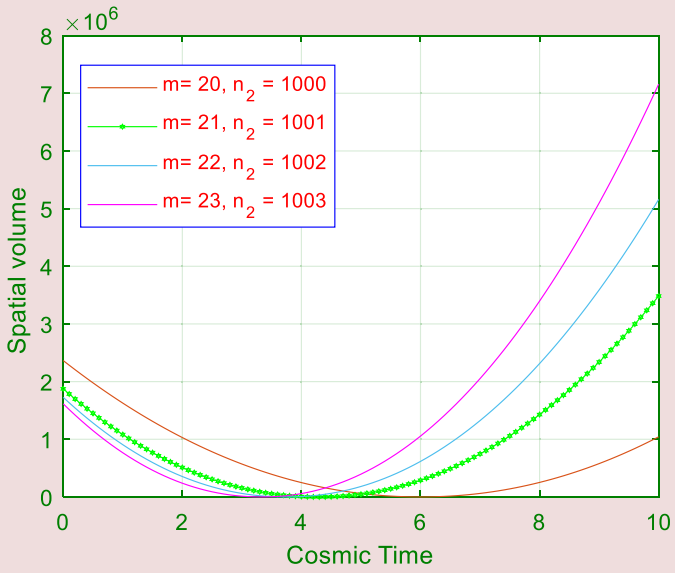

Fig. 9. Variations of spatial volume against cosmic time t (1 unit = 1 billion years).

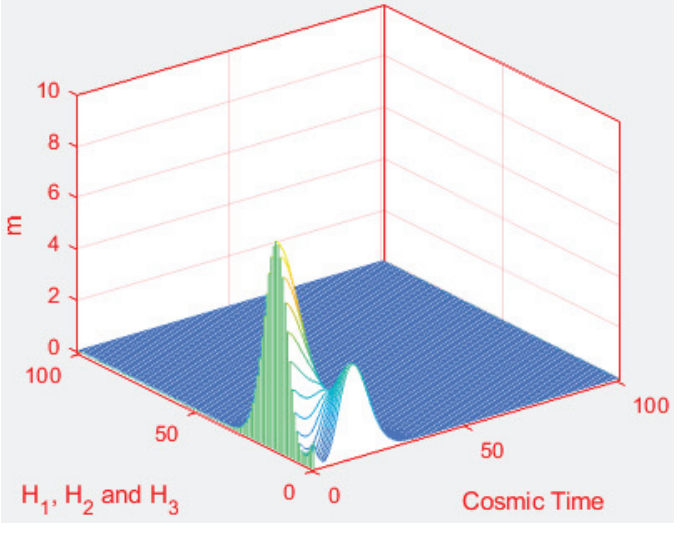

Fig. 10. Variations of rate of expansion H_i against cosmic time t (1 unit = 1 billion years) and m.

The profile of rate of expansion H_i against cosmic time t and m is shown in Fig. 10 by locating the values of $n_2 = (1000, 1001, 1002, 1003)$, $m = (20, 21, 22, 23)$ and $n_1 = -0.3$. The rate of expansion diverges at $T = \left(t = \frac{n_1}{m}\right)$. It is expanded at big rip and stops at big bang.

The density parameter, anisotropy parameter and deceleration parameter of the model are respectively given as

$$\Omega = \frac{(n_2 - m - 2)}{9(m+2)^2},$$
$$\Delta = \frac{2}{3}\left[\frac{2 + (m+1)^2}{(m+2)^2}\right], \tag{24}$$
$$q = -1 + \frac{mn_2}{2(m+2)}.$$

4. Distances in Cosmology

The distance measurement played a significant role for sympathetic about Universe. We have shown some of the different distance measures.

4.1. *Look-back time-redshift*

The look-back time t_L is defined as the difference between the present age of the universe t_0 and the age of the Universe, when a particular light ray at redshift z was emitted. The look-back time t_L is defined as

$$t_L = t_0 - t(z) = \int_a^{a_0} \frac{da}{\dot{a}}, \tag{25}$$

where t_0 is present age of the universe .

The scale factor a in terms of redshift parameter z is written as

$$\frac{a}{a_0} = \frac{1}{1+z}, \tag{26}$$

where a_0 is the present day scale factor of the universe and z denotes redshift of light.

Using Eq. (26), we get

$$(mt - n_1) = (mt_0 - n_1)(1+z)^{\frac{-3m}{m+2}}. \tag{27}$$

From Eq. (27), we get

$$H_0(t_0 - t) = \frac{2(m+2)}{mn_2}\left[1 - (1+z)^{\frac{-3m}{m+2}}\right] \tag{28}$$

where H_0 is the Hubble constant at present. The value of Hubble constant H_0 lies between 50–100 km s^{-1} Mpc^{-1}.

Using Eq. (28), we get

$$H_0(t_0 - t) = \frac{6}{n_2}\left[z - \frac{(1+2m)}{(m+2)}z^2 + \frac{(1+2m)(4+5m)}{(m+2)^2}z^3 + \cdots\right]. \tag{29}$$

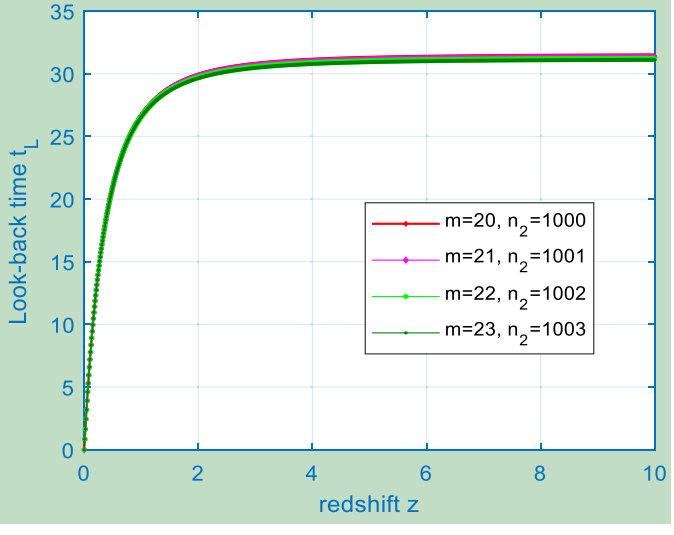

Fig. 11. Variation of look-back time t_L against redshift z.

By using $q = -1 + \frac{mn_2}{2(m+2)}$, we get

$$H_0(t_0 - t) = \frac{3m}{(m+2)(q+1)}\left[z - \frac{(1+2m)mn_2}{2(q+1)}z^2 + \frac{(1+2m)(4+5m)m^2n_2^2}{6(q+1)^2}z^3 + \cdots\right]. \tag{30}$$

In Eq. (28), when $z \to \infty$, we get

$$t_L = t_0 - t = H_0^{-1}\left[\frac{2(m+2)}{mn_2}\right] = \frac{H_0^{-1}}{(1+q)}. \tag{31}$$

For small value of z, using Eq. (30), we get

$$H_0(t_0 - t) \cong \frac{3m}{(m+2)(q+1)}z. \tag{32}$$

The profile of look-back time t_L against redshift z is shown in Fig. 11 by setting the values of $n_2 = (1000, 1001, 1002, 1003)$, $m = (20, 21, 22, 23)$ and $H_0 = 70$.

4.2. *Proper distance*

The proper distance $d(z)$ is defined as the distance between a cosmic source emitting light at any instant $t = t_1$ located at $r = r_1$ with redshift z and the observer receiving the light from the source emitted at $r = 0$ and $t = t_0$.

$$d(z) = r_1 a_0, \tag{33}$$

where $r_1 = \int_t^{t_0} \frac{dt}{a}$.

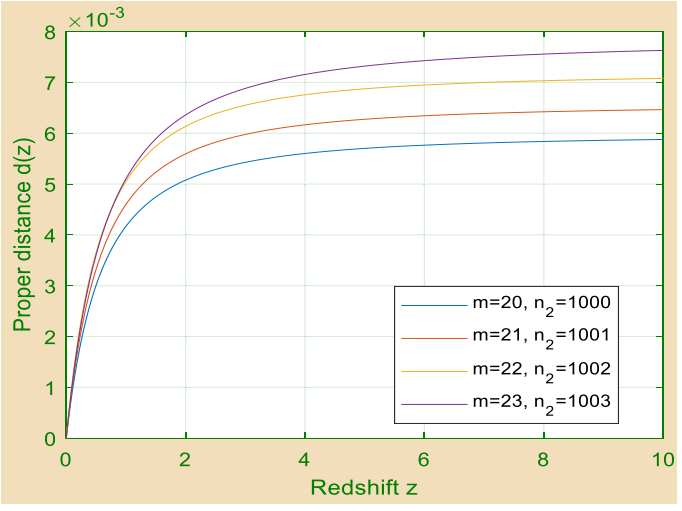

Fig. 12. Variation of proper distance $d(z)$ against redshift z.

The proper distance $d(z)$ is given by

$$d(z) = \frac{(m+2)}{n_2(m-1)} H_0^{-1} \left[1 - (1+z)^{\frac{-2(m-1)}{(m+2)}}\right]. \tag{34}$$

When $z \to \infty$, the proper distance $d(z)$ is $\frac{(m+2)}{n_2(m-1)} H_0^{-1}$.

The profile of proper distance $d(z)$ against redshift z is shown in Fig. 12 by setting the values of $n_2 = (1000, 1001, 1002, 1003)$, $m = (20, 21, 22, 23)$ and $H_0 = 70$.

4.3. *Luminosity distance*

The luminosity distance $d_L$of light source is defined as

$$d_L = a_0 r_1 (1+z) = d(z)(1+z). \tag{35}$$

From Eqs. (34) and (35) we get

$$d_L = \frac{(m+2)}{n_2(m-1)} H_0^{-1} \left[1 - (1+z)^{\frac{-2(m-1)}{(m+2)}}\right](1+z). \tag{36}$$

The profile of luminosity distance d_L against redshift z is shown in Fig. 13 by setting the values of $n_2 = (1000, 1001, 1002, 1003)$, $m = (20, 21, 22, 23)$ and $H_0 = 70$.

4.4. *Angular-diameter distance*

The angular-diameter distance d_A is defined in term of proper distance and luminosity distance as

$$d_A = d(z)(1+z)^{-1} = d_L(1+z)^{-2}. \tag{37}$$

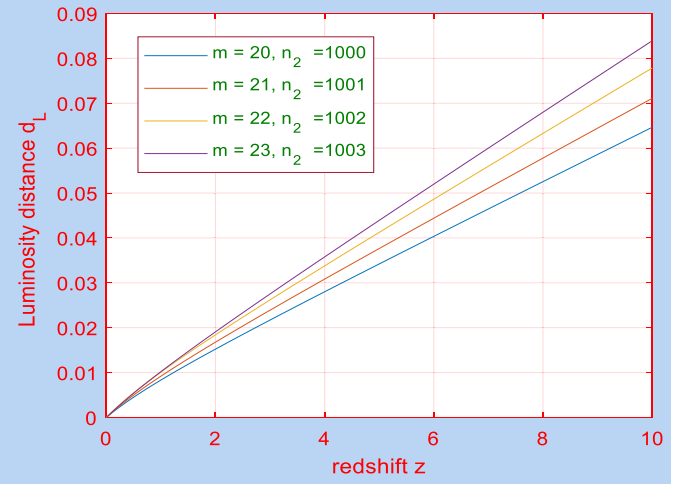

Fig. 13. Variation of luminosity distance d_L against redshift z.

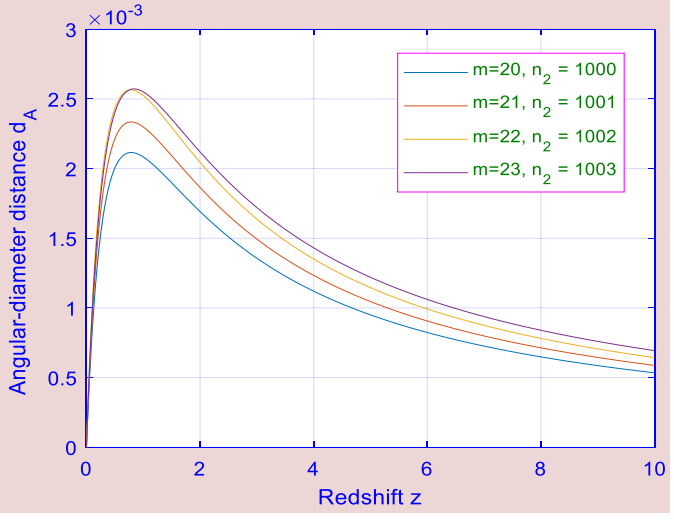

Fig. 14. Variation of angular-diameter distance d_A against redshift z.

From Eqs. (34) and (37) we get

$$d_A = \frac{(m+2)}{n_2(m-1)} H_0^{-1} \left[1 - (1+z)^{\frac{-2(m-1)}{(m+2)}}\right] (1+z)^{-1}. \tag{38}$$

The profile of angular-diameter distance d_A against redshift z is shown in Fig. 14 by setting the values of $n_2 = (1000, 1001, 1002, 1003)$, $m = (20, 21, 22, 23)$ and $H_0 = 70$.

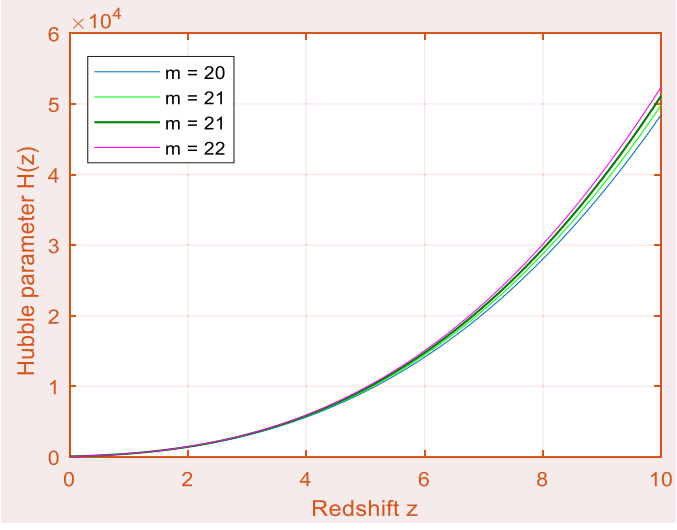

Fig. 15. Variation of Hubble parameter $H(z)$ against redshift z.

4.5. *Distance modulus*

The distance modulus $\mu(z)$ is defined as

$$\mu(z) = 5\log d_L + 25. \tag{39}$$

From Eqs. (36) and (39) we get

$$\mu(z) = 5\log\left\{\frac{(m+2)}{n_2(m-1)}H_0^{-1}\left[1-(1+z)^{\frac{-2(m-1)}{(m+2)}}\right](1+z)\right\} + 25. \tag{40}$$

The Hubble parameter H and deceleration parameter q in terms of redshift z (Ref. 46) are given by

$$H(z) = 2(m+2)n_2^{m-1}(1+z)^{(\frac{3m}{m+2})}, \tag{41}$$

or,

$$H(z) = H_0(1+z)^{\left(\frac{3m}{m+2}\right)}, \tag{42}$$

$$q(z) = -1 - \frac{3m}{2(m+2)^2 n_2^{(m-1)}}(1+z)^{-\left(\frac{3m+n_2+2}{m+2}\right)}, \tag{43}$$

or

$$q(z) = -1 - (1+q_0)(1+z)^{-\left(\frac{3m+n_2+2}{m+2}\right)}, \tag{44}$$

where H_0 is the present value of the Hubble parameter and q_0 is the present value of the deceleration parameter.

The profile of Hubble parameter $H(z)$ against redshift z is shown in Fig. 15 by setting the values $m = (20, 21, 22, 23)$ and $H_0 = 70$.

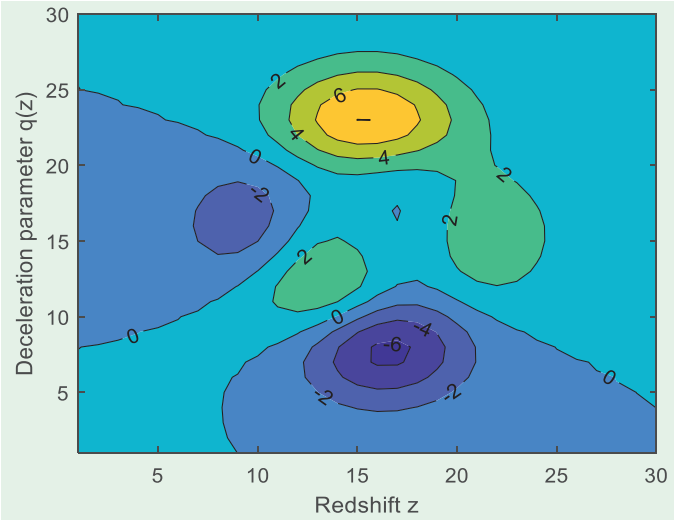

Fig. 16. The contour plot of deceleration parameter $q(z)$ against redshift z.

The contour plot of deceleration parameter $q(z)$ against redshift z is shown in Fig. 16 by setting the values of $n_2 = (1000, 1001, 1002, 1003)$, $m = (20, 21, 22, 23)$ and $H_0 = 70$.

5. Results and Discussion

The pressure p_{WDF} and the energy density ρ_{WDF} of wet dark fluid are vanishing at large cosmic time but when $T \to 0$, the pressure p_{WDF} and the energy density ρ_{WDF} of wet dark fluid are divergent. Tiled angleλ and flow vectors $u^4$are constant. When $M = 1$, the tilt angle λ, the flow vectors $u^4$and heat conduction vectors q_1, q_4 are zero. When $T = \infty$, the flow vectors u^1 and heat conduction vectors q_1, q_4 are disappearing but the flow vectors $u^1$and heat conduction vectors q_1, q_4 are divergent at $T = 0$. At $T = \infty$, the scalar expansion and shear scalar are disappearing but primarily, the scalar expansion and shear scalar are divergent. The shear scalar is zero at$m = 1$ and the scalar expansion is disappearing for $m = -2$. The models are nonexpanding at $m = -2$ and no shearing when $m = 1$. The spatial volume is constant for $m = -2$. When $T = 0$, the rate of expansion is divergent. But for $T \to \infty$, the rate of expansion is zero. The density parameter and anisotropy parameter are constant. The density parameter and anisotropy parameter are divergent for $m = -2$.

6. Conclusion

We have examined the tilted universe with big rip singularity and wet dark fluid in Lyra geometry. The model is expanding, shearing and rotating universe. The

spatial volume, the energy density of wet dark fluid, time dependent displacement field vector and shear scalar have big rip singularity at $T = \left(t = \frac{n_1}{m}\right)$. The models are vanishing at big bang and diverge at big rip i.e. the model is begins at big bang and ends with big rip singularity. The tilted universe has intermediate phase between big bang and big rip singularity. The model initiates with big bang at the initial stage. The expansion in the model decreases as time rises and the expansion in the model rest at large cosmic time. The pan cake-type[47] singularity is observed in the universe when cosmic time is zero. We have discussed physical and geometrical properties of the different parameter. These results match with the results investigated by Sahoo *et al.*[48] and Dagwal.[49]

- The energy density of wet dark fluid is presented by 3D and 2D graphs in Figs. 1 and 2, respectively. The energy density of wet dark fluid approaches toward infinity when cosmic time is at the initial stage. For large value of cosmic time, the energy density of wet dark fluid is zero. The energy density of wet dark fluid has big rip singularity at $T = \left(t = \frac{n_1}{m}\right)$. It has big bang singularity at big value of t. The intermediate phase is between big bang and big rip singularity.
- The variation of γ against cosmic time is shown in Fig. 3. When cosmic time is large, $\gamma \to 0$ but when $T \to 0$, the value of γ is diverging. The model has big rip singularity at $T = \left(t = \frac{n_1}{m}\right)$. The model is vanishing at big bang and diverges at big rip i.e. the model begins at big bang and finishes with big rip singularity.
- The variations of flow vectors versus cosmic time are represented in Fig. 4 by locating the value $n_2 = (1000, 1001, 1002, 1003)$ and $m = (20, 21, 22, 23)$. The flow vectors increases with increase in cosmic time. The flow vectors diverge when $T = \left(t = \frac{n_1}{m}\right)$. The flow vectors approach to zero for large value of cosmic time. The flow vectors start with big bang when$T \to \infty$.
- The profile of heat conduction vectors are represented by 2D and 3D graphs in Figs. 5 and 6, respectively. The heat conduction vectors start at $T \to \infty$ and end with $T = \left(t = \frac{n_1}{m}\right)$. The heat conduction vectors approach to infinite at trivial value of cosmic time.
- The variations of the scalar expansion against cosmic time are represented in Fig. 7 by locating the values $n_2 = (1000, 1001, 1002, 1003)$ and $m = (20, 21, 22, 23)$. The scalar expansion increases with trivial value of cosmic time. When $T \to 0$, scalar expansion expanded the universe. The scalar expansion initiates at big bang and stops with big rip.
- The profile of shear scalar against cosmic time is shown in Fig. 8 by setting the values $n_2 = (1000, 1001, 1002, 1003)$ and $m = (20, 21, 22, 23)$. When $T = \left(t = \frac{n_1}{m}\right)$, the shear scalar is expanding. The shear scalar is in between the values of initial and large cosmic time. The shear scalar starts at $T \to \infty$ and ends at $T \to 0$. The shear scalar has big rip singularity at $T = \left(t = \frac{n_1}{m}\right)$. The shear scalar is beginning at big bang and finishes with big rip singularity. The shear scalar has same singularity like energy density of wet dark fluid and time-dependent displacement field vector.

- The variations of spatial volume against cosmic time are represented in Fig. 9 by setting the values of $n_2 = (1000, 1001, 1002, 1003)$, $m = (20, 21, 22, 23)$ and $n_1 = -0.3$. The spatial volume has same singularity like energy density of wet dark fluid, time-dependent displacement field vector and shear scalar.
- The profile of rate of expansion H_i against cosmic time t and m is show in Fig. 10 by locating the values of $n_2 = (1000, 1001, 1002, 1003)$, $m = (20, 21, 22, 23)$ and $n_1 = -0.3$. The rate of expansion diverges at $T = \left(t = \frac{n_1}{m}\right)$. It is expanded at big rip and stops at big bang.
- The profile of look-back time t_L, proper distance $d(z)$, luminosity distance d_L and angular-diameter distance d_A against redshift z are shown in Figs. 11–14, respectively, by setting the values of $n_2 = (1000, 1001, 1002, 1003)$, $m = (20, 21, 22, 23)$ and $H_0 = 70$.
- The profile of Hubble parameter $H(z)$ against redshift z is shown in Fig. 15 by setting the values $m = (20, 21, 22, 23)$ and $H_0 = 70$.
- The contour plot of deceleration parameter $q(z)$ against redshift z is shown in Fig. 16 by setting the values of $n_2 = (1000, 1001, 1002, 1003)$, $m = (20, 21, 22, 23)$ and $H_0 = 70$.

References

1. R. King and G. G. R. Ellis, *Commun. Math. Phys.* **31**, 209 (1973).
2. G. G. R. Ellis and A. R. King, *Commun. Math. Phys.* **38**, 119 (1974).
3. M. Goliath and G. F. R. Ellis, *Phys. Rev. D* **60**, 023502 (1999).
4. J. Larena, *Phys. Rev. D* **79**, 084006 (2009).
5. L. Herrera, A. Di Prisco and J. Ibáñez, *J. Phys. Rev. D* **84**, 064036 (2011).
6. K. A. Dunn and B. O. J. Tupper, *Astrophys. J.* **222**, 405 (1978).
7. M. Sharif and H. Tahir, *Eur. Phys. J. Plus* **128**, 146 (2013).
8. S. K. Sahu, E. N. Kantila and D. M. Gebru, *Int. J. Theor. Phys.* **55**, 526 (2016).
9. S. K. Sahu and T. Kumar, *Int. J. Theor. Phys.* **012** (2013).
10. V. J. Dagwal and D. D. Pawar, *Mod. Phys. Lett. A* **33**, 1850213 (2018).
11. V. J. Dagwal and D. D. Pawar, *Indian J. Phys.*, doi:10.1007/s12648-019-01625-1.
12. D. D. Pawar and V. J. Dagwal, *Int. J. Theor. Phys.* **53**, 2441 (2014).
13. D. D. Pawar, V. J. Dagwal and Y. S. Solanke, *Int. J. Theor. Phys.* **54**, 1926 (2015).
14. P. Sandin, *Gen. Relat. Gravit.* **41**, 2707 (2009).
15. A. K. Verma, *Astrophys. Space Sci.* **321**, 73 (2009).
16. R. Holman and S. Naidu, arXiv:astro-ph/0408102.
17. P. K. Sahoo and B. Mishra, *Can. J. Phys.* **93**, 1 (2014).
18. R. Chaubey, *Astrophys. Sci.* **321**, 241 (2009).
19. T. Singh and R. Chaubey, *Pramana-J. Phys.* **71**, 447 (2008).
20. G. C. Samanta, S. Jaiswal and S. K. Biswal, *Eur. Phys. J. Plus* **129**, 48 (2014).
21. P. Jain, P. K. Sahoo and B. Mishra, *Int. J. Theor. Phys.* **51**, 2546 (2012).
22. A. T. J. Hayward, *Br. J. Appl. Phys.* **18**, 965 (1967).
23. G. Lyra, *Math. Z.* **54**, 52 (1951).
24. D. K. Sen, *Z. Phys. A*: *Hadrons Nuclei* **149**, 311 (1957).
25. T. M. Karade and S. M. Borikar, *Gen. Relat. Gravit.* **9**, 431 (1978).
26. D. K. Sen and K. A. Dunn, *Math. Phys.* **12**, 578 (1971).
27. W. D. Halford, *Aust. J. Phys.* **23**, 863 (1970).
28. K. S. Bhamra, *Aust. J. Phys.* **27**, 541 (1974).

29. A. Beesham, *Astrophys. Space Sci.* **127**, 189 (1986).
30. G. Mohanty, K. L. Mahanta and R. R. Sahoo, *Astrophys. Space Sci.* **306**, 269 (2006).
31. D. D. Pawar, S. P. Shahare and V. J. Dagwal, *Mod. Phys. Lett. A* **33**, 1850011 (2018).
32. V. J. Dagwal and D. D. Pawar, *Int. J. Math. Arch.* **9**, 120 (2018).
33. C. Aktaş, S. Aygün and I. Yılmaz, *Phys. Lett. B* **707**, 237 (2012).
34. C. Aktaş, S. Aygün and P. K. Sahoo, *Mod. Phys. Lett. A* **33**, 1850135 (2018).
35. S. K. Sahu, T. T. Tole and M. Balcha, *Indian J. Phys.* **92**, 813 (2018).
36. C. Aktaş, *Mod. Phys. Lett. A* **34**, 1950066 (2019).
37. S. Aygün, C. Aktaş and I. Yılmaz, *J. Geom. Phys.* **62**, 100 (2012).
38. İ. Yılmaz, H. Baysal and C. Aktaş, *Gen. Relat. Gravit.* **44**, 2313 (2012).
39. V. J. Dagwal and D. D. Pawar, *Mod. Phys. Lett. A* **35**, 1950357 (2020).
40. V. J. Dagwal and D. D. Pawar, *Indian J. Phys.*, doi:10.1007/s12648-020-01691-w.
41. Abdussattar and S. R. Prajapati, *Astrophys. Space Sci.* **332**, 455 (2011).
42. B. K. Bishi, S. K. J. Pacif, P. K. Sahoo and G. P. Singh, *Int. J. Geom. Methods Mod. Phys.* **14**, 1750158 (2017).
43. Y. S. Solanke, D. D. Pawar and V. J. Dagwal, arXiv:1607.01234v2.
44. K. S. Thorne, *Astrophys. J.* **148**, 51 (1967).
45. C. B. Collins, E. N. Glass and D. A. Wilkinson, *Gen. Relat. Gravit.* **12**, 805 (1980).
46. S. K. J. Pacif, Md. S. Khan, L. K. Paikroy and S. Singh, *Mod. Phys. Lett. A* **35**, 2050011 (2020).
47. M. A. H. MacCallum, *Commun. Math. Phys.* **20**, 57 (1971).
48. P. K. Sahoo, P. Sahoo, B. K. Bishi and S. Aygün, *Mod. Phys. Lett. A* **32**, 1750105 (2017).
49. V. J. Dagwal, *Can. J. Phys.*, doi:10.1139/cjp-2019-0226.
50. L. Herrera, A. Di Prisco, J. Ibáñez and J. Carot, *Phys. Rev. D* **86**, 044003 (2012).
51. R. Kantowski and R. K. Sachs, *J. Math. Phys.* **7**, 433 (1966).
52. M. Sharif and A. Majid, *Astrophys. Space Sci.* **348**, 583 (2013).
53. Z. Yousaf, *Eur. Phys. J. Plus* **132**, 276 (2017).
54. Z. Yousaf, *Eur. Phys. J. Plus* **132**, 71 (2017).


11:07 PM
ugccare.unipune.ac.in/App
University Grants Commission
Consortium for Academic and Research Ethics (UGC-CARE)
Home
About
UGC-CARE List
Feedback
FAQ
Resources
Contact
Logout
UGC-CARE List
UGC-CARE List Group I
Journals found qualified through UGC-CARE protocols.
Search
Alert
UGC-Cell for Journal Analysis, Centre for Publication Ethics (CPE) at Savitribai Phule Pune University(SPPU), Pune, has been notified of cloned and online versions of print-only, authentic Journals on its UGC-CARE List. The ISSN, title, logo etc have been cloned. Scholars are cautioned against such cloned versions of Journals on the UGC-CARE List, and are requested to verify with the CPE whenever they are in doubt about the veracity of any Journal. We also request that news of such cloned Journals be reported to the CPE at the earliest.
UGC, UGC-CARE and CPE bear no responsibility for consequences that may arise from researchers publishing in cloned journals.
Journals found to be involved in unethical practices will be removed immediately.
UGC-CARE List Group II
Journals indexed in globally recognised databases.
These journals are part of UGC-CARE List as Group II and searchable through following links.
Web of Science
1. Arts & Humanities Citation Index
2. Science Citation Index Expanded
3. Social Sciences Citation Index
Scopus
1. Scopus Source List
MLA
Note
Those journals from the Directory of Periodicals by the Modern Language Association that have qualified in accordance with UGC-CARE protocols are included in UGC-CARE Group II. Please note that many MLA journals are already indexed in Scopus/ Web of Knowledge databases, and these have not been separately analysed.
Directory of Periodicals by the Modern Language Association
Note
The journals which are discontinued/ inactive from above databases will not find a place in Group II of the UGC CARE List.


11:11 PM
ugccare.unipune.ac.in/App

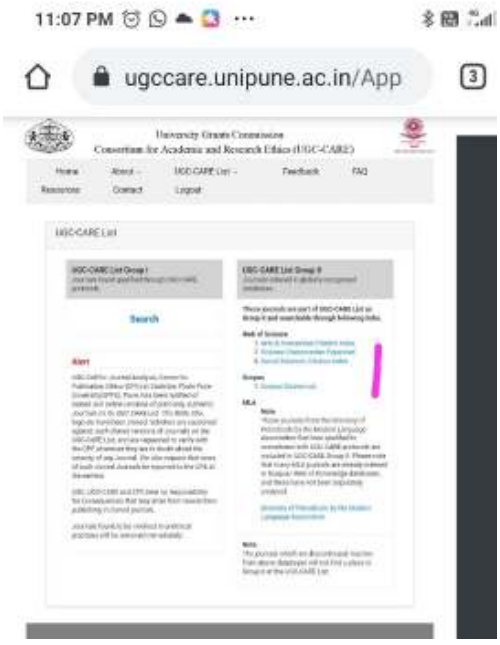
11:07 PM
ugccare.unipune.ac.in/App
University Grants Commission
Consortium for Academic and Research Ethics (UGC-CARE)
Home
About
UGC-CARE List
Feedback
FAQ
Resources
Contact
Logout
UGC-CARE List
Search

Indian J Phys
https://doi.org/10.1007/s12648-020-01795-3

ORIGINAL PAPER

Anisotropic plane symmetric model with massless scalar field

D D Pawar[1], S P Shahare[2]*, Y S Solanke[3] and V J Dagwal[4]

[1]School of Mathematical Sciences, S.R.T.M. University, Nanded, Maharashtra 431606, India

[2]P. R. Pote (Patil) College of Engineering and Management, Amravati, Maharashtra 444604, India

[3]Mungsaji Maharaj Mahavidyalaya, Darwha, Yavatmal, India

[4]Government College of Engineering, Nagpur, Maharashtra, India

Received: 03 January 2019 / Accepted: 24 January 2020

Abstract: This paper deals with the study of tilted plane symmetric cosmological model in the presence of perfect fluid, heat conduction and massless scalar field. We investigate the analytical solution of field equations by imposing power law relation between the metric potentials as well as the equation of state $p = \omega\rho$, $0 \leq \omega \leq 1$. Also, some physical and kinematic parameters of the model are discussed.

Keywords: Tilted model; Plane symmetric; Perfect fluid; Massless scalar field

1. Introduction

In 1920s Albert Einstein and Alexander A. Friedmann proposed a theoretical framework based on general relativity, which is one of the strongest pillars of hot Big Bang theory. It is well known that Einstein's general theory of relativity is the most successful theory of gravitation, used to construct the cosmological models of the universe. Our present understanding of the universe is based upon this hot Big Bang theory, which explains its evolution from the early stage to present stage of the universe. In fact, expansion of the universe, the relative abundance of light elements and the cosmic microwave background (CMB) have helped to establish the hot Big Bang as the preferred model of the universe. Recent modern cosmological observations of Riess et al. [1, 2] and Perlmutter et al. [3] from type Ia Supernovae (SNela) point out that our universe is going through accelerated expansion phase. The intriguing evidence for this is obtained with the support of Bennett et al. [4] and Tegmark et al. [5]. This accelerated expansion of the universe causes due to dark energy which is not yet understood. On the large scales, the universe has a flat geometry and this flatness occurs due to matter present in the universe. But there is neither sufficient ordinary matter nor dark matter in the universe to produce this flatness. Hence, the difference must be attributed to the component with negative pressure which is called a dark energy which composes with □ 3/4 of the critical density. This dark energy causes the accelerated expansion of the universe. The Wilkinson Microwave Anisotropy Probe (WMAP) satellite made precision measurements of CMB fluctuations from which researchers were able to determine several cosmological parameters such as density of the ordinary matter and dark matter, Hubble constant, age of the universe and cosmological constant. Also, WMAP experiment suggested that 73% content of the universe is in the form of dark energy, 23% in the form of non-baryonic dark matter and the rest 4% in the form of the ordinary baryonic matter as well as radiation.

We considered the plane symmetric cosmological model. In recent years, there has been a considerable interest in investigating the plane symmetric cosmologies in spite of spherical symmetry since it plays vital role in understanding inhomogeneities of theoretical cosmology. Inhomogeneous plane symmetric model has been studied by Taub [6, 7], Szekeres [8], Tomimura [9], Singh and Ram [10] and Taruya and Nambu [11]. Plane symmetric model with vacuum and Zel'dovich fluid has been obtained by Mohanty et al. [12]. Pradhan [13] and Venkateswarlu et al. [14] presented inhomogeneous anisotropic non-static plane symmetric model. Also, Mishra [15] has studied the

*Corresponding author, E-mail: sarikashahare83@gmail.com; pawar@yahoo.com; yadaosolanke@gmail.com; vdagwal@gmail.com

Published online: 15 July 2020

effect of vacuum inhomogeneous plane symmetric space time on the evolution of the universe. Pawar et al. [16] investigated plane symmetric model with disordered radiation. Sahoo and Mishra [17] obtained solutions for plane symmetric model with quark matter with the help of Rosen's theory. Recently, Pawar and Agrawal [18] presented homogeneous plane symmetric model in $f(R, T)$ theory with the quark and strange quark matter.

After the development of inflationary model, Linde [19] has discussed the importance of scalar field (mesons) in cosmology. One of the interacting fields is a massless scalar field. From the last few decades, a considerable interest has been focused on the cosmological models with massless scalar field coupled to the gravitational field. Bergmann and Leipnik [20] and Bramhachary [21] have developed the massless scalar field with spherically symmetric gravitational fields. Buchdahl [22], Gautreau [23], Stephenson [24], Rao [25], Singh [26] and Chatterjee and Roy [27] obtained solutions of field equations with massless scalar field (meson field) in the framework of general relativity. The gravitational repulsion in the Einstein's theory with massless scalar field has been investigated by Krori et al. [28]. He noticed that gravitational repulsion is possible for particle velocities lower than those required in the Schwarzchild field in the presence of scalar field. According to Santilli [29], the massless scalar field is basically an attempt to look into yet unsolved problem of unification of gravitational and quantum theories. Further study of massless scalar field has been done by Reddy [30], Pradhan [31], Panigrahi [32] and Katore [33]. Inflationary universe scenario with constant deceleration parameter in the presence of massless scalar field and flat potential taking Bianchi type VI_0 space time as a source is discussed by Bali and Kumari [34]. The massless scalar field acquired a particular importance due to the suggestion given by Weinberg and Wilkzek [35, 36]—there should exist axion (pseudo-scalar) of negligible mass. This idea of axion is further supported by the work of Peccei and Quinn [37].

In the present work, we study tilted cosmological model in the presence of perfect fluid, heat conduction with massless scalar field. King and Ellis [38], Ellis and King [39] and Collins and Ellis [40] have bowed the seed of tilted cosmological models. Particularly, homogeneous cosmological model is said to be tilted if the fluid flow velocity vector is not orthogonal to the group orbits; otherwise, the model is said to be non-tilted. Tilted Bianchi type I model with electromagnetic field has been discussed by Dunn and Tupper [41], Lorenz [42]. Mukherjee [43], Bali and Meena [44], Coley [45] and Pradhan [46] studied tilted cosmological models. Tilted plane symmetric cosmological model with heat conduction and disordered radiation has been discussed by Pawar et al. [47]. Pawar and Dagwal [48, 49] presented tilted two fluid cosmological model in general relativity and Kantowski–Sachs cosmological model in scalar tensortheory of gravitation. Sahu [50, 51] obtained tilted Bianchi type I cosmological model with mesonic stiff fluid and Lyra geometry. Pawar et al. [52] investigated tilted plane symmetric model in the presence of magnetic field with dust fluid. Tilted cosmological model in $f(R, T)$ theory of gravitation has been investigated by Pawar and Dagwal [53]. Recently, Pawar and Shahare [54–56] investigated some tilted cosmological models in presence of perfect fluid.

The present model is characterized by the equation of state (EoS) $p = \omega\rho,\ 0 \leq \omega \leq 1$ by considering some cases. In general relativity, the evolution of the expansion rate is parameterized by the cosmological equation of state (EoS). It is the relation between temperature, pressure, and combined matter, energy and vacuum energy density for any region of space. It plays important role in observational cosmology today. Aÿgun et al. [57] have investigated the cosmological model with the help of equation of states (EOS). We focused our attention to study the tilted plane symmetric homogeneous and anisotropic cosmological model in the presence of perfect fluid, heat conduction and zero-mass scalar field. Physical and kinematical solutions of the field equations are obtained for the applications in cosmology and astrophysics. Homogeneous and anisotropic cosmological models have been studied widely in the framework of general relativity in the search of realistic picture of the universe. The purpose of this paper is to study the effect of tilted congruence of the model. To get the deterministic model, we have used two basic assumptions: (1) equation of state (EoS) and (2) the power law relation between the metric potentials A and B. We also studied the behavior of some physical and geometrical parameters. This paper is organized as follows: Sect. 2 presents the metric and field equations, Sect. 3 provides the solutions of the field equations, Sect. 4 discusses the distance modulus, Sect. 5 presents the results and discussion, and Sect. 6 gives the conclusion.

2. Metric and field equations

We consider the plane symmetric metric in the form

$$ds^2 = -dt^2 + A^2(t)\left(dx^2 + dy^2\right) + B^2(t)dz^2 \tag{1}$$

The field equations determine the values of the components of the metric of a space time for some known content. Once the metric is known, one can begin to compute geodesics in the space time: these are the paths that bundles of light rays travel along or the orbits that planets trace out. This enables GR, as a gravitational theory, to predict directly observable quantities. This also applies to the entire universe: Einstein's field equations

allow the metric for the entire universe to be computed once the content of the universe is known. The Einstein's field equations in the presence of perfect fluid, heat conduction and zero-mass scalar field are given by

$$R_i^j - \frac{1}{2}Rg_i^j = -8\pi\left({}^{P}T_i^j + {}^{v}T_i^j\right) \tag{2}$$

where

$${}^{P}T_i^j = (p+\rho)u_i u^j + pg_i^j + q_i u^j + u_i q^j \tag{3}$$

is the energy momentum tensor for perfect fluid with heat conduction together with

$$g_{ij}u^i u^j = -1, \tag{4}$$

$$q_i q^j > 0 \text{ and } q_i u^i = 0. \tag{5}$$

where p is the pressure, ρ is the energy density, q_i is the heat conduction vector orthogonal to u^i. The fluid flow vector u^i has the components $\left(0, 0, \frac{\sinh\alpha}{B}, \cosh\alpha\right)$ satisfying Eq. (5) and α is the tilt angle.

Further, the stress tensor corresponding to massless scalar field ${}^{v}T_i^j$ is given by

$${}^{v}T_i^j = \frac{1}{4\pi}\left(U_i U^j - \frac{1}{2}g_i^j U_a U^a\right) \tag{6}$$

The Klein–Gordon equation corresponding to the scalar field U is given by

$$g^{ij}U_{;ij} = 0 \tag{7}$$

The field equations of metric (1) reduce to

$$\frac{A_{44}}{A} + \frac{B_{44}}{B} + \frac{A_4}{A}\frac{B_4}{B} = -8\pi p - U_4^2, \tag{8}$$

$$\left(\frac{A_4}{A}\right)^2 + 2\frac{A_{44}}{A} = -8\pi\left[(p+\rho)\sinh^2\alpha + p + 2q_3\frac{\sinh\alpha}{B} + \frac{1}{8\pi}U_4^2\right], \tag{9}$$

$$\left(\frac{A_4}{A}\right)^2 + 2\frac{A_4}{A}\frac{B_4}{B} = -8\pi\left[-(p+\rho)\cosh^2\alpha + p - 2q_3\frac{\sinh\alpha}{B} - \frac{1}{8\pi}U_4^2\right], \tag{10}$$

$$-8\pi\left[(p+\rho)B\sinh\alpha\cosh\alpha + q_3\cosh\alpha + q_3\frac{\sinh^2\alpha}{\cosh\alpha}\right] = 0, \tag{11}$$

$$U_{44} + U_4\left[\log\left(A^2B\right)\right]_{,4} = 0. \tag{12}$$

where suffix 4 after field variable denotes ordinary differentiation with respect to cosmic time t.

For the plane symmetric cosmological model, the average scale factor R and the spatial volume V are given by

$$R(t) = \left(A^2B\right)^{\frac{1}{3}} \tag{13}$$

$$V = R^3 = A^2B \tag{14}$$

The directional mean Hubble's parameter for this model is given by

$$H = \frac{R_4}{R} = \frac{1}{3}(H_1 + H_2 + H_3). \tag{15}$$

where H_1, H_2 and H_3 are the directional Hubble's parameters in the directions of x, y and z axes, respectively.

The anisotropic expansion parameter A_m for the universe is defined as

$$A_m = \frac{1}{3}\sum_{i=1}^{3}\left(\frac{\Delta H_i}{H}\right)^2, \quad \text{where } \Delta H_i = H_i - H \tag{16}$$

This anisotropic parameter can be used to examine whether the universe expands anisotropically or isotropically. The universe expands anisotropically for nonzero value of anisotropic parameter, and that of it expands isotropically if $A_m = 0$.

The deceleration parameter is given by

$$q = -\frac{RR_{44}}{R_4^2} = \frac{\mathrm{d}}{\mathrm{d}t}\left(\frac{1}{H}\right) - 1 \tag{17}$$

Also, the expansion scalar Θ and the shear scalar σ are given by

$$\Theta = 3H = 2\frac{A_4}{A} + \frac{B_4}{B} \tag{18}$$

$$\sigma^2 = \frac{1}{2}\left(\sum_{i=1}^{3}H_i^2 - 3H^2\right) \tag{19}$$

3. Cosmological solutions

In order to obtain explicit solution of field equations (8)–(12), which are highly nonlinear differential equations in seven unknowns, namely B, U, p, ρ, α and q_3, we have imposed two extra constraints:

(a) Equation of state (EOS). In principle, there is no compelling reason for this choice.

$$p = \omega\rho, \quad 0 \le \omega \le 1. \tag{20}$$

This gives rise to the following cases:

(1) For mesonic fluid, $\omega = 0$.
(2) For a stiff fluid or Zel'dovich fluid, we have $\omega = 1$.
(3) For a radiation dominated solution, we have $\omega = \frac{1}{3}$.

(b) The power law relation between metric potentials A and B is

$$B = A^n, \quad \text{where } n \neq 1 \text{ is constant.} \tag{21}$$

Using Eqs. (20) and (21) in Eq. (8) gives

$$-8\pi p = (n+1)\frac{A_{44}}{A} + n^2\left(\frac{A_4}{A}\right)^2 + U_4^2 \tag{22}$$

$$-8\pi\rho = \frac{1}{\omega}\left[(n+1)\frac{A_{44}}{A} + n^2\left(\frac{A_4}{A}\right)^2 + U_4^2\right]. \tag{23}$$

From Eq. (12), scalar field U is given by

$$U_4 = \frac{C}{A^2 B} \tag{24}$$

The directional mean Hubble's parameter for this model is given by

$$H = \frac{1}{3}\left(2\frac{A_4}{A} + \frac{B_4}{B}\right). \tag{25}$$

where the directional Hubble's parameters along directions of x, y and z axes, respectively, are given by

$$H_1 = \frac{A_4}{A}, \quad H_2 = \frac{A_4}{A}, \quad H_3 = \frac{B_4}{B}. \tag{26}$$

The anisotropic expansion parameter A_m for the universe is given by

$$A_m = 2\left(\frac{n-1}{n+2}\right)^2, \quad \text{where } n \neq 1,\ n \neq -2 \tag{27}$$

The present value of anisotropic expansion parameter A_m nearly matches with that of value obtained by Rao and Prasanthi [58], Sahoo et al. [59] and Mishra et al. [60].

Also, the expansion scalar Θ and the shear scalar σ are given by

$$\Theta = 3H = 2\frac{A_4}{A} + \frac{B_4}{B} \tag{28}$$

$$\sigma^2 = \frac{1}{3}(n-1)^2, \quad \text{where } n \neq 1 \tag{29}$$

From Eq. (27) and (29), it is observed that values of anisotropic expansion parameter A_m and shear scalar σ are independent of ω and hence remain the same in all the cases.

The heat conduction vectors are

$$q_1 = q_2 = 0,$$
$$q_3 = \frac{-(\omega+1)\rho A^n \sinh\alpha\cosh^2\alpha}{\cosh 2\alpha}, \tag{30}$$
$$q_4 = (\omega+1)\rho\sinh^2\alpha\cosh\alpha$$

Case I For mesonic fluid $\omega = 0$:

For mesonic fluid, solution of our model is as follows:

Solving field equations (8)–(12) with the help of (21) gives

$$A = T^m, \quad B = T^{mn} \tag{31}$$

where $T = c_1 t + c_2$, $m = \frac{n^2}{n+1} + 1$, $n \neq 1$. Also, c_1 and c_2 are constants of integrations.

$$V = T^{m(n+2)} \tag{32}$$

Also, from Eq. (24) scalar field U is

$$U = \frac{c_3 T^{1-(n+2)m}}{1-(n+2)m} \tag{33}$$

where c_3 is constant of integration.

Using Eqs. (22)–(23), (31)–(32) with $\omega = 0$, the pressure and energy density become

$$p = 0 \tag{34}$$

$$8\pi\rho = 2(n+1)\frac{c_3^2 m^2}{T^2} + \frac{2c_3^2 m(m-1)}{T^2} \tag{35}$$

The directional mean Hubble's parameter for this model is given by

$$H = \frac{mc_1}{3}\left(\frac{n+2}{T}\right). \tag{36}$$

where the directional Hubble's parameters are

$$H_1 = \frac{mc_1}{T}, \quad H_2 = \frac{mc_1}{T}, \quad H_3 = \frac{mnc_1}{T}. \tag{37}$$

The anisotropic expansion parameter A_m for the universe is given by

$$A_m = 2\left(\frac{n-1}{n+2}\right)^2, \quad \text{where } n \neq 1,\ n \neq 2 \tag{38}$$

Also, the expansion scalar Θ and the shear scalar σ are given by

$$\Theta = mc_1\left(\frac{n+2}{T}\right) \tag{39}$$

$$\sigma^2 = \frac{1}{3}(n-1)^2, \quad \text{where } n \neq 1 \tag{40}$$

The deceleration parameter q is

$$q = \frac{1-n}{n+2} \tag{41}$$

Tilted angle is

$$\cosh^2\alpha = \frac{n+1}{2n}, \quad \sinh^2\alpha = \frac{1-n}{2n} \tag{42}$$

The heat conduction vectors are

$$q_1 = q_2 = 0, \quad q_3 = \frac{-1}{8\pi}\left[2(n+1)\frac{c_3^2 m^2}{T^2} + \frac{2c_3^2 m(m-1)}{T^2}\right]$$
$$T^m\left(\frac{1+n}{2}\right)\sqrt{\frac{1-n}{2n}},$$

$$q_4 = \frac{1}{8\pi}\left[2(n+1)\frac{c_3^2m^2}{T^2} + \frac{2c_3^2m(m-1)}{T^2}\right]\left(\frac{1-n}{2n}\right)\sqrt{\frac{1+n}{2n}} \tag{43}$$

$$ds^2 = -dT^2 + T^{2m}\left(dx^2 + dy^2\right) + T^{2mn}dz^2 \tag{44}$$

Case II For a stiff fluid or Zel'dovich fluid, we have $\omega = 1$:

Equations (9), (10), (20) and (23) result in

$$\frac{A_{44}}{A_4} + (n+1)\frac{A_4}{A} = 0 \tag{45}$$

Integrating Eq. (45) gives

$$A = (k_1t + k_2)^{\frac{1}{n+2}} = T_1^{\frac{1}{n+2}},$$
$$B = (k_1t + k_2)^{\frac{n}{n+2}} = T_1^{\frac{n}{n+2}}. \tag{46}$$

where $T_1 = k_1t + k_2$.

The spatial volume is

$$V = T_1 \tag{47}$$

where k_1 and k_2 are constants of integration.

Scalar field U is

$$U = \frac{\log(k_1t + k_2)}{k_1} \tag{48}$$

Using Eqs. (22), (46)–(47) with $\omega = 1$, the pressure and energy density become

$$8\pi p = 8\pi\rho = \frac{1}{T_1^2}\left[\frac{k_1^2(1-2n)}{(n+2)^2} - C^2\right], \quad n \neq -2,\ n \neq 1 \tag{49}$$

The directional mean Hubble's parameter for this model is given by

$$H = \frac{mk_1}{3}\left(\frac{n+2}{T_1}\right). \tag{50}$$

where the directional Hubble's parameters are

$$H_1 = \frac{mk_1}{T_1}, \quad H_2 = \frac{mk_1}{T_1}, \quad H_3 = \frac{mnk_1}{T_1}. \tag{51}$$

The anisotropic expansion parameter A_m for the universe is given by

$$A_m = 2\left(\frac{n-1}{n+2}\right)^2, \quad \text{where } n \neq 1,\ n \neq 2 \tag{52}$$

Also, the expansion scalar Θ and the shear scalar σ are given by

$$\Theta = mk_1\left(\frac{n+2}{T_1}\right) \tag{53}$$

$$\sigma^2 = \frac{1}{3}(n-1)^2, \quad \text{where } n \neq 1 \tag{54}$$

The deceleration parameter q is

$$q = \frac{3(n+1)}{(n+2)(n^2+n+1)} - 1 \tag{55}$$

Tilted angle is

$$\cosh^2\alpha = 1,$$
$$\sinh^2\alpha = 0 \tag{56}$$

The heat conduction vectors are

$$q_1 = q_2 = q_3 = q_4 = 0 \tag{57}$$

$$ds^2 = -dT_1^2 + T_1^{\frac{2}{n+2}}\left(dx^2 + dy^2\right) + T_1^{\frac{2n}{n+2}}dz^2 \tag{58}$$

Case III For a radiation dominated solution, we have $\omega = \frac{1}{3}$:

For this case, Eqs. (9), (10), (21) and (24) result in

$$2A_{44} + 2\left(\frac{n^2+n+1}{n+2}\right)\frac{A_4^2}{A} = \frac{-2C^2}{(n+2)A^{2n+3}}$$

This equation can be written as

$$\frac{df^2}{dA} + \left(\frac{n^2+n+1}{n+2}\right)\frac{2}{A}f^2 = \frac{-2C^2}{(n+2)A^{2n+3}}. \tag{59}$$

where $A_4 = f(A), \quad A_{44} = f\frac{df}{dA}$

Equation (59) gives

$$f^2 = \left(\frac{dA}{dt}\right)^2 = \frac{C^2A^{-2n-2}}{2n+1} + d_1A^{-2\left(\frac{n^2+n+1}{n+2}\right)} \tag{60}$$

where d_1 is constant of integration.

For this solution metric (1) reduces to

$$ds^2 = -\left[\frac{C^2T_2^{-2n-2}}{2n+1} + d_1T_2^{-2\left(\frac{n^2+n+1}{n+2}\right)}\right]^{-1}dT_2^2 + T_2^2\left(dX^2 + dY^2\right) + T_2^{2n}dZ^2 \tag{61}$$

where $A = T_2,\ dx = dX,\ dy = dY,\ dz = dZ.$

So that $A = T_2,\ B = T_2^n.$ (62)

For this case, the spatial volume is

$$V = T_2^{n+2} \tag{63}$$

Using Eqs. (23)–(26) with $\omega = 1$, the pressure and energy density become

$$8\pi p = d_1\left(\frac{2n+1}{n+2}\right)T_2^{\frac{-2n^2-4n-6}{n+2}}, \quad n \neq -2 \tag{64}$$

$$8\pi\rho = 3d_1\left(\frac{2n+1}{n+2}\right)T_2^{\frac{-2n^2-4n-6}{n+2}},\ n \neq -2 \tag{65}$$

The directional mean Hubble's parameter for this model is given by

$$H = \frac{n+2}{3}\left(\frac{1}{T_2}\right). \tag{66}$$

where the directional Hubble's parameters are

$$H_1 = \frac{1}{T_2}, \quad H_2 = \frac{1}{T_2}, \quad H_3 = \frac{n}{T_2}. \tag{67}$$

The anisotropic expansion parameter A_m for the universe is given by

$$A_m = 2\left(\frac{n-1}{n+2}\right)^2, \quad \text{where } n \neq 1,\ n \neq 2 \tag{68}$$

Also, the expansion scalar Θ and the shear scalar σ are given by

$$\Theta = \frac{n+2}{T_2} \tag{69}$$

$$\sigma^2 = \frac{1}{3}(n-1)^2, \quad \text{where } n \neq 1 \tag{70}$$

The deceleration parameter$q$ is

$$q = \frac{1-n}{n+2},\ n \neq 1. \tag{71}$$

Tilted angle is

$$\cosh^2\alpha = \frac{n+3}{2(n+1)}, \quad \sinh^2\alpha = \frac{1-n}{2(n+1)}, \quad n \neq -1. \tag{72}$$

The heat conduction vectors are

$$q_1 = q_2 = q_4 = 0$$

$$q_3 = -\frac{1}{8\pi}\frac{(n+3)(2n+1)}{n+2}\sqrt{\frac{1-n}{2(n+1)}}T_2^{\frac{-n^2-2n-6}{n+2}} \tag{73}$$

4. Distance modulus

The direct evidence for the current acceleration of the universe is related to the observation of luminosity distances of high redshift supernovae [1–3]. The apparent magnitude ɱ of the source with an absolute magnitude M is related to the luminosity distance d_L. Distance modulus (μ) is the distance between apparent magnitude (ɱ) and absolute magnitude (M). It is the measure of distance to the object.

$$\mu(z) \equiv \text{ɱ} - M = 5log_{10}\left(\frac{d_L(z)}{Mpc}\right) + 25 \tag{74}$$

If redshift $z \ll 1$, then $H_0 d_L \approx z$

$$d_L = \frac{1+z}{H_0}\int_0^z \frac{dz'}{\sqrt{\Omega_{m0}(1+z')^3 + \Omega_{\Lambda 0}}}, \tag{75}$$

satisfying $\Omega_{m0} + \Omega_{\Lambda 0} = 1$, where Ω_{m0} and $\Omega_{\Lambda 0}$ are non-relativistic matter density and dark energy density, respectively (Tables 1, 2).

We can measure the apparent magnitude ɱ and the redshift z observationally; it depends upon the objects which we observe. In order to get a feeling of the phenomenon, we consider two supernovae: 1990O at low-redshift z=0.03 with ɱ=16.26 and 1997R at high redshift z =0.657 with m=23.83 [1, 2]. For $z \ll 1$, the luminosity distance is approximately given by $d_L(z) \approx z/H_0$. Using the apparent magnitude ɱ=16.26 of 1990O at z=0.03, the absolute magnitude is estimated as M=−19.28 from Eq. (74). Here, we adopted the value H_0^{-1}=2998 h^{-1} Mpc with h=0.70. Then, the luminosity distance of 1997R is obtained by substituting ɱ=23.83 and M=−19.15 in Eq. (74):

$$H_0 d_L \approx 0.92, \quad \text{for } z = 0.657. \tag{76}$$

Also, for ɱ=23.83 and M=−19.15,

$$H_0 d_L \approx 0.817, \quad \text{for } z = 0.656. \tag{77}$$

From Eq. (75) the theoretical estimate for the luminosity distance in a two-component flat universe is

$$H_0 d_L(z = 0.657) \approx 0.740, \quad \Omega_{m0} \approx 1 \tag{78}$$

$$H_0 d_L(z = 0.657) \approx 0.92, \quad \Omega_{m0} \approx 0.3, \quad \Omega_{\Lambda 0} \approx 0.7 \tag{79}$$

$$H_0 d_L(z = 0.656) \approx 0.817, \quad \Omega_{\Lambda 0} \approx 0.38 \tag{80}$$

In fact, two data points are not sufficient to conclude that the present cosmological expansion is accelerating and dark energy required. But by assuming a flat universe, Perlmutter et al. [3] found that about 70% of the energy density of the present universe consists of dark energy. Hence, dark energy is required to best fit the theoretical data and observational data (Fig. 1).

5. Results and discussion

Case I For mesonic fluid $\omega = 0$:

Recent astrophysical observations show that the observed value of deceleration parameter of the universe is in the range $-1 < q \leq 0$ which is $q_0 \approx -0.77$. In the present case for n=2.5, we have obtained $q_0 = -0.76$ which is consistent with respect to the observed value of DP of the universe at present epoch [61]. Here, $q < 0$ for $n > 1$; hence, our model is accelerating. For $0.6 \leq n < 1$, $\epsilon(-1, 0)$; also, for $n > 1$, $q < 0$ and hence our model is accelerating.

Table 1 Illustration of SNeIa apparent magnitude data at low-redshift $z \ll 1$

Name of SN	Redshift (z)	Apparent magnitude (m)	Luminosity distance ($H_0 d_L$)	Absolute magnitude (M)
1990O	0.03	16.26	0.03	−19.28
1992bg	0.036	16.66	0.036	−19.29

Table 2 Illustration of SNeIa apparent magnitude data at high redshift z, Perlmutter et al. [3]

Name of SN	Absolute magnitude (M)	Redshift (z)	Apparent magnitude (m)	Luminosity distance ($H_0 d_L$)
1997R	−19.15	0.657	23.83	0.92
1995ck	−19.15	0.656	23.57	0.817

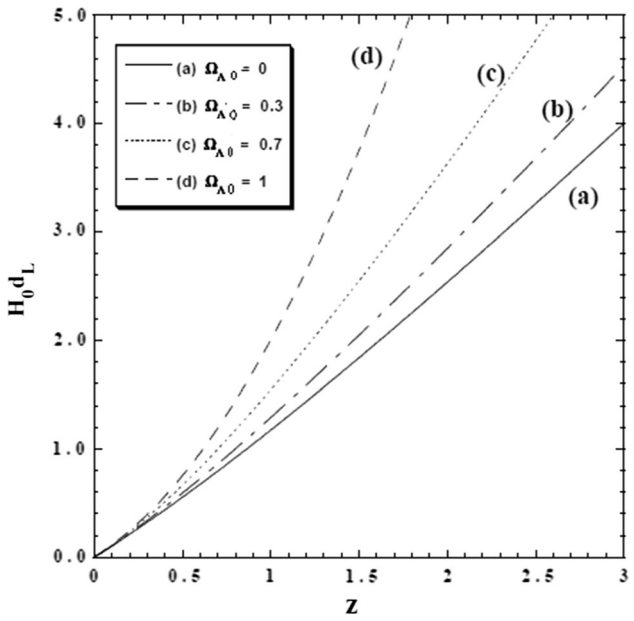

Fig. 1 Variation of $H_0 d_L$ against redshift z

Figure 2a and b shows the variation of energy density, Hubble parameter versus cosmic time t in an accelerating mode of the universe for different values of n=1.5, 1.6, 1.65 and $C_1 = 2.5$, $C_2 = 3.1$. It is observed that energy density and Hubble parameter are decreasing functions of cosmic time and they vanish for large value of T and become infinite at T=0. Also, it remains positive throughout the evolution of the universe. It starts with a positive value and approaches to zero as $T \to \infty$. Also, since $-1 < q \leq 0$, the present model represents accelerating universe. Hence, the universe starts evolving with big bang singularity at T=0. That's why the model obtained here is not only expanding but also accelerating which represents early stages of evolution of the universe which is in good agreement with recent observations.

Also, Fig. 3a and b shows variation of spatial volume V, expansion scalar Θ versus cosmic time. It is observed that the spatial volume increases with an increase in cosmic time. Also, $V \to 0$ as $T \to 0$ and $V \to \infty$ as $T \to \infty$, which show that the universe starts expanding with zero

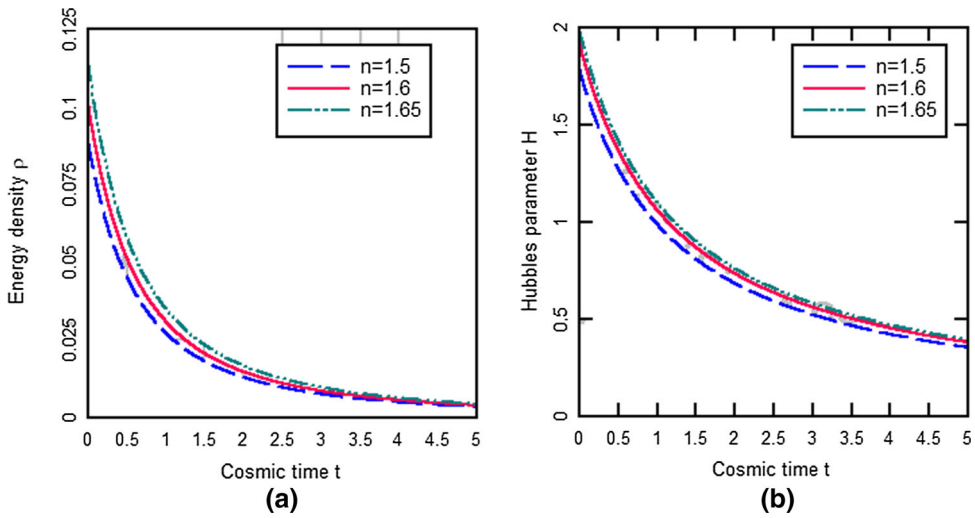

Fig. 2 Variation of energy density and variation of Hubble parameter against cosmic time for $C_1 = 2.5$, $C_2 = 3.1$ with varying $n = 1.5,\ 1.6,\ 1.65$

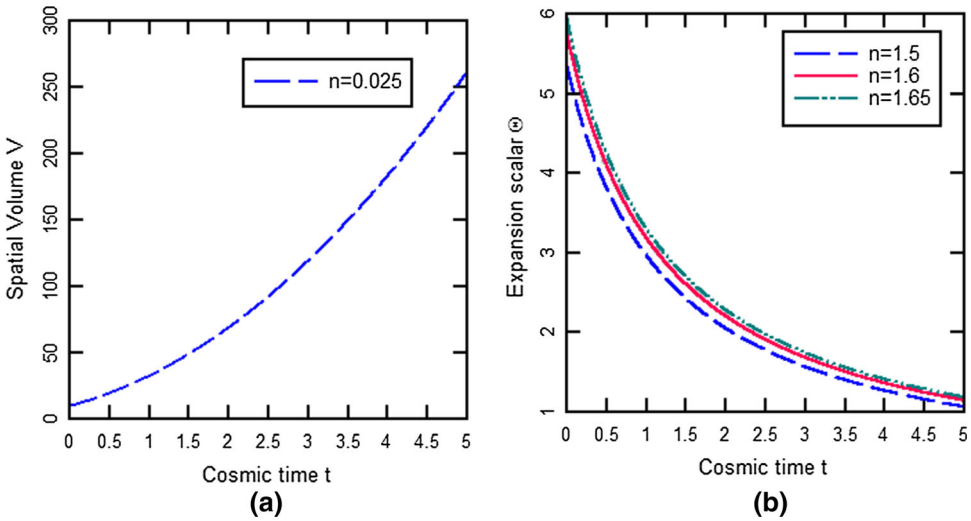

Fig. 3 Variation of spatial volume and variation of expansion scalar against cosmic time for $C_1 = 2.5,\ C_2 = 3.1$ with varying $n = 1.5,\ 1.6,\ 1.65$

volume and explode at infinite past. The expansion scalar is a decreasing function of cosmic time. It is observed that the expansion rate is faster at the beginning and becomes slow in the later stage. It starts with the positive value approaching to zero as $T \to \infty$. Tilted angle and heat conduction vector are functions of cosmic time.

Case II For a stiff fluid or Zel'dovich fluid, we have $\omega = 1$

In this case, the model (58) admits a singularity at $T_1 \to \infty$. Also, the metric potentials A and B tend to zero as $T_1 \to 0$ and hence the space time collapses at $T_1 \to 0$. It is observed from Eq. (48) that the massless scalar field U is a logarithmic function of cosmic time and hence Big Bang of the universe can be avoided by introducing scalar field U. The mean anisotropy parameter Am and shear scalar σ of the model are constant and same as that of previous case. Tilted angle is independent of cosmic time, and heat conduction vectors are zero. Figure 4a shows the variation of pressure (p) with respect to cosmic time for different values of n and it is observed that pressure decreases with an increase in cosmic time. Also, it remains positive throughout the evolution of the universe. Figure 4b depicts the variation of energy density (ρ) with respect to cosmic time for different values of n, and it is observed that energy density starts with a positive value and then decreases with an increase in cosmic time. Also, it is observed that for infinite value of T_1, pressure and energy density tend to zero. Figure 5a and b represents variation of Hubble parameter and expansion scalar versus cosmic time. We observed that Hubble parameter and expansion scalar are positive decreasing functions of cosmic time and they approaches to zero as $T_1 \to \infty$. Figure 6 depicts variation of the spatial volume against cosmic time. The universe starts its expansion with zero volume and expands exponentially with an increase in cosmic time and becomes infinite when $T_1 \to \infty$ which indicates that the present model starts expanding with big bang singularity at $T_1 \to 0$. In this case, the shear scalar and the mean anisotropy parameter A_m are constant throughout the evolution

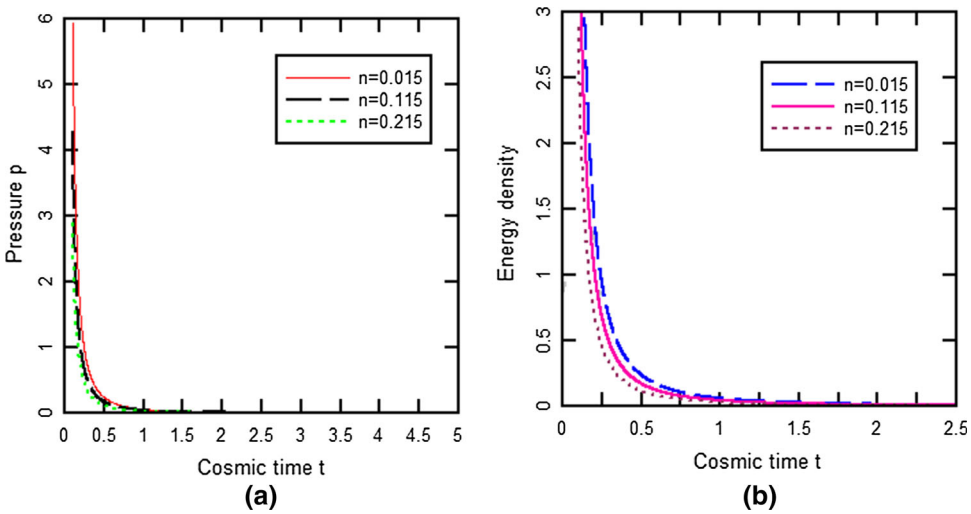

Fig. 4 Variation of pressure and energy density against cosmic time for $k_1 = 2.5,\ k_2 = 3.1,\ C = 0.012$ with varying $n = 0.015,\ 0.115,\ 0.215$

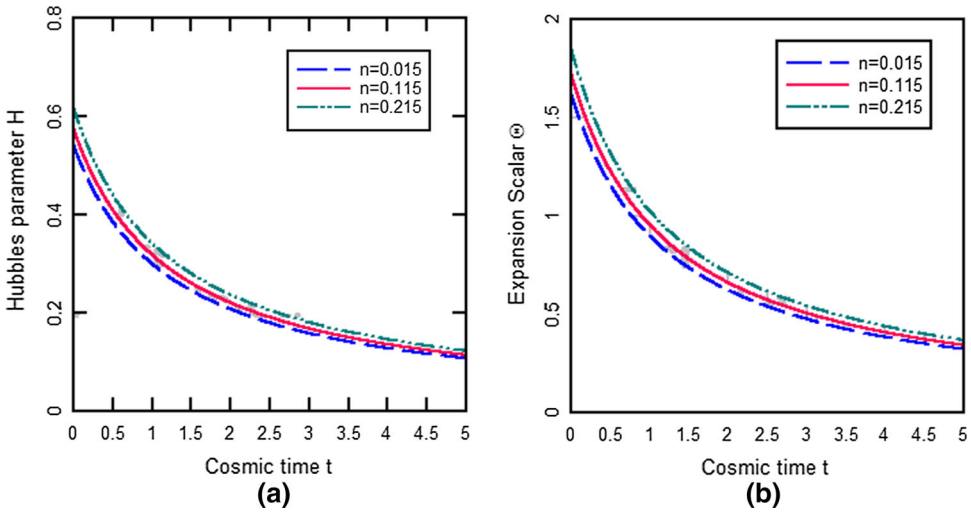

Fig. 5 Variation of Hubble parameter and variation of expansion scalar against cosmic time for $k_1 = 2.5,\ k_2 = 3.1,$ $C = 0.012$ with varying $n = 0.015,\ 0.115,\ 0.215$

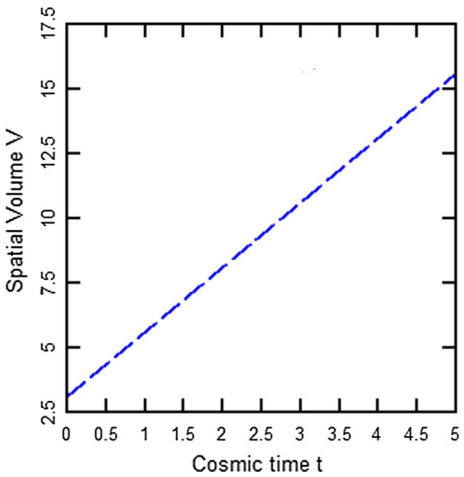

Fig. 6 Variation of Hubble parameter and variation of expansion scalar against cosmic time for $k_1 = 2.5,\ k_2 = 3.1,\ C = 0.012$

of the universe; however, these values are exactly same as the previous case.

Case III For a radiation dominated solution, we have $\omega = \frac{1}{3}$:

Equation (71) shows that the deceleration parameter $q < 0$. The metric potentials A and B tend to zero as T_2. The tilted angle is constant, and one of the heat conduction vectors is time dependent. In this case, it is observed that the spatial volume, pressure, energy density, mean generalized Hubble parameter, directional Hubble's and expansion scalar are functions of cosmic time. All these parameters tend to zero as cosmic time tends to infinity except the spatial volume. Tilted angle in all cases is independent of cosmic time. Figure 7a and b shows variation of pressure and energy density with respect to cosmic time for $d_1 = 2.5$ with varying $n = 2,\ 2.1,\ 2.2$. It is observed that both pressure and energy density are decreasing functions of cosmic time which tend to zero as $T_2 \to \infty$. Also, Fig. 8a and b depicts the variations of the Hubble parameter and the expansion scalar against the cosmic time. From these graphs, it is observed that Hubble parameter and the expansion scalar are decreasing positive valued functions of cosmic time. These two parameters tend to zero as $T_2 \to \infty$. Hence, in the present case, expansion in the model decreases with an increase in time and the expansion stops as $T_2 \to \infty$. Figure 9 depicts the variation of spatial volume. It is observed that spatial volume in the present case increases with an increase in cosmic time. Also, $V \to 0$ as $T_2 \to 0$; hence, the model obtained here starts expanding with zero volume and that of $V \to \infty$ as $T_2 \to \infty$, which shows that the present model is expanding with Big Bang singularity at $T_2 = 0$. This model does not approach to isotropy due to nonzero value of $\left(\frac{\sigma}{\Theta}\right)^2$ as $T_2 \to \infty$. The value of anisotropic parameter and shear scalar is same as that of previous two cases. Hence, the model obtained here is expanding, shearing with anisotropic universe. These results are compatible with the present observations; also, these results match with results obtained by Singh [62–64].

6. Conclusion

In this paper, we have studied the evolution of universe with heat conduction and massless scalar field filled with perfect fluid. For that we considered tilted plane symmetric cosmological model. We have obtained the general solution of the gravitational field equations with the help of power law relation between the metric potentials and EoS $p = \omega\rho,\ 0 \le \omega \le 1$. Also, some physical parameters of the model are discussed in three different cases.

From Figs. 3a, 6 and 9, it is observed that at the initial epoch the spatial volume V of the model is zero and it is increasing function of cosmic time. Also, V tends to infinity

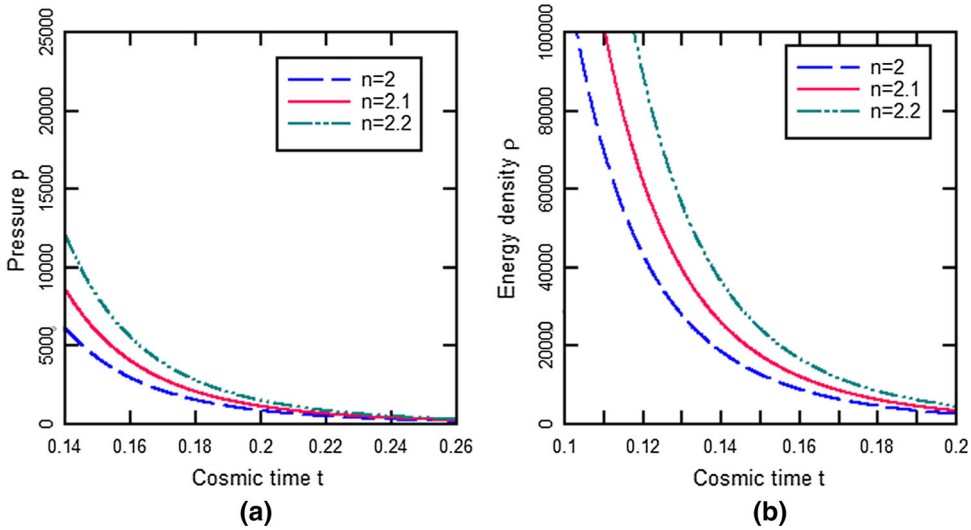

Fig. 7 Variation of pressure and variation of energy density against cosmic time for $d_1 = 2.5$ with varying $n = 2,\ 2.1,\ 2.2$

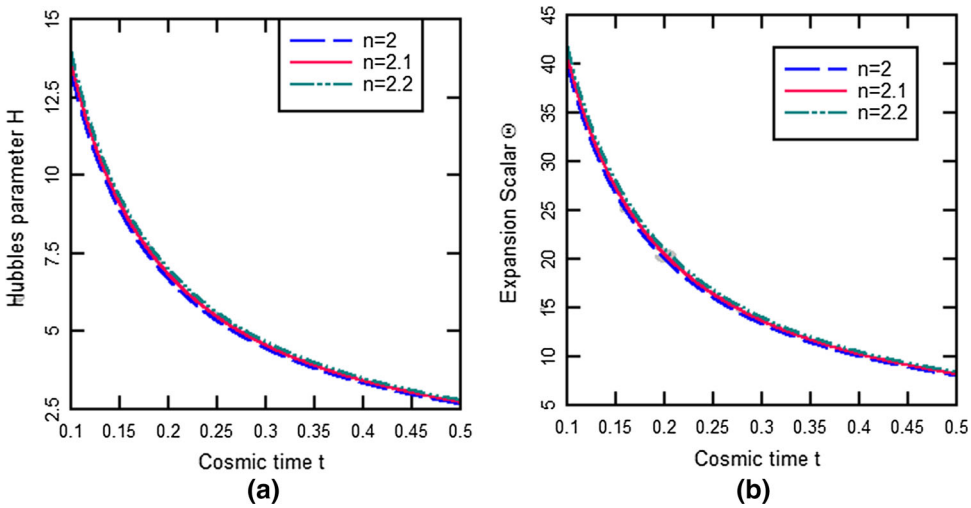

Fig. 8 Variation of Hubble parameter and variation of expansion scalar against cosmic time for $d_1 = 2.5$ with varying $n = 2,\ 2.1,\ 2.2$

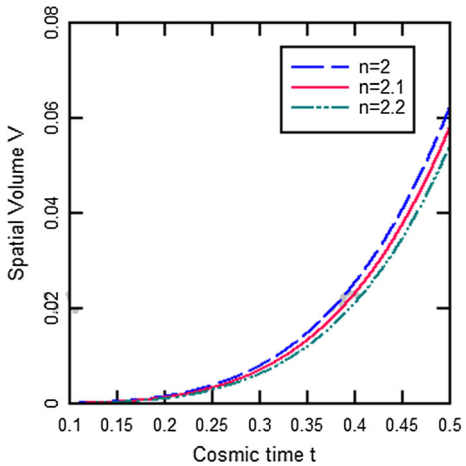

Fig. 9 Variation of spatial volume against cosmic time with varying $n = 2,\ 2.1,\ 2.2$

as time tends to infinity and hence the present model is expanding.

The Hubble parameter and the expansion scalar are two measure observational parameters in astrophysics and cosmology which help to analyze the rate of expansion of the universe as well as the fractional increase in the scale of the universe in unit time. In all the three cases, Hubble parameter and the expansion scalar are positive-valued decreasing functions of cosmic time. From Figs. 3b, 5b and 8b, it is seen that at the beginning expansion rate is faster and in the late stage this expansion rate slows down. In other words, the expansion in the model decreases with an increase in time and the expansion stops as time tends to infinity.

The interesting and remarkable observation of the present paper is that the mean anisotropy parameter Am and the shear scalar σ^2 in all the three cases of the model are same and constant throughout the evolution of the universe, having nonzero values. Hence, the model obtained here

with different deceleration parameters represents expanding, shearing and anisotropic universe. These results are compatible with the present observations; also, these results match with results obtained by Singh [62–64]. These models not approach to isotropy due to nonzero value of $\left(\frac{\sigma}{\Theta}\right)^2$ as cosmic time tends to infinity. Another remarkable observation made in the second case is that the massless scalar field U is a logarithmic function of cosmic time and hence Big Bang of the universe can be avoided by introducing scalar field U.

Recent astrophysical observations show that the observed value of deceleration parameter of the universe is in the range $-1 < q \leq 0$ which is $q_0 \approx -0.77$. In first two cases for n=2.5, we have obtained $q_0 = -0.76$ which is consistent with respect to the observed value of DP of the universe at the present epoch [61]. In these cases $q < 0$ for $n > 1$ and $q\epsilon(-1, 0)$ as $0.6 \leq n < 1$; also, for $n > 1, q < 0$. In the third case, $q < 0$ for $n > 1$. Hence, the models obtained here are not only expanding but also accelerating which represents early stages of evolution of the universe which is in good agreement with recent observations.

References

1. A G Riess, A V Filippenko, P Challis et al. *Astron. J.* **116** 1009 (1998)
2. A G Riess, A V Filippenko, P Challis et al. *Astron. J.* **117** 707 (1999)
3. S Perlmutter, G Aldering, G Goldhaber et al. *Astrophys. J.* **517** 565 (1999)
4. C L Bennett, M Halpern, G Hinshaw et al. *Astrophys. J. Suppl. Ser.* **148** 1 (2003)
5. M Tegmark, M A Strauss, M R Blanton et al. *Phys. Rev. D* **69** 103501 (2004)
6. A H Taub *Ann. Math.* **53** 472 (1951)
7. A H Taub *Phys. Rev.* **103** 454 (1956)
8. P Szekeres *Commun. Math. Phys.* **41** 55 (1975)
9. N Tomimura *Nuovo Cimento* B **44** 372 (1978)
10. J K Singh and S Ram *Astrophys. Space Sci.* **236**, 277 (1996)
11. A Taruya and Y Nambu *Prog. Theor. Phys.* **95** 295 (1996)
12. G Mohanty, B Mishra and R Das *Bull. Inst. Math. Acad. Sin. (ROC)* **28** 43 (2000)
13. A Pradhan and A K Vishwakarma *Int. J. Mod. Phys. D* **11** 1195 (2002)
14. R Venkateswarlu, S Janjeti and P Kakarlapati *Res. Astron. Astrophys*. **12** 63 (2012)
15. B Mishra *Commun. Phys*. **15** 229 (2005)
16. D D Pawar, S N Bayaskar and V R Patil *Bulg. J. Phys*. **36** 68 (2009)
17. P K Sahoo and B Mishra *J. Theor. Appl. Phys.* **7** 12 (2013)
18. P K Agrawal and D D Pawar *J. Astrophys. Astron.* **38** 2 (2017)
19. A Linde *Phys. Lett*. **108** 389 (1982)
20. O Bergmann and R Leipnik *Phys. Rev*. **107** 1157 (1957)
21. R L Bramhachary *Prog. Theor. Phys.* **23** 749 (1960)
22. H A Buchdahl *Phys. Rev*. **115** 1325 (1959)
23. R Gautreau *Nouv. Cim. B* **62** 360 (1969)
24. G Stephenson *Proc. Camb. Philos. Soc*. **58** 521 (1972)
25. J R Rao, A R Roy and R N Tiwari *Ann. Phys*. **69** 473 (1972)
26. T Singh *Gen. Rel. Gravity* **5** 657 (1974)
27. B Chatterjee and A R Roy *Acta Phys. Pol. B* **13** 385 (1982)
28. K D Krori, J C Sarmah and D Goswami *Can. J. Phys*. **62** 629 (1984)
29. R M Santilli *Found. Phys. Lett*. **10** 307 (1997)
30. D R K Reddy *Astrophys. Space Sci.* **140** 161 (1988)
31. A Pradhan, K L Tiwari and A Beesham *Ind. J. Pure Appl. Math* **32** 789 (2001)
32. U K Panigrahi and R C Sahu *Theor. Appl. Mech*. **30** 163 (2003)
33. S D Katore, A Y Shaikh, M M Sancheti and J L Pawade *Prespacetime J*. **3** 83 (2012)
34. R Bali and P Kumari *Adv. Astrophys.* **2** 67 (2017)
35. S Weinberg *Phys. Rev. Lett*. **40** 223 (1978)
36. F Wilczek *Phys. Rev. Lett.* **40** 279 (1978)
37. R D Peccei and H R Quinn *Phys. Rev. Lett.* **38** 1440 (1977)
38. A R King and G F R Ellis *Commun. Math. Phys*. **31** 209 (1973)
39. G F R Ellis and A R King *Comm. Maths. Phys*. **38** 119 (1974)
40. C B Collins and G F R Ellis *Phys. Rep*. **56** 65 (1979)
41. K A Dunn and B O J Tupper *Astrophys. J*. **235** 307(1980)
42. D Lorenz *Phys. Lett*. **83A** 155 (1981)
43. G Mukherjee *Astrophys. Astron. J*. **4** 295 (1983)
44. R Bali and B L Meena *Pramana J. Phys.* **62** 1007 (2004)
45. A A Coley, S Hervik and W C Lim arXiv:gr-qc/0605128v1 (2006)
46. A Pradhan and S K Shrivastava arXiv:gr-qc/0408043v3 (2008)
47. D D Pawar, S W Bhaware and A G Deshmukh *Rom. J. Phys*. **54** 187 (2009)
48. D D Pawar and V J Dagwal *Int. J. Theor. Phys* **53** 2441 (2014)
49. D D Pawar, V J Dagwal and S P Shahare *IOSR J. Math.* **12** 104 (2016) arXiv:1602.05223 [gr-qc]
50. S K Sahu and T Kumar *Int. J Theor. Phys* **52** 793 (2013)
51. S K Sahu *Int. J. Theor. Phys*. **50** 3368 (2011)
52. D D Pawar, V J Dagwal and Y S Solanke *Prespacetime J*. **5** 368 (2014)
53. D D Pawar and V J Dagwal *Aryabhatta J. Math. Inform.* **7** 17 (2015)
54. D D Pawar, S P Shahare and V J Dagwal *Mod. Phys. Lett. A* **33** 1850011 (2018). https://doi.org/10.1142/s0217732318500116
55. D D Pawar and S P Shahare *J. Astrophys. Astron.* **40**(4) 31(2019)
56. D D Pawar and S P Shahare *New Astron.* **75** 101318 (2020)
57. S Aÿgun, C Halife, C Aktas *Eur. Phys. J. Plus* **130**, 12 (2015)
58. V U M Rao, D U Y Prasanthi *Afr. Rev. Phys.* **11** 0001(2016)
59. P K Sahoo, P Sahoo, B K Bishi and S Aÿgun ĆarXiv:1707.00979v2 [gr-qc] (2017)
60. B Mishra, S K Tripathy and S Tarai arXiv:1803.05302v1 (physics. gen-ph) (2018)
61. C E Cunha, M Lima, H Ogaizu, J Frieman and H. Lin *Mon. Not. R. Astron. Soc.* **396** 2379 (2009)
62. C P Singh and S Kumar *Int. J. Mod. Phys. D* **15** 419 (2006)
63. C P Singh and S Kumar *Pramana J. Phys*. **68** 707 (2007)
64. C P Singh *Pramana J. Phys.* **72** 429 (2009)

International Journal of Geometric Methods in Modern Physics
Vol. 18, No. 4 (2021) 2150062 (27 pages)

DOI: 10.1142/S0219887821500626

World Scientific
www.worldscientific.com

Accelerating dark energy universe with LRS Bianchi type-I space-time

Y. S. Solanke*,§, D. D. Pawar†,¶ and V. J. Dagwal‡,‖

*Mungsaji Maharaj Mahavidyalaya, Darwha, Yavatmal 445202, India

†School of Mathematical Sciences, Swami Raman and Teerth Marathwada University, Vishnupuri Nanded 431 606, India

‡Department of Mathematics
Government College of Engineering, Nagpur 441 108, India

§yadaosolanke@gmail.com

¶dypawar@yahoo.com

‖vdagwal@gmail.com

Received 14 April 2020
Accepted 31 December 2020
Published 22 February 2021

The main purpose of this paper is to investigate LRS Bianchi type I metric in the presence of perfect fluid and dark energy. In order to obtain a deterministic solution of the field equations we have assumed that the two sources of the perfect fluid and dark energy interact minimally with separate conservation of their energy–momentum tensors as well EoS parameter of the perfect fluid is assumed to be constant. In addition to this we have used a special law of variation of Hubble parameter proposed by Berman that yields constant deceleration parameter. For the two different constant values of deceleration we have obtained two different cosmological models. The physical behaviors of both the models have been discussed by using MATLAB.

Keywords: LRS Bianchi type I models; perfect fluid and dark energy; EoS parameter.

1. Introduction

In the modern cosmology the numbers of recent astrophysical observational data suggest that the present universe is not only expanding but also accelerating and this accelerating phase of the universe is a recent phenomenon. Therefore, naturally it is to be assumed that dark energy was insignificant in early evolution of the universe while it has the dominant contribution at the present accelerating epoch [1–4]. These observations also suggest that a transition of the universe from earlier deceleration phase to the accelerated stage of universe can be due to the domination of dark energy over other kinds of matter. In order to study the universe, the cosmologists

‖Corresponding author.

have decided to obtain the large scale structure of the universe. In the formation of the large scale structure of the universe it should have decelerating expansion in early phase of matter era. Thus the formation of structure in the universe is supported by decelerating model, also model should have decelerating as well as accelerating phase of universe to give a precise form for this reasoning [5–7]. The simplest expanding cosmological models are those which are spatially homogeneous and isotropic. The evolution of isotropic cosmological models filled with perfect fluid dark energy has been extensively studied by many researchers. As it is predicted that the cosmic accelerated expansion of the universe is due to some kind of matter with negative pressure called the dark energy. The experimental observations such as cosmic microwave background radiation and large scale structure provide an indirect proof for the late time accelerated expansion of the universe [8–10]. The numbers of models have been studied by considering ordinary matter as a perfect fluid in the universe, but it is not sufficient to describe the dynamics of an accelerating phase of universe. This problem motivates the researchers to consider the models of the universe filled with dark energy along with perfect fluid [11–14]. In order to explain why the cosmic accelerated expansion of the universe happens, many candidates have been proposed. The cosmological constant is the prime candidate for dark energy even though having two well-known problems such as the fine tuning and cosmic coincidence. The alternative candidates for the dark energy are dynamical dark energy scenario. The quintessence, k-essence, chaplygin gas models, tachyon field, phantom field are some of the examples of dynamical dark energy models [15–18].

The observational data exhibit that our current Universe has an accelerated expansion. The concept of dark energy is used to define an accelerated expansion of the Universe proposed by Einstein's general relativity. This model successfully describes the current acceleration of the universe, and fits fine with observational data [45, 46]. The cosmological models with unbalanced matter equation of state in the class of equation $\omega = \frac{p}{\rho}$ are used, where p is the fluid pressure and ρ its energy density. As it is well known that the vacuum energy for which $\omega = -1$, mathematically equivalent to the cosmological constant $\wedge$ is one of the most prominent candidates used by the cosmologists to explain the dark energy component of the universe [9, 47, 48]. The dark energy represented by minimally coupled scalar fields called quintessence for which $\omega > -1$ [49, 50], and phantom energy for which $\omega < -1$ [5, 51]. The equation of state parameter is represented by stiff fluid era $\omega = 1$, the radiation dominated era $\omega = -1/3$, matter dominated era $\omega = 0$, transition era $\omega = -1/3$ and DE dominated era $\omega = -1$ [52, 53]. There are two methods used to describe this accelerated expansion of the universe. First method is the dark energy, in the framework of general relativity and second method is to modify the gravitational theory. The researchers Odintsov *et al.* [54], Harko *et al.* [55], Wu and Yu [56], Myrzakulov [57] and Li *et al.* [58] have investigated several modified theories of gravity such as $f(R)$ theory of gravity, $f(R,T)$ theory of gravity, $f(T)$ theory of gravity, $f(G)$ theory of gravity, etc.

In this paper, we have studied LRS Bianchi type model in the presence of perfect fluid and dark energy with variable EoS parameter for DE component whereas EoS parameter for perfect fluid is assumed to be constant. In order to obtain the exact solution of Einstein's field equations we have assumed a special law of variation of Hubble's parameter that yields constant parameter. We have obtained two different cosmological models by using two different explicit forms of scale factors depending on the value of constant decelerating parameters. The paper is organized as follows. In Sec. 2, the metric and the field equations are presented. In Sec. 3, an exact solution of the field is obtained to get two different models for $n = 0$ and $n \neq 0$. In Sec. 4, exponential expansion model I for $n = 0$ is derived. In Sec. 4.1, geometrical behavior of the model I for $n = 0$ is discussed and in Sec. 4.2 some more physical parameters are also discussed. In Sec. 5, power expansion model II for $n \neq 0$ is derived. In Sec. 5.1, geometrical behavior of the model II for $n \neq 0$ is discussed and in Sec. 5.2 some more physical parameters are also discussed. In Sec. 6, results and discussion are presented. Finally, we have concluded the opinion about the models in Sec. 7.

2. Metric and the Field Equations

We consider LRS Bianchi type I metric [19–23] in the form given by

$$ds^2 = -dt^2 + A^2(t)\left\{dx^2 + dy^2 + \left(1 + \beta \int \frac{dt}{A^3}\right)^2 dz^2\right\}, \tag{1}$$

where $A(t)$is a metric potential being a function of cosmic time t and β is positive constant.

We have selected metric (Eq. (1)) because this is one of the simplest models of an anisotropic universe which is homogeneous and spatially flat. If we consider$\beta = 0$, the metric (Eq. (1)) reduces to the Friedmann models with space-sections.

LRS Bianchi type-I metric is the spatially homogeneous and anisotropic flat universe. FRW universe has the equivalent scale factor for each of the three spatial directions whereas LRS Bianchi type-I metric has dissimilar scale factors. The singularity of LRS Bianchi type-I metric behaves like Kasnser metric. It has been studied that a metric filled with matter, the early anisotropy in LRS Bianchi type-I metric speedily expires away and evolves into a FRW universe. It has simple mathematical form and motivating because of the capability to clarify the cosmic evolution of the early universe. Due to its prominence, several authors have explored LRS Bianchi type-I metric from different aspects.

An anisotropic cosmological model plays an important role in the large scale structure of the Universe. The various researchers studying on cosmology by using relativistic cosmological models have not given proper details of explanation to believe in a regular expansion of the early stages of the Universe. At the present state of evolution, the Universe is spherically symmetric and the matter dispersal in it is on the whole isotropic and homogeneous. But at the beginning stages of

evolution, it could not have such a smoothed out picture because near the big bang singularity neither the supposition of spherical symmetry nor of isotropy can be strictly valid. Anisotropy of the cosmic expansion is an important quantity because it is supposed to be damped out in the course of cosmic evolution but the recent experimental data and critical arguments support the existence of an anisotropic phase of the cosmic expansion that approaches an isotropic one. Therefore it makes sense to consider models of the Universe with an anisotropic background.

In natural units ($8\pi G = 1, c = 1$), the Einstein field equations in case of a mixture of perfect fluid and dark energy components are given by

$$G_{ij} = R_{ij} - \frac{1}{2} g_{ij} R = -T_{ij}, \tag{2}$$

where $T_{ij} = T_{ij}^{(m)} + T_{ij}^{(de)}$ is the overall energy–momentum tensor with $T_{ij}^{(m)}$ as the energy–momentum tensors of the ordinary matter (perfect fluid) and $T_{ij}^{(de)}$ as the energy–momentum tensors of the dark energy components which are, respectively, given by

$$T_j^{(m)i} = \text{diag}[-\rho^{(m)}, p^{(m)}, p^{(m)}, p^{(m)}] = \text{diag}[-1, \omega^{(m)}, \omega^{(m)}, \omega^{(m)}]\rho^{(m)}, \tag{3}$$

$$T_j^{(de)i} = \text{diag}[-\rho^{(de)}, p^{(de)}, p^{(de)}, p^{(de)}] = \text{diag}[-1, \omega^{(de)}, \omega^{(de)}, \omega^{(de)}]\rho^{(de)}, \tag{4}$$

where $\rho^{(m)}$ and $p^{(m)}$ are the energy density and pressure of the perfect fluid components respectively whereas$\rho^{(de)}$ and $p^{(de)}$ are the corresponding energy density and pressure of the DE components while $\omega^{(m)} = \frac{p^{(m)}}{\rho^{(m)}}$ and $\omega^{(de)} = \frac{p^{(de)}}{\rho^{de}}$ are the corresponding EoS parameters.

By assuming the comoving co-ordinate system, field equation (2) with Eqs. (3) and (4) for the metric (1) turns into

$$\frac{\dot{A}^2}{A^2} + \frac{2\ddot{A}}{A} = -\omega^{(m)}\rho^{(m)} - \omega^{(de)}\rho^{(de)}, \tag{5}$$

$$3\frac{\dot{A}^2}{A^2} + \frac{2\beta\dot{A}}{A^4(1 + \beta\int \frac{dt}{A^3})} = \rho^{(m)} + \rho^{(de)}. \tag{6}$$

By the equation of law of energy conservation (Bianchi identity) $T_{;j}^{ij} = 0$, we have

$$\dot{\rho}^{(m)} + 3[1 + \omega^{(m)}]H\rho^{(m)} + \dot{\rho}^{(de)} + 3[1 + \omega^{(de)}]H\rho^{(de)} = 0. \tag{7}$$

3. Solution of the Field Equations

The field equations (5) and (6) involve five unknown variables, $\omega^{(de)}$. Therefore, in order to obtain the deterministic solution of the field equations we require three more suitable assumptions relating these unknown variables.

According to Pacif and Abdussattar [11], Akarsu and Kilinc [12], Abdussattar and Prajapati [13], let us first assume that the perfect fluid and DE components interact minimally. Therefore, equation of conservation of energy (7) can be split up into two separately additive conserved components which are as follows.

The energy conservation equation of the perfect fluid $T^{(m)ij}_{;j} = 0$ leads to

$$\dot{\rho}^{(m)} + 3[1 + \omega^{(m)}]H\rho^{(m)} = 0. \tag{8}$$

Similarly, energy conservation equation of the DE components $T^{(de)ij}_{;j} = 0$ leads to

$$\dot{\rho}^{(de)} + 3[1 + \omega^{(de)}]H\rho^{(de)} = 0. \tag{9}$$

Here, overhead dot represents the differentiation with respect to cosmic time whereas superscript (m) and (de) stand for perfect fluid (matter) and DE components, respectively.

Second, we have assumed that the EoS parameter of the perfect fluid to be a constant. Thus

$$\omega^{(m)} = \frac{p^{(m)}}{\rho^{(m)}} = \text{Constant}, \tag{10}$$

whereas $\omega^{(de)}$ has been allowed to be a function of cosmic time. Since the line element (1) is completely characterized by Hubble parameter H therefore finally, we have assumed that the mean generalized Hubble parameter H is related to the scale factor R by the relation [24]

$$H = lR^{-n} = l\left[A^3\left(1 + \beta\int\frac{dt}{A^3}\right)\right]^{-\frac{n}{3}}, \tag{11}$$

where $l > 0$ and $n \geq 0$ are constants.

As the deceleration parameter $q = -1 - \frac{\dot{H}}{H^2}$, Eq. (11) yields the constant value

$$q = n - 1. \tag{11a}$$

The universe with $n < 1$ corresponds to inflate the universe, whereas the universe with $n > 1$ defines decelerating universes. The universe with $n = 0$ has non-singular origin while the universe with $n \neq 0$ has singular origin. However, the present observations of SN Ia and CMBR favor accelerating models, i.e. $q < 0$. An arresting chance is that all the known cosmological models of Brans–Dicke theory with flat space-times unsurprisingly render a constant deceleration parameter are presented by Johri and Desikan [36]. Already such types of relations (Eq. (11)) for different space-times have been presented by Berman and Gomide [28]; Pradhan *et al.* [29]; Singh and Beesham [37]. Several authors have investigated the solutions of Einstein's equations using Berman's law in unlike contexts of GR such as Berman [38, 39]; Beesham [40, 41]. A number of authors like as Pradhanet *et al.* [42], Singh and Desikan [43], Singh and Singh [44] have also been used this law in cosmological models in alternative and modified theories of gravity. All these referred works were carried out in homogenous and isotropic space-times.

Now, we discuss the dark energy cosmological model for $n = 0$ and $n \neq 0$ by using Eq. (11) in the following two respective sections.

4. DE Cosmological Model-I for $n = 0$

Comparing Eq. (11) with the definition $H = \frac{\dot{R}}{R}$ and integrating, we get

$$R(t) = k_1 e^{lt}, \quad l > 0, \tag{12}$$

where k_1 is constant of integration.

Berman's law is a generalization of the de Sitter and power-law expansions.

The average scale factor for $n = 0$ is represented by 2D graph in Fig. 1. The average scale factor rises monotonically with respect to cosmic time t and the universe expands with acceleration for large values of the average scale factor. When $t \to 0$, the average scale factor is constant. The average scale factor diverges when $t \to \infty$. The average scale factor is performing like exponential expansion. This outcome decides with the studies of Berman and Gomide [28]; Pradhan *et al.* [29]; Dagwal and Pawar [22].

From given metric (1) the overall average scale factor R is defined as

$$R(t) = \left[A^3 \left(1 + \beta \int \frac{dt}{A^3}\right)\right]^{\frac{1}{3}}. \tag{13}$$

After little manipulations with Eqs. (12) (3.1.1) and (13) (3.1.2), we get

$$A(t) = \exp\{lt + k_0 e^{-3lt}\} \tag{14}$$

and

$$\left(1 + \beta \int \frac{dt}{A^3}\right) = k \exp\{-3k_0 e^{-3lt}\}, \tag{15}$$

where

$$k = k_1^3 \quad \text{and} \quad k_0 = \frac{\beta}{9kl}. \tag{16}$$

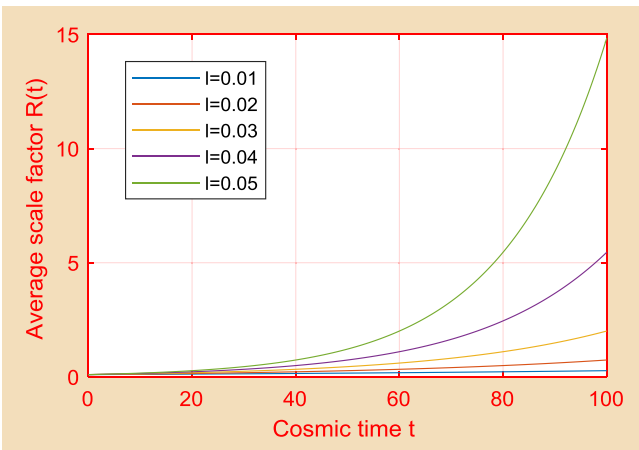

Fig. 1. Behavior of average scale factor $R(t)$ versus cosmic time t(Gyr) with $k_1 = 0.1$ and different value of l.

Thus our required cosmological model for the given metric (1) takes the form

$$ds^2 = -dt^2 + \{\exp 2[lt + k_0 e^{-3lt}]\}[dx^2 + dy^2] + k^2\{\exp 2[lt - 2k_0 e^{-3lt}]\}dz^2. \tag{17}$$

4.1. *Geometrical behavior of the model I (17)*

The directional Hubble parameters for the model along $x-$, $y-$ and z-axis are, respectively, given by

$$H_x = H_y = l(1 - 3k_0 e^{-3lt}) \quad \text{and} \quad H_z = l(1 + 6k_0 e^{-3lt}). \tag{18}$$

Thus the mean generalized Hubble parameter for the model found to be

$$H = \frac{1}{3}(H_x + H_y + H_z) = l = \text{constant}. \tag{19}$$

The mean anisotropy parameter Δ is defined and takes the value

$$\Delta = \frac{1}{3}\sum_{i=1}^{3}\left(\frac{H_i - H}{H}\right)^2 = 18k_0^2 e^{-6lt}. \tag{20}$$

The mean anisotropy parameter for $n = 0$ is represented by 3D graph in Fig. 2. The mean anisotropy parameter decreases monotonically with respect to cosmic time and tends to a constant value in the large-time limit. When $t \to 0$, the mean anisotropy parameter is constant. It is zero, when $t \to \infty$. Also, the mean anisotropy parameter dominates the physical sources in the sufficiently early times of the Universe.

The spatial volume of the required model is obtained as

$$V = A^3\left(1 + \beta\int\frac{dt}{A^3}\right) = k^{\frac{1}{3}}e^{lt}. \tag{21}$$

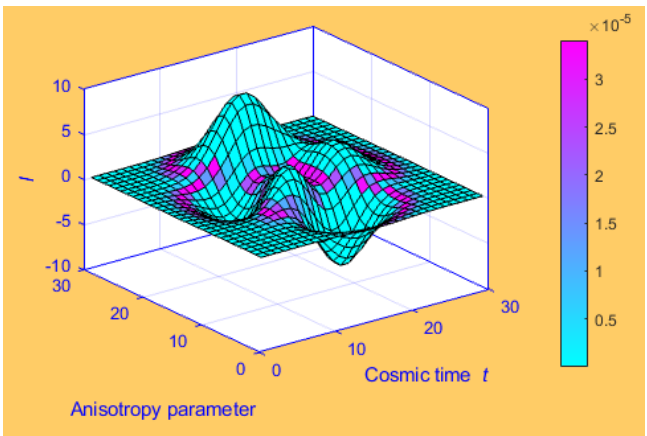

Fig. 2. Behavior of anisotropy parameter versus cosmic time t(Gyr) and l with $k_0 = \frac{\beta}{9kl}, \beta = 0.5$ and $k = 0.1$.

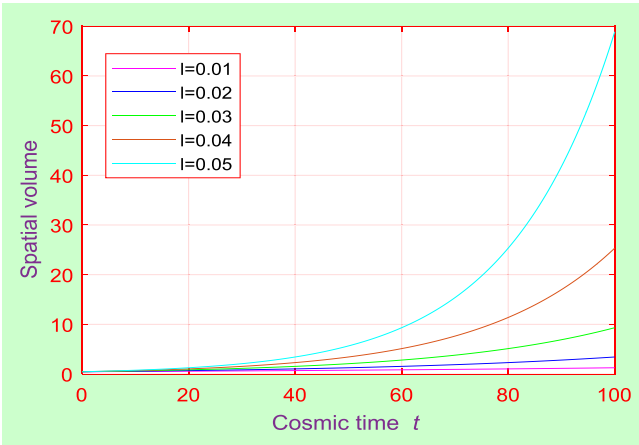

Fig. 3. Behavior of spatial volume versus cosmic time t(Gyr) with $k = 0.1$ and different value of l.

The spatial volume for $n = 0$ is represented by 2D graph in Fig. 3. The spatial volume rises monotonically with respect to cosmic time t. When $t \to 0$, spatial volume is constant. The spatial volume diverges when $t \to \infty$.

Similarly, shear scalar as well as scalar expansion of the model, respectively, given by

$$\sigma^2 = 54k_0 l^2 e^{-6lt} \tag{22}$$

and

$$\theta = 3H = 3l = \text{constant}. \tag{23}$$

The shear scalar for $n = 0$ is represented by 3D graph in Fig. 4. The shear scalar decreases monotonically with respect to cosmic time and tends to a constant value in the large-time limit. When $t \to 0$, shear scalar is constant. The shear scalar is zero when $t \to \infty$.

The value of the constant deceleration parameter for this model is found to be

$$q = -\frac{R\ddot{R}}{\dot{R}^2} = -1. \tag{24}$$

4.2. *Some physical parameters for the model I (17)*

The energy density of the perfect fluid by assuming its EoS parameter $\omega^{(m)}$ to be constant with the help of Eqs. (8), (14) and (23) is given by

$$\rho^{(m)} = k_2 e^{-3[1+\omega^{(m)}]lt}, \tag{25}$$

where k_2 being constant of integration.

The energy density of the perfect fluid for $n = 0$ versus cosmic time t is shown in Fig. 5 by setting the values $k_2 = 0.9, \omega^{(m)} = 1$ and different value of l. The

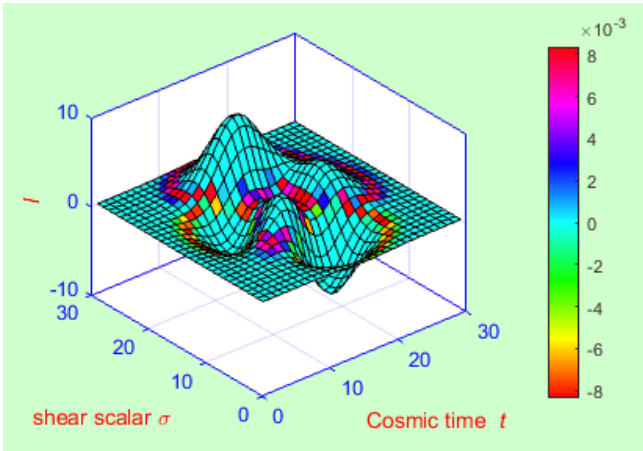

Fig. 4. Behavior of shear scalar versus cosmic time t(Gyr) and l with $k_0 = \frac{\beta}{9kl}, \beta = 0.5$ and $k = 0.1$.

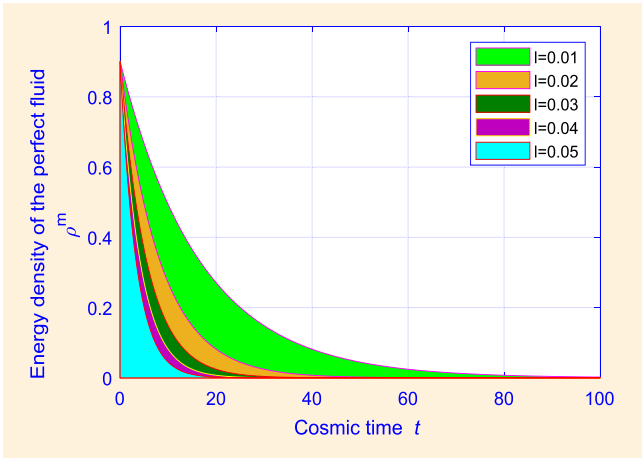

Fig. 5. Behavior of energy density of the perfect fluid versus cosmic time t(Gyr) with $k_2 = 0.9, \omega^{(m)} = 1$ and different value of l.

energy density decreases monotonically with respect to cosmic time $t$and tends to a constant value in the large-time limit. The energy density of the perfect fluid is constant for small value of cosmic time t. The energy density of the perfect fluid is zero for big value of cosmic time t. Figure 6 represents the variation of the energy density of the perfect fluid against cosmic time t with $k_2 = 0.9, l = 0.01$ and different value of $\omega^{(m)}$. The energy density of the perfect fluid for dust universe, radiation universe, hard universe and Zel'dovich universe decreases monotonically with respect to cosmic time t and tends to a constant value in the large-time limit. This result agrees with the studies of Saha [30, 31]; Singh and Chaubey [32].

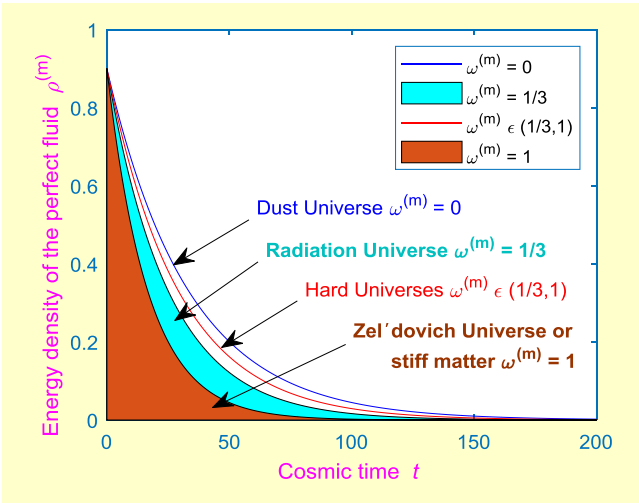

Fig. 6. Behavior of energy density of the perfect fluid versus cosmic time t(Gyr) with $k_2 = 0.9, l = 0.01$ and different value of $\omega^{(m)}$.

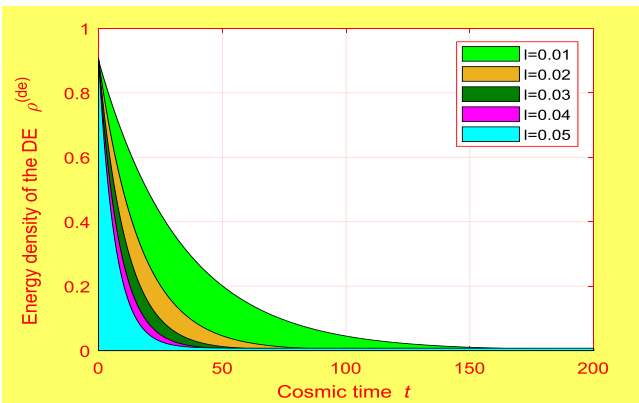

Fig. 7. Behavior of energy density of the DE versus cosmic time t(Gyr) with $k_0 = \frac{\beta}{9kl}, \beta = 0.5, k = 0.1, k_2 = -0.9, \omega^{(m)} = 1$ and different value of l.

The energy density of the DE component by using Eq. (6) with Eqs. (14), (15) and (25) is found to be

$$\rho^{(de)} = 3l^2(1 - 9k_0^2 e^{-6lt}) - k_2 e^{-3[1+\omega^{(m)}]lt}. \tag{26}$$

The profile of the energy density of the DE for $n = 0$ versus cosmic time t is shown in Fig. 7 by setting the values $k_0 = \frac{\beta}{9kl}, \beta = 0.5, k = 0.1, k_2 = -0.9, \omega^{(m)} = 1$ and different value of l. The energy density of the DE decreases monotonically with respect to cosmic time $t$and tends to a constant value in the large-time limit. The

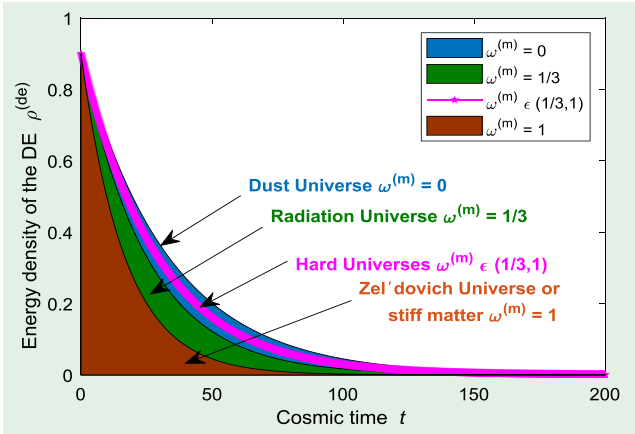

Fig. 8. Behavior of energy density of the DE versus cosmic time t(Gyr) with $k_0 = \frac{\beta}{9kl}, \beta = 0.5, k = 0.1, k_2 = -0.9, l = 0.01$ and different value of $\omega^{(m)}$.

energy density of the perfect fluid is constant for small value of cosmic time t. The energy density of the DE is zero for big value of cosmic time t. Figure 8 represents the variation of the energy density of the DE against cosmic time t with $k_0 = \frac{\beta}{9kl}, \beta = 0.5, k = 0.1, k_2 = -0.9, l = 0.01$ and different value of $\omega^{(m)}$. The energy density of the DE for dust universe, radiation universe, hard universe and Zel'dovich universe decreases monotonically with respect to cosmic time t and tends

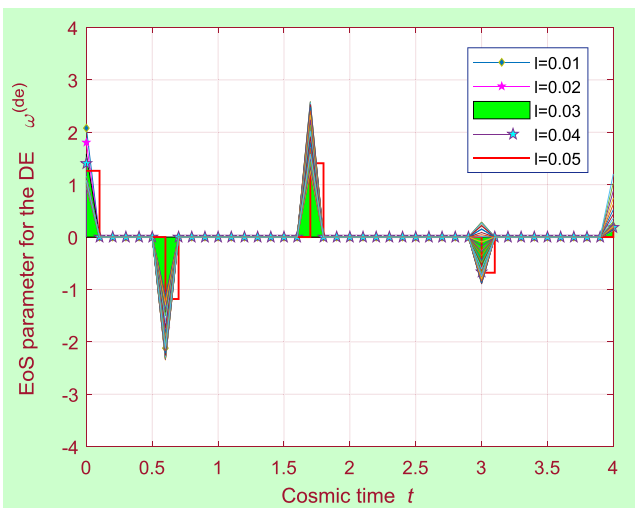

Fig. 9. Behavior of EoS parameter for the DE versus cosmic time t(Gyr) with $k_0 = \frac{\beta}{9kl}, \beta = 0.5, k = 0.1, k_2 = -0.9, \omega^{(m)} = 1$ and different value of l.

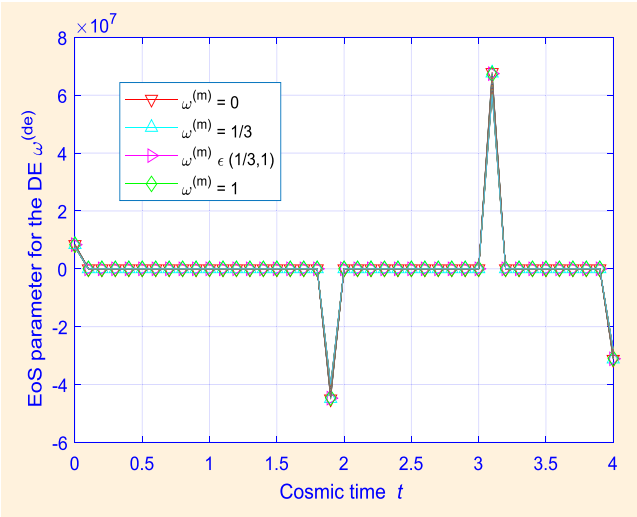

Fig. 10. Behavior of EoS parameter for the DE versus cosmic time t(Gyr) with $k_0 = \frac{\beta}{9kl}, \beta = 0.5, k = 0.1, k_2 = -0.9, l = 0.01$ and different value of $\omega^{(m)}$.

to a constant value in the large-time limit. This result agrees with the studies of Saha [30, 31]; Singh and Chaubey [32].

Similarly, Eq. (5) by using Eqs. (14), (15), (25) and (26) gives EoS parameter for the DE component as

$$\omega^{(de)} = -\frac{\{3l^2(1+9k_0^2e^{-6lt}) + k_2\omega^{(m)}e^{-3[1+\omega^{(m)}]lt}\}}{\{3l^2(1-9k_0^2e^{-6lt}) - k_2e^{-3[1+\omega^{(m)}]lt}\}}, \tag{27}$$

The behavior of EoS parameter for the DE for $n = 0$ versus cosmic time t is shown in Fig. 9.

Figure 10 represents the EoS parameter of the DE for $n = 0$ against cosmic time t with $k_0 = \frac{\beta}{9kl}, \beta = 0.5, k = 0.1, k_2 = -0.9, l = 0.01$ and different value of $\omega^{(m)}$. The profile of EoS parameter of the DE for dust universe, radiation universe, hard universe and Zel'dovich universe is discussed in Fig. 10. This result agrees with the studies of Saha [30, 31]; Singh and Chaubey [32].

5. DE Cosmological Models II for $n \neq 0$

Comparing Eq. (11) with the definition $H = \frac{\dot{R}}{R}$ and integrating we get

$$R(t) = (nlt + c_1)^{\frac{1}{n}}, \quad l > 0, \tag{28}$$

where c_1 is constant of integration.

The profile of the average scale factor for $n \neq 0$ versus cosmic time t is shown in Fig. 11 by setting the values $c_1 = 0.1$, $n = 0.5$ and different value of l. The average scale factor for $n \neq 0$ increases monotonically with respect to cosmic time

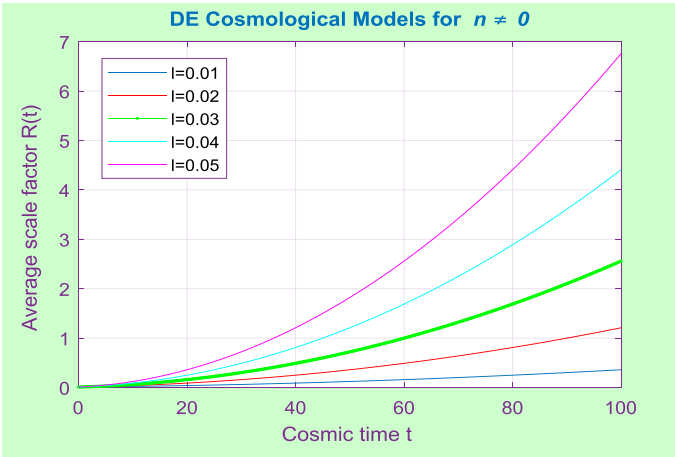

Fig. 11. Behavior of average scale factor $R(t)$ versus cosmic time t(Gyr) with $c_1 = 0.1$, $n = 0.5$ and different value of l.

t and the universe expands with acceleration for large values of the average scale factor. When $t \to 0$, the average scale factor for $n \neq 0$ is constant. The average scale factor for $n \neq 0$ diverges when $t \to \infty$. The average scale factor is performing like exponential expansion. This result agrees with the studies of Pacif *et al.* [6]; Berman and Gomide [28]; Pradhan *etal.* [29]; Dagwal and Pawar [22].

From equation of a given metric (1) the overall average scale factor R is defined as

$$R(T) = \left[A^3\left(1 + \beta \int \frac{dT}{A^3}\right)\right]^{\frac{1}{3}}. \tag{29}$$

After little manipulation with Eqs. (28) and (29), we get

$$A(T) = T^{\frac{1}{n}} \exp\left\{\frac{\beta}{3(3-n)l} T^{\frac{(n-3)}{n}}\right\} \tag{30}$$

and

$$\left(1 + \beta \int \frac{dT}{A^3}\right) = \exp\left\{\frac{\beta}{(n-3)l} T^{\frac{(n-3)}{n}}\right\}, \tag{31}$$

where, for the sake of simplicity, we have chosen

$$T = nlt + c_1. \tag{32}$$

Thus from Eqs. (28) and (32) the average scale factor of this model takes the form

$$R = T^{\frac{1}{n}}. \tag{33}$$

Thus our required cosmological model for the metric (11) becomes

$$ds^2 = \left(\frac{-1}{n^2l^2}\right)dT^2 + \left\{T^{\frac{2}{n}}\exp\frac{2\beta}{3(3-n)l}T^{\frac{(n-3)}{n}}\right\} \times \left[dx^2 + dy^2 + \left\{\exp\frac{2\beta}{(n-3)l}T^{\frac{(n-3)}{3}}\right\}dz^2\right]. \tag{34}$$

5.1. *Geometrical behavior of the model II (34)*

The directional Hubble parameters for the model along x^-, y^- and z^- axis are, respectively, given by

$$H_x = H_y = \frac{\dot{A}}{A} = \frac{1}{nT} - \frac{\beta}{3nlT^{\frac{3}{n}}}$$

and

$$H_z = \frac{\frac{d}{dT}[A(T)(1+\beta\int\frac{dT}{A^3})]}{A(T)(1+\beta\int\frac{dT}{A^3})} = \frac{1}{nT} + \frac{2\beta}{3nlT^{\frac{3}{n}}}. \tag{35}$$

Thus, the mean generalized Hubble parameter for the model is

$$H = \frac{1}{3}(H_x + H_y + H_z) = \frac{1}{nT}. \tag{36}$$

The Hubble parameter for $n \neq 0$ against cosmic time t and l is represented by 3D graph in Fig. 12 by locating the values $c_1 = 0.1$, $n = 0.5$. When $t \to 0$, the Hubble parameter for $n \neq 0$ is constant.

The Hubble parameter for $n \neq 0$ vanishes at $t \to \infty$. The Hubble parameter diverges when $t \to -\frac{c_1}{nl}$. The Hubble parameter has big rip singularity at $t \to -\frac{c_1}{nl}$. It has big bang singularity when $t \to \infty$. The intermediate phase is between big

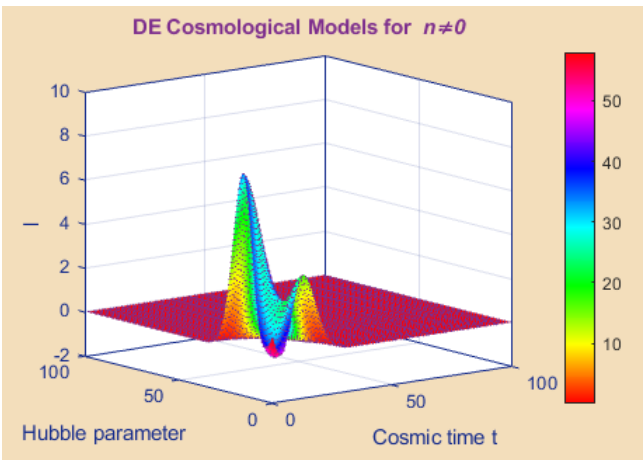

Fig. 12. Behavior of Hubble parameter versus cosmic time t(Gyr) and l with $c_1 = 0.1$, $n = 0.5$.

bang and big rip singularity. The Hubble parameter starts with big bang and ends with big rip singularity. This result agrees with the studies of Dagwal [21]; Berman and Gomide [28]; Pradhan *et al.* [29]; Sahoo *et al.* [33]; Dagwal *et al.* [34].

The mean anisotropy parameter Δ_1 of the expansion for the model is

$$\Delta_1 = \frac{1}{3}\sum_{i=1}^{3}\left(\frac{H_i - H}{H}\right)^2 = \frac{2\beta^2}{9l^2T^{\frac{2(3-n)}{n}}}. \tag{37}$$

The mean anisotropy parameter for $n \neq 0$ against cosmic time t and l is represented by 3D graph in Fig. 13 by locating the values $n = 0.5, \beta = 0.5$ and $c_1 = 0.1$. The mean anisotropy parameter for $n \neq 0$ has big rip singularity when $t \to -\frac{c_1}{nl}$ and big bang singularity when $t \to \infty$. When $n \to 3$, the mean anisotropy parameter is constant.

The spatial volume V of the model is found to be

$$V = A\left(1 + \beta\int\frac{dT}{A^3}\right)^{\frac{1}{3}} = T^{\frac{1}{n}}. \tag{38}$$

The spatial volume for $n \neq 0$ against cosmic time t is shown in Fig. 14 by locating the values $c_1 = 0.1$, $n = 0.5$ and different value of l. The spatial volume for $n \neq 0$ increases monotonically with respect to cosmic time t. When $t \to 0$, spatial volume is constant. The spatial volume diverges when $t \to \infty$.

Similarly shear scalar σ^2 and scalar expansion θ are, respectively, found to be

$$\sigma^2 = \frac{2\beta^2}{3n^2l^2T^{\frac{6}{n}}} \quad \text{and} \quad \theta = 3H = \frac{3}{nT}. \tag{39}$$

The shear scalar for $n \neq 0$ against cosmic time t and l is represented by 3D graph in Fig. 15 by setting the values $n = 0.5, \beta = 0.5$ and $c_1 = 0.1$. The shear

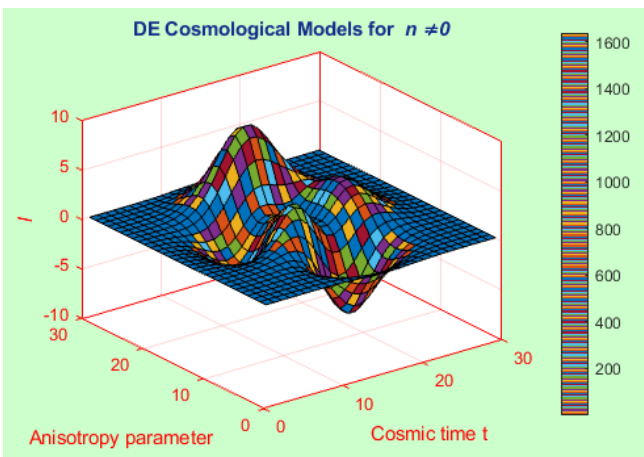

Fig. 13. Behavior of anisotropy parameter versus cosmic time t(Gyr) and l with $n = 0.5, \beta = 0.5$ and $c_1 = 0.1$.

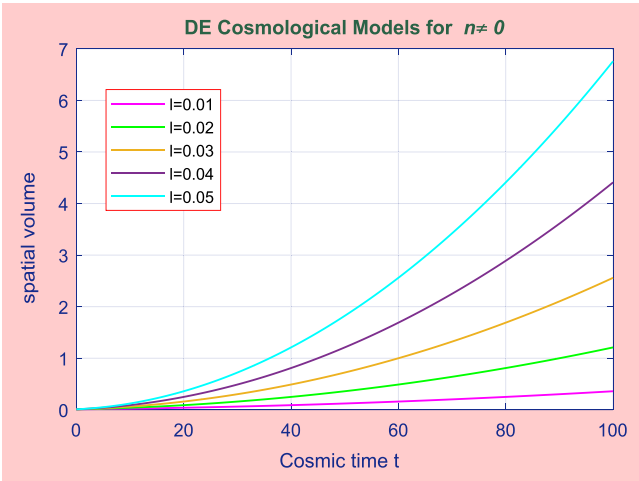

Fig. 14. Behavior of spatial volume versus cosmic time t(Gyr) with $c_1 = 0.1$, $n = 0.5$ and different value of l.

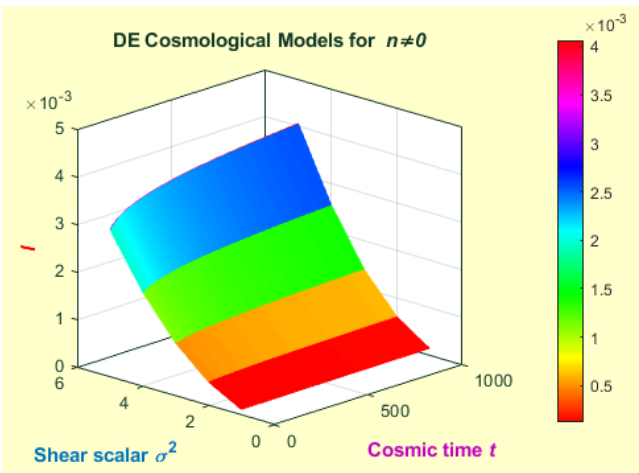

Fig. 15. Behavior of shear scalar versus cosmic time t(Gyr) and l with $n = 0.5, \beta = 0.5$ and $c_1 = 0.1$.

scalar for $n \neq 0$ has big rip singularity at $t \to -\frac{c_1}{nl}$. It has big bang singularity at $t \to \infty$. The shear scalar for $n \neq 0$ starts with big bang singularity and ends with big rip.

The value of the deceleration parameter for this model is obtained as

$$q = -\frac{R\ddot{R}}{\dot{R}^2} = n - 1. \tag{40}$$

5.2. *Some more physical parameters of the model II (34)*

As per our proposed assumption EoS parameter $\omega^{(m)}$ of perfect fluid being constant energy density for the perfect fluid by using Eq. (8) with the help of Eqs. (30) and (31) is given by

$$\rho^{(m)} = c_2 T^{\frac{-3[1+\omega^{(m)}]}{n}}, \tag{41}$$

where c_2 being constant of integration.

The energy density of the perfect fluid for $n \neq 0$ versus cosmic time t is presented in Fig. 16 by setting the values $c_1 = 0.1, c_2 = 0.3, n = 3, \omega^{(m)} = 1$ and different value of l. The energy density of the perfect fluid for $n \neq 0$ decreases monotonically with respect to cosmic time t and tends to a constant value in the large-time limit. The energy density of the perfect fluid for $n \neq 0$ is constant at beginning of the Universe. The energy density of the perfect fluid for $n \neq 0$ is disappearing for large value of the Universe. The energy density of the perfect fluid for $n \neq 0$ has big rip singularity when and big bang singularity when $t \to \infty$. It starts with big bang singularity and ends with big rip. The energy density of the perfect fluid for $n \neq 0$ has intermediate phase between big bang and big rip singularity. This result agrees with the studies of Dagwal [21]; Berman and Gomide [28]; Pradhanet. *et al.* [29]; Sahoo *et al.* [33]; Dagwal *et al.* [34]; Kumar and Akarsu [35]. Figure 17 represents the variation of the energy density of the perfect fluid for $n \neq 0$ against cosmic time t with $c_1 = 0.1, c_2 = 0.3, n = 3, l = 0.01$ and different value of . The energy density of the perfect fluid for $n \neq 0$, dust universe, radiation universe, hard universe and Zel'dovich universe decreases monotonically with respect to cosmic time t and tends to a constant value in the large-time limit. This result agrees with the studies of Saha [30, 31]; Singh and Chaubey [32]; Kumar and Akarsu [35].

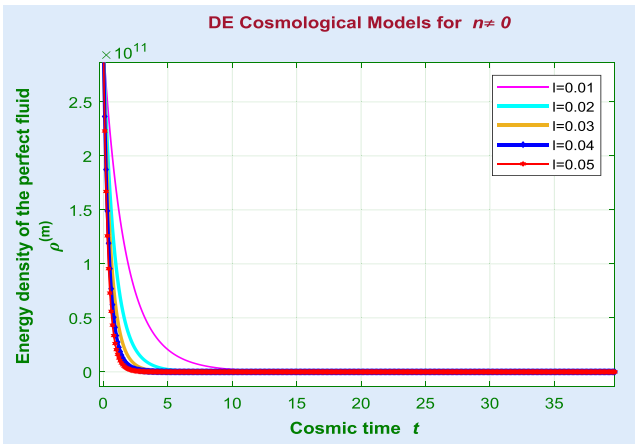

Fig. 16. Behavior of energy density of the perfect fluid versus cosmic time t(Gyr) with $c_1 = 0.1, c_2 = 0.3, n = 3, \omega^{(m)} = 1$ and different value of l.

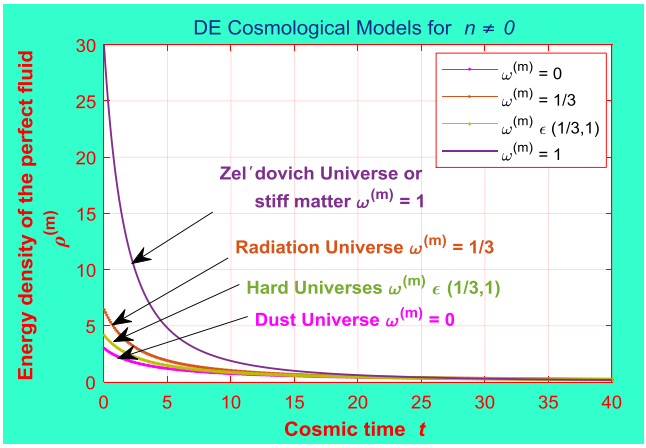

Fig. 17. Behavior of energy density of the perfect fluid versus cosmic time t(Gyr) with $c_1 = 0.1, c_2 = 0.3, n = 3, l = 0.01$ and different value of $\omega^{(m)}$.

Equation (6) with Eqs. (30), (31) and (41) gives energy density of the DE component for the model (34) as

$$\rho^{(de)} = \left(\frac{1-2nl}{3n^2l^2}\right)\frac{\beta^2}{T^{\frac{6}{n}}} + \frac{2(nl-1)\beta}{n^2lT^{\frac{(n+3)}{n}}} + \frac{3}{n^2T^2} - \frac{c_2}{T^{\frac{3[1+\omega^{(m)}]}{n}}}, \tag{42}$$

The energy density of the DE for $n \neq 0$ versus cosmic time t is presented in Fig. 18 by setting the values $c_1 = 0.1, c_2 = 0.3, n = 3, \omega^{(m)} = 1, \beta = 0.5$ and different value of l. The energy density of the DE for $n \neq 0$ is constant at

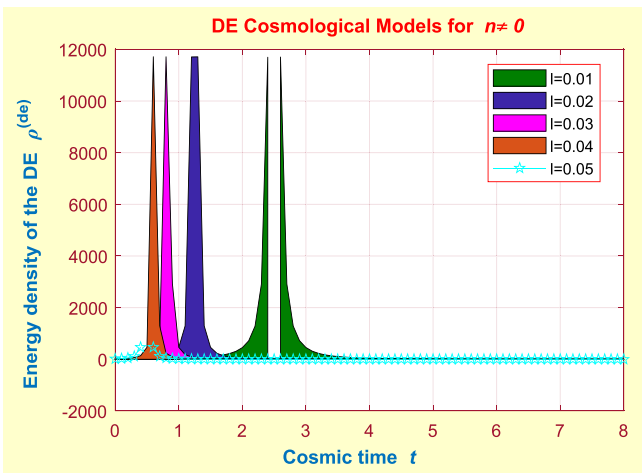

Fig. 18. Behavior of energy density of the DE versus cosmic time t(Gyr) with $c_1 = 0.1, c_2 = 0.3, n = 3, \omega^{(m)} = 1, \beta = 0.5$ and different value of l.

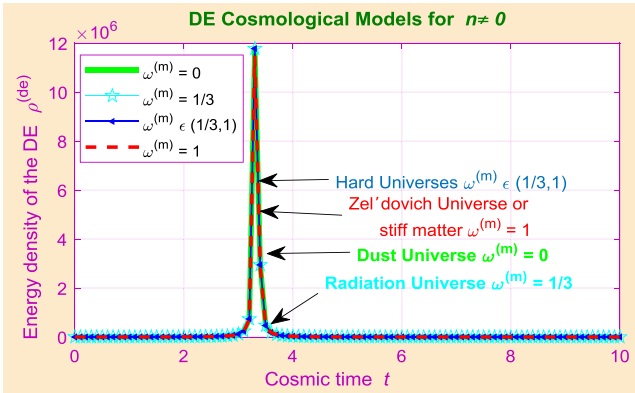

Fig. 19. Behavior of energy density of the DE versus cosmic time t(Gyr) with $c_1 = 0.1, c_2 = 0.3, n = 3, l = 0.91, \beta = 0.5$ and different value of $\omega^{(m)}$.

beginning of the Universe. The energy density of the DE for $n \neq 0$ is disappearing for large value of the Universe. The energy density of the DE for $n \neq 0$ has big rip singularity when $t \to -\frac{c_1}{nl}$ and big bang singularity when $t \to \infty$. It starts with big bang singularity and ends with big rip. The energy density of the DE for $n \neq 0$ has intermediate phase between big bang and big rip singularity. Figure 19 represents the variation of the energy density of the DE for $n \neq 0$ against cosmic time t with $c_1 = 0.1, c_2 = 0.3, n = 3, l = 0.91, \beta = 0.5$ and different value of $\omega^{(m)}$. This outcome approves with the studies of Dagwal [21]; Sahoo *et al.* [33]; Dagwal *et al.* [34]. The energy density of the DE for $n \neq 0$, dust universe $\omega^{(m)} = 0$, radiation universe $\omega^{(m)} = 1/3$, hard universe $\omega^{(m)} \in (1/3, 1)$ and Zel'dovich universe $\omega^{(m)} = 1$ have big bang singularity when $t \to \infty$ and big rip singularity when $t \to -\frac{c_1}{nl}$. It has intermediate phase between big bang and big rip singularity. This result agrees with the studies of Berman and Gomide [28]; Pradhan *et al.* [29]; Saha [30, 31]; Singh and Chaubey [32]; Kumar and Akarsu [35].

Similarly, Eq. (5) with Eqs. (30), (31), (41) and (42) gives EoS parameter of DE component as

$$\omega^{(de)} = -\frac{1}{\rho^{(de)}}\left\{\frac{(3-2n)}{n^2T^2} + \frac{\beta^2}{3n^2l^2T^{\frac{6}{n}}} + \frac{c_2\omega^{(m)}}{T^{\frac{3[1+\omega^{(m)}]}{n}}}\right\}, \tag{43}$$

where $\rho^{(de)}$ is given by Eq. (42).

The behavior of EoS parameter for the DE for $n \neq 0$ versus cosmic time t is shown in Fig. 20 by setting the values $c_1 = 0.1, c_2 = 0.3, n = 3, \omega^{(m)} = 1, \beta = 0.5$ and different value of l. Figure 21 represents the EoS parameter of the DE for $n \neq 0$ against cosmic time t with $k_0 = \frac{\beta}{9kl}, \beta = 0.5, k = 0.1, k_2 = -0.9, l = 0.01$ and different value of $\omega^{(m)}$. The profile of EoS parameter of the DE for $n \neq 0$, dust universe $\omega^{(m)} = 0$, radiation universe $\omega^{(m)} = 1/3$, hard universe $\omega^{(m)} \in (1/3, 1)$ and Zel'dovich universe $\omega^{(m)} = 1$ are discussed in Fig. 21. The EoS parameter of

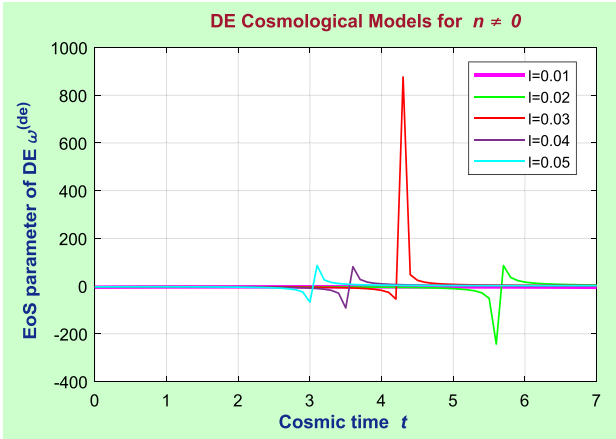

Fig. 20. Behavior of EoS parameter of DE versus cosmic time t(Gyr) with $c_1 = 0.1, c_2 = 0.3, n = 3, \omega^{(m)} = 1, \beta = 0.5$ and different value of l.

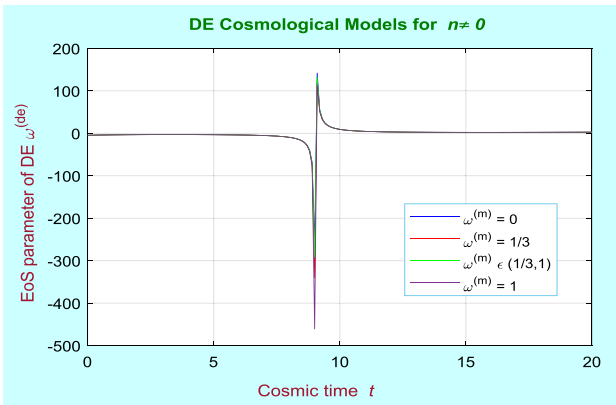

Fig. 21. Behavior of EoS parameter of DE versus cosmic time t(Gyr) with $c_1 = 0.1, c_2 = 0.3, n = 3, l = 0.91, \beta = 0.5$ and different value of $\omega^{(m)}$.

the DE for $n \neq 0$positive value, the universe matter dominate phase and it has negative value, the universe is at the present epoch. The previous real matter later on changed to the dark energy dominated phase of the models in both accelerating and decelerating approaches. This result agrees with the studies of Pradhan *et al.* [29]; Saha [30, 31]; Singh and Chaubey [32].

6. Results and Discussion

6.1. *DE cosmological model-I for* $n = 0$

The directional Hubble parameters $H_x = H_y$ and H_z are finite when the cosmic time is zero as well as infinity. Thus, the model represents the inflationary era in the early

universe and the very late time of the universe. The spatial volume of this model is finite when $t = 0$ and expands exponentially as t increases and becomes infinitely large at $t = \infty$. This shows that universe starts with constant volume and expands with exponential rate. The shear scalar σ^2, the mean anisotropy parameter Δ are finite at $t = 0$ and tend to zero as cosmic time tends to infinity. The energy density $\rho^{(m)}$ of the perfect fluid is constant k_2 when cosmic time is zero and decreases exponentially so as to converge at zero when EoS parameter of the perfect fluid $\omega^{(m)} \geq 0$ as per the proposed assumption. But energy density $\rho^{(de)}$ of the DE component changes slightly when cosmic time is zero and decreases exponentially as time increases further it converges to nonzero constant $3l^2$ as well as DE component isfinite at $t = 0$ and tends to zero as cosmic time tends to infinity. In the present model ratio of $\frac{\rho^{(de)}}{\rho^{(de)}+\rho^{(m)}}$ converges to 1 as t increases and this is sufficient to show that the dark energy dominates the perfect fluid in the inflationary era. The mean anisotropy parameter of expansion decreases monotonically when time increases and converges to zero when time is infinite. Also $\lim_{t\to\infty} \frac{\sigma^2}{\theta} = 0$ indicates that model approach to isotropy for large value of cosmic time. The EoS parameter of the dark energy exhibits nontrivial behavior of the early time of the universe and converges to -1 for late time [25]. Thus, when cosmic time $t = \infty$ EoS parameter $\omega^{(de)} = -1$. This is the simplest form of dark energy called vacuum energy, which is mathematically equivalent to the cosmological constant. But in some cosmological models value of the EoS parameter $\omega = -1$ is rejected so as to get the exact solution of the field equations [26].

Graphical presentation for model-I:

- The average scale factor for $n = 0$ is represented by 2D graph in Fig. 1. The average scale factor rises monotonically with respect to cosmic time t and the universe expands with acceleration for large values of the average scale factor. When $t \to 0$, the average scale factor is constant. The average scale factor diverges when $t \to \infty$. The average scale factor is performing like exponential expansion. This outcome decides with the studies of Berman and Gomide [28]; Pradhan *et al.* [29]; Dagwal and Pawar [22].
- The mean anisotropy parameter for $n = 0$ is represented by 3D graph in Fig. 2. The mean anisotropy parameter decreases monotonically with respect to cosmic time and tends to a constant value in the large-time limit. When $t \to 0$, the mean anisotropy parameter is constant. It is zero when $t \to \infty$. Also, the mean anisotropy parameter dominates the physical sources in the sufficiently early times of the Universe.
- The spatial volume for $n = 0$ is represented by 2D graph in Fig. 3. The spatial volume rises monotonically with respect to cosmic time t. When $t \to 0$, spatial volume is constant. The spatial volume diverges when $t \to \infty$.
- The shear scalar for $n = 0$ is represented by 3D graph in Fig. 4. The shear scalar decreases monotonically with respect to cosmic time and tends to a constant

value in the large-time limit. When $t \to 0$, shear scalar is constant. The shear scalar is zero when $t \to \infty$.

- The energy density of the perfect fluid for $n = 0$ versus cosmic time t is shown in Fig. 5 by setting the values $k_2 = 0.9, \omega^{(m)} = 1$ and different value of l. The energy density decreases monotonically with respect to cosmic time t and tends to a constant value in the large-time limit. The energy density of the perfect fluid is constant for small value of cosmic time t. The energy density of the perfect fluid is zero for big value of cosmic time t. Figure 6 represents the variation of the energy density of the perfect fluid against cosmic time t with $k_2 = 0.9, l = 0.01$ and different value of $\omega^{(m)}$. The energy density of the perfect fluid for dust universe, radiation universe, hard universe and Zel'dovich universe decreases monotonically with respect to cosmic time t and tends to a constant value in the large-time limit. This result agrees with the studies of Saha [30, 31]; Singh and Chaubey [32].
- The profile of the energy density of the DE for $n = 0$ versus cosmic time t is shown in Fig. 7 by setting the values $k_0 = \frac{\beta}{9kl}, \beta = 0.5, k = 0.1, k_2 = -0.9, \omega^{(m)} = 1$ and different value of l. The energy density of the DE decreases monotonically with respect to cosmic time t and tends to a constant value in the large-time limit. The energy density of the perfect fluid is constant for small value of cosmic time t. The energy density of the DE is zero for big value of cosmic time t. Figure 8 represents the variation of the energy density of the DE against cosmic time t with $k_0 = \frac{\beta}{9kl}, \beta = 0.5, k = 0.1, k_2 = -0.9, l = 0.01$ and different value of $\omega^{(m)}$. The energy density of the DE for dust universe, radiation universe, hard universe and Zel'dovich universe decreases monotonically with respect to cosmic time $t$and tends to a constant value in the large-time limit. This result agrees with the studies of Saha [30, 31]; Singh and Chaubey [32].
- The behavior of EoS parameter for the DE for $n = 0$ versus cosmic time t is shown in Fig. 9. Figure 10 represents the EoS parameter of the DE for n =0 against cosmic time t with$k_0 = \frac{\beta}{9kl}, \beta = 0.5, k = 0.1, k_2 = -0.9, l = 0.01$ and different value of $\omega^{(m)}$. The profile of EoS parameter of the DE for dust universe, radiation universe, hard universe and Zel'dovich universe is discussed in Fig. 10. This result agrees with the studies of Saha [30, 31]; Singh and Chaubey [32].

6.2. *DE cosmological models-II for $n \neq 0$*

The directional Hubble parameters $H_x = H_y \,\&\, H_z$ are infinitely large at $T = 0 (\because T = nlt + c_1)$ and becomes null when $T = \infty$. It is observed that at $T = 0$, the spatial volume vanishes while all other parameters diverge. Thus the derived model starts evolving with zero volume and expands with cosmic time. This singularity is point type because metric potential $A(T)$ vanishes at the initial moment. The mean anisotropy parameter Δ_1, the expansion scalar θ and shear scalar σ^2 all vanish when $T \to \infty$, which indicates that universe is expanding with increase in cosmic time. Also $\lim_{T\to\infty} \frac{\sigma^2}{\theta} = 0$ provided $n < 6$ which shows that the model approaches isotropic for large value of cosmic time. According to Collins and Hawking [27]

all the candidates for homogeneity and isotropizations are satisfied by the present model. Thus the present model approaches isotropic during the late time of its evolution.

Graphical presentation for model-II:

- The profile of the average scale factor for $n \neq 0$ versus cosmic time t is shown in Fig. 11 by setting the values $c_1 = 0.1$, $n = 0.5$ and different value of l. The average scale factor for $n \neq 0$ increases monotonically with respect to cosmic time t and the universe expands with acceleration for large values of the average scale factor. When $t \to 0$, the average scale factor for $n \neq 0$ is constant. The average scale factor for $n \neq 0$ diverges when $t \to \infty$. The average scale factor is performing like exponential expansion. This result agrees with the studies of Pacif *et al.* [6]; Berman and Gomide [28]; Pradhan *et al.* [29]; Dagwal and Pawar [22].
- The Hubble parameter for $n \neq 0$ against cosmic time t and l is represented by 3D graph in Fig. 12 by locating the values $c_1 = 0.1$, $n = 0.5$. When $t \to 0$, the Hubble parameter for $n \neq 0$ is constant. The Hubble parameter for $n \neq 0$ vanishes at $t \to \infty$. The Hubble parameter diverges when $t \to -\frac{c_1}{nl}$. The Hubble parameter has big rip singularity at $t \to -\frac{c_1}{nl}$. It has big bang singularity when $t \to \infty$. The intermediate phase is between big bang and big rip singularity. The Hubble parameter starts with big bang and ends with big rip singularity. This result agrees with the studies of Dagwal [21]; Berman and Gomide [28]; Pradhan *et al.* [29]; Sahoo *et al.* [33]; Dagwal *et al.* [34].
- The mean anisotropy parameter for $n \neq 0$ against cosmic time t and l is represented by 3D graph in Fig. 13 by locating the values $n = 0.5, \beta = 0.5$ and $c_1 = 0.1$. The mean anisotropy parameter for $n \neq 0$ has big rip singularity when $t \to -\frac{c_1}{nl}$ and big bang singularity when $t \to \infty$. When $n \to 3$, the mean anisotropy parameter is constant.
- The spatial volume for $n \neq 0$against cosmic time t is shown in Fig. 14 by locating the values $c_1 = 0.1$, $n = 0.5$ and different value of l. The spatial volume for $n \neq 0$ increases monotonically with respect to cosmic time t. When $t \to 0$, spatial volume is constant. The spatial volume diverges when $t \to \infty$.
- The shear scalar for $n \neq 0$ against cosmic time t and l is represented by 3D graph in Fig. 15 by setting the values $n = 0.5, \beta = 0.5$ and $c_1 = 0.1$. The shear scalar for $n \neq 0$ has big rip singularity at $t \to -\frac{c_1}{nl}$. It has big bang singularity at $t \to \infty$. The shear scalar for $n \neq 0$ starts with big bang singularity and endswith big rip.
- The energy density of the perfect fluid for $n \neq 0$versus cosmic time t is presented in Fig. 16 by setting the values $c_1 = 0.1, c_2 = 0.3, n = 3, \omega^{(m)} = 1$ and different value of l. The energy density of the perfect fluid for $n \neq 0$ decreases monotonically with respect to cosmic time $t$and tends to a constant value in the large-time limit. The energy density of the perfect fluid for $n \neq 0$ is constant at beginning of the Universe. The energy density of the perfect fluid for $n \neq 0$ is disappearing for large value of the Universe. The energy density of the perfect fluid for $n \neq 0$ has big rip singularity when $t \to -\frac{c_1}{nl}$ and big bang singularity when $t \to \infty$.

It starts with big bang singularity and ends with big rip. The energy density of the perfect fluid for $n \neq 0$ has intermediate phase between big bang and big rip singularity. This result agrees with the studies of Dagwal [21]; Berman and Gomide [28]; Pradhan *et al.* [29]; Sahoo *et al.* [33]; Dagwal *et al.* [34]; Kumar and Akarsu [35]. Figure 17 represents the variation of the energy density of the perfect fluid for $n \neq 0$ against cosmic time t with $c_1 = 0.1, c_2 = 0.3, n = 3, l = 0.01$ and different value of $\omega^{(m)}$. The energy density of the perfect fluid for $n \neq 0$, dust universe, radiation universe, hard universe and Zel'dovich universe decreases monotonically with respect to cosmic time t and tends to a constant value in the large-time limit. This result agrees with the studies of Saha [30, 31]; Singh and Chaubey [32]; Kumar and Akarsu [35].

- The energy density of the DE for $n \neq 0$ versus cosmic time t is presented in Fig. 18 by setting the values $c_1 = 0.1, c_2 = 0.3, n = 3, \omega^{(m)} = 1, \beta = 0.5$ and different value of l. The energy density of the DE for $n \neq 0$ is constant at beginning of the Universe. The energy density of the DE for $n \neq 0$ is disappearing for large value of the Universe. The energy density of the DE for $n \neq 0$ has big rip singularity when $t \to -\frac{c_1}{nl}$ and big bang singularity when $t \to \infty$. It starts with big bang singularity and ends with big rip. The energy density of the DE for $n \neq 0$ has intermediate phase between big bang and big rip singularity. Figure 19 represents the variation of the energy density of the DE for $n \neq 0$ against cosmic time t with $c_1 = 0.1, c_2 = 0.3, n = 3, l = 0.91, \beta = 0.5$ and different value of $\omega^{(m)}$. This outcome approves with the studies of Dagwal [21]; Sahoo *et al.* [33]; Dagwal *et al.* [34]. The energy density of the DE for $n \neq 0$, dust universe $\omega^{(m)} = 0$, radiation universe $\omega^{(m)} = 1/3$, hard universe $\omega^{(m)} \in (1/3, 1)$ and Zel'dovich universe $\omega^{(m)} = 1$ have big bang singularity when $t \to \infty$ and big rip singularity when $t \to -\frac{c_1}{nl}$. It has intermediate phase between big bang and big rip singularity. This result agrees with the studies of Berman and Gomide [28]; Pradhan *et al.* [29]; Saha [30, 31]; Singh and Chaubey [32]; Kumar and Akarsu [35].
- The behavior of EoS parameter for the DE for $n \neq 0$ versus cosmic time t is shown in Fig. 20 by setting the values $c_1 = 0.1, c_2 = 0.3, n = 3, \omega^{(m)} = 1, \beta = 0.5$ and different value of l. Figure 21 represents the EoS parameter of the DE for $n \neq 0$ against cosmic time t with $k_0 = \frac{\beta}{9kl}, \beta = 0.5, k = 0.1, k_2 = -0.9, l = 0.01$ and different value of$\omega^{(m)}$. The profile of EoS parameter of the DE for $n \neq 0$, dust universe $\omega^{(m)} = 0$, radiation universe $\omega^{(m)} = 1/3$, hard universe $\omega^{(m)} \in (1/3, 1)$ and Zel'dovich universe $\omega^{(m)} = 1$ are discussed in Fig. 21. The EoS parameter of the DE for $n \neq 0$ positive value, the universe matter dominate phase and it has negative value, the universe is at the present epoch. The previous real matter later on changed to the dark energy dominated phase of the models in both accelerating and decelerating approaches. This result agrees with the studies of Pradhan *et al.* [29]; Saha [30, 31]; Singh and Chaubey [32].

7. Conclusion

In this paper, we have investigated accelerating LRS Bianchi type-I dark energy cosmological model for $n = 0$ and $n \neq 0$. As we have defined the Hubble's parameter in Eq. (11) it gives rise to two types of cosmological models depending on the nature of the value of constant deceleration parameter whether it is positive or negative. The first form of the universe having negative value of deceleration parameter shows the exponential expansion of the universe while second form of the universe having positive value of deceleration parameter shows the power law expansion of the universe. For the exponential expansion model all the parameters $H_x, H_y, H_z, \Delta, \sigma^2$ are constant at $t = 0$. As $t \to \infty$ the EoS parameter of the DE component is -1, i.e. $\omega^{(de)} = -1$ which may be considered as vacuum energy density. Obviously, it is equivalent to cosmological constant and it is important to note that this class of solution is consistent with the recent observations of the supernova I_a [1–4]. For the power law expansion model $H_x, H_y, H_z, \Delta_1, \sigma^2, \theta$ all these parameters are infinitely very large at initial moment and decrease with increase in time and vanish at large value of cosmic time.

Finally, we conclude that there is no singularity in dark energy cosmological model-I for $n = 0$ but in dark energy cosmological model-II for $n \neq 0$ we have big bang, big rip and point type singularity [59]. This result agrees with the studies of Ashtekar and Singh [60]; Bojowald [61]; Singh [62]; Shamir [63]; Pradhan and Amirhashchi [64]; Bali and Kumawat [65], etc. Model-II has intermediate phase between big bang and big rip singularity. In both model-I and II, it is investigated that, in early stage, the EoS parameter ω is positive, i.e. the universe is matter dominated in early stage but in late time, the universe is evolving with negative values, i.e. the present epoch. Thus our DE models represent realistic models.

References

[1] S. Perlmutter *et al.*, *Nature* **391** (1988) 51.
[2] A. Reiss *et al.*, *Astrophys. J.* **517** (1999) 565.
[3] R. A. Knop *et al.*, *Astrophys. J.* **598** (2003) 102.
[4] S. K. J. Pacif, Md. S. Khan, L. K. Paikroy and S. Singh, *Mod. Phys. Lett. A* **35**(5) (2020) 2050011.
[5] R. R. Caldwell, *Phys. Lett. B* **545** (2002) 23.
[6] S. K. J. Pacif, R. Myrzakulov and S. Myrzakul, *Int. J. Geom. Methods Mod. Phys.* **14**(7) (2017) 1750111.
[7] Z. Y. Haung, B. Wang, Abdulla and R. K. E. Sul, *J. Cosmol. Astropart. Phys.* **05** (2006) 013.
[8] S. K. J. Pacif and B. Mishra, *Res. Astron. Astrophys.* **15**(12) (2015) 2141.
[9] P. Peebles and B. Ratra, *Rev. Mod. Phys.* **75** (2003) 559.
[10] M. Tegmark *et al.*, *Phys. Rev. D* **69** (2004) 103501.
[11] S. K. J. Pacif and Abdussattar, *Eur. Phys. J. Plus* **129** (2014) 244.
[12] Ö. Akarsu and C. B. Kilink, *Gen. Relativ. Gravit* **42** (2010b) 763.
[13] A. Sattar and S. R. Prajapati, *Astrophys. Space Sci.* **331** (2011) 657–663.

[14] A. K. Yadav and V. L. Yadav, *Int. J. Theor. Phys.* **50** (2011) 218.
[15] B. Ratra and J. Peebles, *Phys. Rev. D* **37** (1988) 321.
[16] C. Aktas, *Mod. Phys. Lett. A* **34**(11) (2019) 1950066.
[17] C. Aktas, S. Aygün and I. Yılmaz, *Phys. Lett. B* **707** (2012) 237–242.
[18] T. Padmanabhan, *Phys. Rev. D* **66** (2002) 021301.
[19] A. Sattar and S. R. Prajapati, *Astrophys.Space Sci.* **331** (2011) 657.
[20] D. D. Pawar and V. J. Dagwal, *Int. J. Theor. Phys.* **53**(7) (2014) 2441.
[21] V. J. Dagwal, *Can. J. Phys.* **98** (2020) 636–642
[22] V. J. Dagwal and D. D. Pawar, *Mod. Phys. Lett. A* **34** (2019) 1950357.
[23] V. J. Dagwal and D. D. Pawar, *Indian J. Phys.* (2020), https://doi.org/10.1007/s12648-020-01691- w.
[24] M. S. Berman, *Nuovo Cimento B* **74** (1983) 182.
[25] D. D. Pawar and Y. S. Solanke, *Int. J. Theor. Phys.* **53** (2014) 3052–3065.
[26] D. D. Pawar, Y. S. Solanke and S. N. Bayskar, *Prespacetime.* **5**(2) (2014) 60–68.
[27] C. B. Collins and S. W. Hauking, *Astrophys. J.* **180** (1973) 317.
[28] M. S. Berman and F. de Mello Gomide, *Gen. Relat. Gravit.* **20** (1988) 191–198.
[29] A. Pradhan, H. Amirhashchi and B. Saha, *Int. J. Theor. Phys.* **50** (2011) 2923–2938.
[30] B. Saha, *Chin. J. Phys.* **43** (2005) 1035–1043.
[31] B. Saha, *Astrophys. Space Sci.* **302** (2006) 83–91.
[32] T. Singh and R. Chaubey, *Astrophys. Space Sci.* **319** (2009) 149–154.
[33] P. K. Sahoo, P. Sahoo, B. K. Bishi and S. Aygün, *Mod. Phys. Lett. A* **32**(21) (2017) 1750105.
[34] V. J. Dagwal, D. D. Pawar, Y. S. Solanke and H. R. Shaikh, *Mod. Phys. Lett. A* **35**(24) (2020) 2050196.
[35] S. Kumar and Ö. Akarsu, *Eur. Phys. J. Plus* **127** (2012) 64.
[36] V. B. Johri and K. Desikan, *Gen. Relativ. Gravit.* **12** (1994) 1217.
[37] V. Singh and A. Beesham, *Gen. Relativ. Gravit.* **51** (2019) 166.
[38] M. S. Berman, *Phys. Rev. D* **43** (1991) 1075.
[39] M. S. Berman, *Gen. Relativ. Gravit.* **23** (1991) 465.
[40] A. Beesham, *Gen. Relativ. Gravit.* **25** (1992) 561.
[41] A. Beesham, *Phys. Rev. D* **48** (1993) 3539.
[42] A. Pradhan, V. K. Yadav and I. Chakrabarty, *Int. J. Mod. Phys. D* **10** (2001) 339.
[43] G. P. Singh and K. Desikan, *Pramana J. Phys.* **49** (1997) 205.
[44] V. Singh and C. P. Singh, *Astrophys. Scace Sci.* **346** (2013) 285.
[45] P. A. R. Ade *et al.*, *Astron. Astrophys.* **594** (2016) A13.
[46] E. Komatsu *et al.*, *Astrophys. J. Suppl.* **192** (2011) 18.
[47] T. Padmanabhan, *Phys. Rep.* **380** (2003) 235–320.
[48] S. M. Carroll, *Living Rev. Rel.* **4** (2001) 1.
[49] T. Chiba, *Phys. Rev. D* **60** (1999) 083508.
[50] L. Amendola, *Phys. Rev. D* **62** (2000) 043511.
[51] R. R. Caldwell, M. Kamionkowski and N. N. Weinberg, *Phys. Rev. Lett.* **91** (2003) 071301.
[52] J. Kujat *et al.*, *Astrophys. J.* **572** (2002) 1–14.
[53] M. Bartelmann *et al.*, *New Astron. Rev.* **49** (2005).
[54] S. D. Odintsov, V. K. Oikonomou and E. N. Saridakis, *Ann. Phys.* **336** (2015) 141.
[55] T. Harko, F. S. N. Lobo, S. Nojiri and S. D. Odintsov, *Phys. Rev. D* **84** (2011) 024020.
[56] P. Wu and H. Yu, *Phys. Lett. B* **707** (2011) 223.
[57] R. Myrzakulov, *Eur. Phys. J. C* **71** (2011) 1752.
[58] B. Li, T. P. Sotiriou and J. D. Barrow, *Phys. Rev. D* **83** (2011) 064035.

[59] M. A. H. MacCallum, *Commun. Math. Phys.* **18** (1971) 2116.
[60] M. Bojowald, *Rev. Rel.* **8** (2005) 11.
[61] A. Ashtekar and P. Singh, *Class. Quantum Grav.* **28** (2011) 213001.
[62] P. Singh, *Phys. Rev. D* **85** (2012) 104011.
[63] M. F. Shamir, *Eur. Phys. J. C.* **75** (2015) 354.
[64] A. Pradhan and H. Amirhashchi, *Astrophys. Space Sci.* **332** (2011) 441–448.
[65] R. Bali and P. Kumawat, *Phys. Lett. B* **665** (2008) 332.

International Journal of Scientific Research in Science and Technology
Print ISSN: 2395-6011 | Online ISSN: 2395-602X (www.ijsrst.com)
© 2021 | IJSRST | Volume 8 - Issue 1

Comparison of Free Length Thermodynamically and Acoustically of alpha-Alumina (α-Al_2O_3) Nano Suspension in Ethanol Base Fluid

P. D. Bageshwar[1], V. K. Jadhao[2] and N. R. Pawar[3]

[1]Department of Physics, Mungsaji Maharaj Mahavidyalaya, Darwha, Maharashtra, India

[2]Department of Physics, B. B. Arts, N. B. Commerce and B. P. Science College, Digras, Maharashtra, India

[3]Department of Physics, Arts, Commerce and Science College, Maregaon, Maharashtra, India

*Corresponding Author : pdbageshwar@gmail.com

ABSTRACT

The present paper reports the comparison of free length thermodynamically and acoustically of alpha alumina (α-Al_2O_3) nano suspension in ethanol base fluid. α-Al_2O_3 nanoparticles were synthesized through alkoxide route using sol-gel method. Intermolecular free length has been calculated by thermo acoustical method at different temperatures over the entire range of concentrations and compared with the valued obtained from well established thermodynamic method. The ultrasonic velocity measurement at 4 MHz with an interferometric technique has been made on alpha alumina (α-Al_2O_3) nano suspension in ethanol base fluid. Measurement was taken for the density. The intermolecular free length was calculated from the velocity and density measurements. Free length is related with the surface of nanoparticles and nanoparticle surfactant interactions and help for the study of thermo acoustic and thermodynamic properties of nanosuspension.

Keywords : α-Al_2O_3, Ethanol, Free Length, Nanosuspension

I. INTRODUCTION

Extensive use of free length has been made to study the attraction and repulsion forces between the nanoparticles in nanosuspension. Thermo acoustically free length of nanoparticles in nanosuspension is given by, $L_f = K (\beta a)^{1/2} = K/U\rho^{1/2}$

Where βa, U and ρ respectively the adiabatic compressibility, ultrasonic velocity and density of nanoparticles in suspended medium. The constant K is called Jacobson's constant, which depends on temperature. Jacobson determined the value of K empirically between 0 and 50^{0}C.

Thermodynamically, free length of nanoparticles in nanosuspension is given by,

$$L_f = 2V_a/A$$

Where V_a and A represents the available volume and the surface area of nanoparticles in nanosuspension. Also,

$$V_a = V - V_O$$

$$A = (36\pi N V_O^2)^{1/3}$$

Where N is the Avogadro number V_O, and V is the molar volume at zero temperature and at temperature T, respectively.

Thermodynamically, the value of V_a can be calculated using critical temperature from the following relation,

$$V_a = V [1- (1- T/Tc)^{0.3}]$$

Where Tc is the critical temperature.

The free length has been widely used to interpret the interactions between nano suspensions in the base fluid. There has been an increasing interest in the study of interactions between the nanoparticles in the suspended medium [1-2]. Ultrasonic study of nanosuspension has been extensively carried out in different branches of science to measure the thermodynamic properties to predict the nature of interactions of nanosuspension in base fluid [3-4]. Ultrasonic velocity and thermo acoustic parameters as a function of the concentration in nanoparticle suspension are useful in gaining insight into the structure and bonding of associated nano complexes and other processes in nanosuspension. The materials of interest in this study are α-Al_2O_3 and ethyl alcohol (C_2H_5OH). Thus ethyl alcohol has an OH group that might be expected to lead to the formation of a hydrogen-bonded nano complex with α-Al_2O_3 at the oxygen site and perhaps electrostatic bonding at the other sites. These types of nanosuspension are of interest to organic chemists who want to know about the type of bond and the number of each kind of nanoparticles in the α-Al_2O_3 nano complex.

In this work, measurements of free length acoustically and thermodynamically are functions of concentration and temperatures are reported. The data presented may stimulate other researchers to consider the interactions of nanoparticles in nanosuspension. Such data are valuable in building a core of basic information about nanosuspension. The method used in the measurement of ultrasonic velocity at 4 MHz was the interferometric method over the temperature range 25-40^{0}C.

The main objective of present work is to contribute the free length of α-Al_2O_3 nanosuspension properties database in current literature in order to better understand the effects of various parameters such as particle size and temperatures. Free length is highly dependent on specific surface area of nanoparticle in nanosuspension.

II. EXPERIMENTAL AND METHODS

The test liquid samples used were spectroquality. All these samples are of BDH analar grade and were assume to be sufficiently pure so that no further purification was necessary. In this study the ultrasonic measurements have been made by interferometric method at fixed frequency 4 MHz over the entire range of concentrations and in the temperature range 25 – 40^{0}C. The velocity of ultrasound thus measured was accurate to within 0.01%. The densities were measured with an Anton Paar DMA 35 N vibrating tube densimeter with a $\pm 0.5 \times 10^{-3}$g/cm^3 resolution. The temperature of nanosuspension medium was controlled to within 0.2^{0}C. Nanoparticles of alpha alumina (α-Al_2O_3) was prepared by sol-gel method [6-11] from Aluminum isopropoxide [Al (OC_3H_7)$_3$] and aluminum nitrate. The average particle size α-Al_2O_3 has been estimated by using Debye-Scherrer formula. The average estimate size of α-Al_2O_3 nano particles is found to be 20-30 nm Pawar et.al. The prepared α-Al_2O_3 nano particles were suspended in ethanol.

III. RESULTS AND DISCUSSION

The intermolecular forces, which in one way or another determine the said properties of nanosuspension, consist of attractive forces and repulsive forces. These forces have opposite directions but are numerically equal under given external conditions. The attractive forces are dependent on the distance between what are called the centres of attraction of the nanoparticles, whereas the repulsive forces are dependent on the distance between the surfaces of the nanoparticles. Centres of attraction do not coincide with the geometrical centre of the nanoparticles. The distances between the surfaces have a clear physical significance, and thus lend themselves

more easily. Surface tension, viscosity, thermal expansion and molecular association will be related to the intermolecular free length. The acoustic wave which was excited in the nano suspended medium is momentarily to the intermolecular length. Free length is long, ultrasonic velocity has a low value. Its value corresponded to the molecular shape Fig.11 contains the plot of free length computed acoustically versus molar concentration. It shows similar trend as that of adiabatic compressibility and reverse trend as that of ultrasonic velocity which is in good agreement with the theoretical requirement.

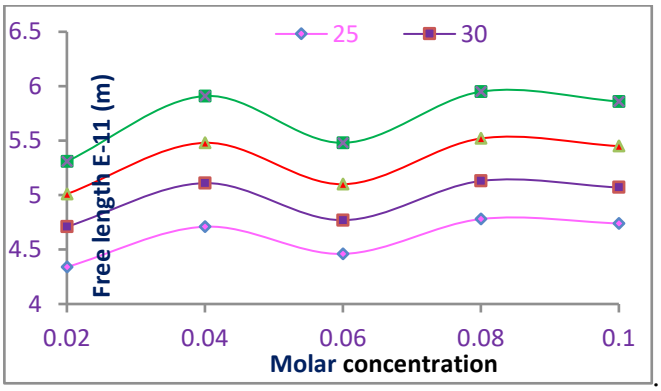

Figure.1 Free length versus molar concentration of α-Al_2O_3 nanosuspension in ethanol

IV. CONCLUSION

1. The free length computed acoustically and thermodynamically shows considerable deviation from any linear variation with respect to molar concentrations.
2. Non linear variation of free length versus molar concentration is due to Brownian motion of nanoparticles in nanosuspension.
3. Behavior of nanoparticles in ethanol base fluid nano suspension dependent on its specific surface area.
4. Free length study of nanoparticles in nanosuspension highly useful in understanding nature of interactions, internal structure and the aggregation behavior.

V. REFERENCES

[1]. D.H. Kumar, H.E. Patel, V.R.R. Kumar, T. Sundararajan, T. Pradeep, S.K. Das, Model for heat conduction of nanofluids, Physical Review Letters, 2004, 94, 14, 1-3.

[2]. S. Rajagopalan, S. J. Sharma and V. Y. Nanotkar, Ultrasonic Characterization of Silver Nanoparticles, Journal of Metastable and Nanocrystalline Materials 2005, 23 271-274.

[3]. Gan Z, Ning G, Lin Y, Cong Y, Morphological control of mesoporous alumina nanostructures via template-free solvothermal synthesis. Mater Lett 2007, 61, 31, 3758–3761.

[4]. Zhan X, Honkanen M, Leva E Transition alumina nanoparticles and nanorods from boehmite nanoflakes. J Crystal Growth, 2008, 310, 30, 3674–3679.

[5]. Y. K. Park, E. H. Tadd, M. Zubris, and R. Tannenbaum, Size controlled synthesis of alumina nanoparticles from aluminum alkoxides, Materials Reasearch Bulletin, 2005, 40, 9, 1512.

[6]. D. G. Wang, F. Guo, J. F. Chen, H. Liu, and Z. Zhag, Preparation of nano aluminium trihydroxide by high gravity reactive precipitation, Chemical Engineering Journal, 2006, 121, 2-3, 109-114.

[7]. R. Aghababazadeh, A. R. Mirhabibi, J. Pourasad, A. Brown, A. Brydson, and N. Ameri Mahabad, Economical synthesis of Nanocrystalline alumina using an environmentally low-cost binder, Journal of Surface Science, 2007, 601,13,2864-2867

[8]. P. Christian and M. Bromfield, Preparation of small silver, gold and copper nanoparticles which disperse in both polar and non-polar solvents, J. Mater. Chem, 2010, 20, 1135 – 1139.

[9]. Rogojan R, Andronescu E, Ghitulica C, Stefan B, Synthesis and characterization of alumina nano-powder by sol-gel method. UPB Sci Bull Ser B , 2011, 73, 2, 27, 67–76.

[10].Bhalla V., Kumar R., Tripathi S. and Sing D., Mechanical and thermal properties of praseodymium nanoparticles: an ultrasonic study, Int. J. Mod. Phys. B, 2013, 27, 1350116.
[11].Pawar N. R., Ph.D thesis Summary on Investigation of Ultrasonic wave absorption in some Bio-liquids, J Pure and Appl Ultrasonic, 2014, 36, 69.
[12].Pawar N. R. and Chimankar O. P., Comparative Study ultrasonic absorption and relaxation behavior of polar solute and non-polar solvent, Pure and Appl Ultrasonic, 2015, 37, 11.
[13].Johari G K & Mishra R L, Acustica, 1984, 56, 66.

Peer Reviewed Refereed
and UGC Listed Journal
Journal No. 47023

ISSN 2319 - 8508
AN INTERNATIONAL
MULTIDISCIPLINARY
HALF YEARLY
RESEARCH JOURNAL

GALAXY LINK

Volume - IX, Issue - II
May - October - 2021
English / Marathi Part - I

Impact Factor /
Indexing
2019 - 6.571
www.sjifactor.com

Ajanta
Prakashan

ISSN 2319 - 8508

AN INTERNATIONAL MULTIDISCIPLINARY
HALF YEARLY RESEARCH JOURNAL

GALAXY LINK

Volume - IX Issue - II May - October - 2021

English / Marathi Part - I

Peer Reviewed Refereed
and UGC Listed Journal
Journal No. 47023

ज्ञान-विज्ञान विमुक्तये

IMPACT FACTOR / INDEXING
2019 - 6.571
www.sjifactor.com

❖ EDITOR ❖

Assit. Prof. Vinay Shankarrao Hatole
M.Sc (Math's), M.B.A. (Mkt), M.B.A (H.R),
M.Drama (Acting), M.Drama (Prod & Dirt), M.Ed.

❖ PUBLISHED BY ❖

Ajanta Prakashan
Aurangabad. (M.S.)

CONTENTS OF MARATHI PART - I

१३. भारतीय अर्थव्यवस्थेवर कोविड - १९ चा प्रभाव

प्रा. डॉ. के. व्ही. ढवळे
वाणिज्य विभाग प्रमुख, मुंगसाजी महाराज महाविद्यालय, दारव्हा.

कोविड–19 काळात भारताची अर्थव्यवस्था या पूर्वीच मंदावली आहे. कोविड–19 लॉकडाउनच्या काळात अव्वल जोखिमेमूळे देशात कोरोना व्हायरसचा प्रादुर्भाव वाढतच गेला. देशातील कोरोना रुग्णाची संख्या ही वाढतच गेली. हा प्रादुर्भाव रोखण्यासाठी सरकारने लॉकडाऊन घोषीत केला होता. हा लॉकडाऊन दीर्घकाळ चालल्याने त्याचा आंतराष्ट्रीय नाणेनिधी भारतीय अर्थव्यवस्थेवर या काळाचा धक्कादायक अंदाज व्यक्त केल्या जात होता. 2020 मध्ये भारतीय अर्थव्यवस्था 4.5 टक्यानी घसरेल आणि ही घसरण ऐतिहासीक असेल असं नाणेनिधीने म्हटलं होत. तर ती घसरण 3.3 टक्क्यांनी खाली आली आहे. जी 11 वर्षातील सर्वात कमी आहे. अर्थशास्त्राच्या मते 'पुरवठा साइड संकुचित परिणाम ' उत्पादन, शेती आणि औषधे उद्योगावर परीणाम करेल. कोरोना विषाणू संपूर्ण देशाच्या आर्थिक घडामोडींमूळे कोरोना विषाणूला बाधा येते म्हणून भाराताला सरकारच्या महसुलात आणि कमीतकमी दोन तिमाहीच्या उत्पन्नातील वाढीची घट आहे. गुंतवणूकदाराच्या भावना कमी झाल्यामूळे खासगीकरण योजना सरकार आणि उद्योग यांच्यावर परिणाम झाला.

जागतिक आरोग्य संघटनेने (डब्ल्यूएचओ) 12 मार्च रोजी कोरोना रोग (सीओव्हीआयडी–1) या कादंबरीचा नुकताच उर्देक झाल्याची घोषणा केली. 11.4 ट्रिलियन भागधारकांची संपत्ती पर्यटन, विमानचालन, अतिथ्य आणि व्यापार या सारख्या क्षेत्रांना कोरोना आव्हानांचा सामना करावा लागतो. इतर क्षेत्रांनाही चकीय परिणामाचा सामना करावा लागला. देशाचे अहवाला नुसार देशांतर्गत प्रवासामध्ये 20 टक्के घट झाली आहे आणि आंतरराष्ट्रीय प्रवासी बुकींगमध्ये 75 टक्के कपात झाली आहे. हॉटेल बुकींगचे दरही 70 टक्के वरुन 20 टक्के पर्यंत खाली आले आहेत. रेस्टॉरंट व्यवसायात 30 ते 35 टक्के पर्यंत खाली आले होते. पोल्ट्री क्षेत्राची विकीही जवळपास दररोज 1,500 ते 2,000 कोटी एवढी घट झाली. कोरोना विषाणूचा प्रादूर्भाव हा जागतिक अर्थव्यवस्था आणि वित्तीय बाजारपेठेसाठी सर्वात मोठा धोका बनला आहे. ग्लोबल व्हीलेज इंडीयाचा एक भाग असल्याने या विषाणू पासून मुक्ती नाही. भारत सरकार तसेच राज्य सरकारने कोरोना विषाणूच्या साथीच्या रोगाचा प्रसार रोखण्यासाठी परिस्थितीवर बारीक लक्ष ठेवून उपचार घेत आहेत. या समस्येचे स्पष्ट चित्र प्राप्त करण्यास बराच काळ लागू शकतो. या करीता जागरुक आणि सतर्क राहणे देशातील प्रत्येक नागरीकाला फार महत्वाचे आहे.

आरबीआय देशातील संकट परिस्थितीला तोंड देण्यासाठी आवश्यक पावले उचलत आहे. उदयोन्मुख परिस्थितीत रिझर्व्ह बॅंकेने बिझिनेस सातत्य योजना तयार केली आणि कर्मचारी इतर ग्राहक यांच्यात रणनीती आखून सूचनांचे वाटप करीत आहे. आरबीआय ने ओपन मार्केट देखिल सुरु केले आहे.

प्रधानमंत्री मा. नरेंद्र मोदी यांनी आश्वासन दिले की सरकार आपल्या पाठीशी आहे आणि आपण स्वतःची अलग ठेवणे करुन स्वतः मदत केली पाहिजे नागरिक म्हणून आपण जागतिक हातानी संकटात अढावे आणि भारत

सरकारच्या निर्देशानुसार मुलभूत आरोग्य व स्वच्छताविषयक सुचना पाळणे आवश्यक आहे. आम्हाला आपल्या कृतीबद्दल सावधगिरी बाळगण्याची आवश्यकता आहे आणि एकत्र आपण निश्चितपणे या विषाणूवर मात करु आणि या ग्रहाचे जगणे अधिक चांगले बनवू. आशा आहे की बाजारपेठेतील चिंता लवकरच मरेल आाणि अर्थव्यवस्थेची प्रगती होईल.

कोविड–19 ने समाजातील सर्वच घटकावर परिणाम केला आहे, ही बाब गंभीर आणि चिंतेची बाब आहे. शंभराहून अधिक देशाच्या अर्थव्यवस्थेवर याचा गंभीर परिणाम झाला आहे. अशा प्रकारे अनेक देशांनी आंतरराष्ट्रीय नाणेनिधी कडून आर्थिक मदतीसाठी विचारणा केली आहे. करमणूक, विमानचालन, अतिथ्य इत्यादी सारख्या जगभरातील व्यवसायावर लक्षणीय नकारात्मक प्रभाव दिसला. ऑलंम्पिक किकेट 20–20 विश्वचषक असे विविध खेळाचे कार्यकम पुढे ढकलले गेलेले आहेत. अमेझॉन, फ्लिपकार्ड इत्यादी विविध ऑनलाइन दिग्गज कंपण्यांच्या कामकाजावरही याचा परिणाम झाला आहे. अमेरीका, भारत, ब्राझील,इटली आणि स्पेनसारख्या देशांमध्ये त्यांचे मृत्यूचे प्रमाणे खूपच जास्त आहे. ही बाबही फार चिंतेची व गंभीर आहे.

कोरोना विषाणूमूळे देशाच्या आर्थिक घडामोडीचा फटका बसत असल्याने कमीतकमी दोन चतुर्थांश सरकारच्या महसुलात आणि उत्पन्नाच्या वाढीमध्ये भारताला मोठ्या प्रमाणात घट झाली आहे. गुंतवणूकदाराच्या भावना कमी झाल्यामूळे खाजगीकरण योजना, उद्योग, सरकार यावर परिणाम होतो. जागतिक अर्थव्यवस्थेत महत्वपूर्ण बदल झाला आहे. रेस्टॉरंट्स , पब, बाजार, विद्यापीठे आणि महाविद्यालये इत्यादी बंद पडले आहेत. या भीतीमूळे व्यक्तीची हालचाल मर्यादीत झाली आहे. जनता दररोज वापरलेली उत्पादने खरेदी करत नव्हते. या सर्वांचा परिणाम जगाच्या अर्थव्यवस्थेवर होत आहे. आर्थिक सहकार आणि विकास संस्थेने नोंदवले आहे की जागतिक वाढीची अपेक्षा 2.9 टक्के वरुन 2.4 टक्के वर कमी केल्या गेली आहे. आणि ती 1.5 टक्के पर्यंत खाली येऊ शकते. आकडेवारीनुसार भारताची जीडीपीमधील जीडीपी गमावण्याची शक्यता अंदाजे 5–10 अब्ज डॉलर्स (जीडीपीच्या 0. 15–0.35 टक्के) असेल. बेंचमार्क निर्देशांकामध्ये 20 टक्के पेक्षा जास्त कपात भारतीय समता बाजार अस्वलाच्या बाजारपेठेत दाखल झाला आहे. नवीन कोरोना विषाणूमूळे गुंतवणूकदारांना बॉन्डच्या किंमती वाढविण्यास प्रवृत्त केले जाते. परिणामी प्रमुख अर्थव्यवस्थांमध्ये उत्पादन कमी होते. आणखी वाईट विचार करणे म्हणजे रशियाच्या सौदी अरविया दरम्यान कच्चा तेलाचे युध्द आहे ज्याने इतर मालमत्ता मध्ये अस्थिरता आणली आहे. कुडच्या किंमती कमी झाल्यामूळे पेंट्स, स्पेशालिटी केमिकल्स, हेअर ऑईल, सिमेंट, प्रीव्हीसी पाईप्स इत्यादी विभागांना फायदा होईल. मोठ्यया वित्तीय संस्थांच्या अपयशामुळे होणारी घरगुती वापराची मंदी, येस बँक संकटाच्या रुपाने आणखी एक परिस्थिती वनली आहे. अन्य वस्तू खाली असतांना अनिश्चिततेत सुरक्षित आसराची मागणी केल्यामूळे सोन्याची वाढ झाली आहे.

भारतातील लॉकडाऊनने अर्थव्यवस्थेवर परिणाम केला आहे. मुख्यतः उपभोग, जीडीपीतील सर्वात महत्वाचा घटक आहे. चीनसारख्या इतर देशाकडून कच्चा मालाच्या आयातीवर अवलंबून असणारी इलेक्ट्रॉनिक्स, खत, औषध या क्षेत्रावर भारताच्या आयात आणि निर्यातवर गंभीर परिणाम झाला आहे.

कोरोना व्हायरस या साथीच्या रोगाने सर्व देशभर या साथीच्या आजाराचा परिणाम भारतावर मोठ्या प्रमाणात झाला आहे. आर्थिक कियाकलाप तसेच मानवी जीवितहानीच्या दृष्टीने विघटनकारी ठरला आहे. देशांतर्गत मागणी

आणि निर्यातीमध्ये काही प्रमाणात लक्षणिय अपवाद आहेत ज्यामध्ये उच्च वाढ दिसून आली आहे. जवळजवळ सर्वच क्षेत्रावर विपरीत परिणाम झाला आहे. काही महत्वाच्या क्षेत्राकरीता होणारे परिणाम आणि संभाव्य समाधानाचे विश्लेषण करण्याचा प्रयत्नद केला जात आहे.

कृषि आणि खाद्य

कृषि हे आपल्या देशाचा कणा आहे. शासनाच्या एका भागाने अत्यावश्यक प्रवर्गाची घोषणा केली असल्याने प्राथमिक शेती उत्पादन आणि कृषि साधनाचा वापर या दोन्ही बाबींवर त्याचा परिणाम कमी होण्याची शक्यता आहे. अनेक राज्य सरकारांनी फळे, भाज्या दूध इत्यादींची मुक्त हालचाल करण्यास या पूर्वीच परवाणगी दिली आहे. ऑनलाईन फूड किराणा मालाचे प्लॅटफार्मवर हालचालींवर अस्पष्ट निर्बंध आणि लॉजिस्टिक वाहने थांबविल्यामूळे याचा मोठा परिणाम होतो. आरबीआय आणि अर्थमंत्र्यांनी घोषित केले की, या उपाययोजनांनमूळे उद्योग आणि कर्मचाऱ्यांना अल्पावधीत मदत होईल. येत्या आठवड्यात ग्रामिण अन्न उत्पादन क्षेत्राला इन्सूलेट केल्याने कोविड –19 च्या भारतीय खाद्य क्षेत्रावर तसेच मोठ्या अर्थव्यवस्थेवर होणाऱ्या या मॅको परिणामास मोठे उत्तर मिळेल.

विमानचालन आणि पर्यटन

जीडीपीमध्ये उड्डान क्षेत्र आणि पर्यटनाचे योगदान अनुकमे 2.4 टक्के आणि 2.2 टक्के आहे. आर्थीक वर्ष 18–19 मध्ये पर्यटन क्षेत्राने अंदाजे मिलियन 43 दशलक्ष लोकांना सेवा दिली. विमानचालन आणि पर्यटन हे पहिले उद्योग होते ज्यांना साथीचे रोगाचा फारसा परिणाम झाला होता. सर्वसाधारण एकमत असे दिसते की, कोरोनामूळे या उद्योगांना 9/11 आणि 2008 च्या आर्थिक संकटापेक्षा अधिक मोठा कठोर फटका बसणार आहे. साथीचे रोग सुरु होण्यापासून हे दोन उद्योग गंभीर रोख प्रवाहाच्या मुद्द्यांशी संबंधीत आहेत. आणि संभाव्य 38 दशलक्ष लोकांकडे लक्ष वेदत आहेत. कामगाराच्या 70 टक्के भाषांतरित करतात. याचा परिणाम व्हाईट आणि ब्ल्यू कॉलर या दोन्ही जॉबवर पडणार आहे. आयएटीओच्या अंदाजानुसार प्रवासी निर्बंधामूळे या उद्योगांना सुमारे 85 अब्ज रुपयाचे नुकसान होऊ शकते. कॉन्टॅक्टलेस बोर्डिंग आणि ट्रॅव्हल्स टेक्नॉलॉजी या क्षेत्रांनाही साथीचा हा रोग नवनिर्मीतीची लाट आणल्याचे दिसते.

दुरध्वनी

सेवा पुरवठ्यामधील अल्प किंमतीच्या युध्दांमूळे कोविड–19 च्या आधीपासून भारताच्या दुरसंचार क्षेत्रात काही प्रमाणात वदल झालेत. निर्बंधामुळे Work from home ' घरातून काम ' अंमलात आणल्याबद्दल साथीच्या आजारात सर्वात चौर्य सेवा आणि क्षेत्र चालू आहे. 1 अब्जाहून अधिक कनेक्शनसह दूरसंचार क्षेत्र जीडीपीच्या .5 टक्के वाटा जवळजवळ मिलीयन दशलक्ष लोकांना रोजगार देते. वाढलेल्या ब्राडबॅंड वापराचा थेट परिणाम झाला आणि त्याचा परिणाम नेटवर्कवर दवाव निर्माण झाला. मागणीत सुमारे 10 टक्के वाढ झाली आहे. तथापी, टेलको नवीन ग्राहक जोडण्यात मोठ्या प्रमाणात घट करीत आहेत. धोरणात्मक शिफारस म्हणून सरकार नियामक अनुपालन शिथील करुन या क्षेत्राला मदत करु शकते आणि स्पेक्ट्रमच्या थकबाकीसाठी मोटोरियम देऊ शकते. ज्याचा उपयोग कंपन्यांव्दारे नेटवर्क विस्तारासाठी केला जाऊ शकतो.

फार्मासिअटिकल

कोविड–19 या साथीच्या रोगाने संपूर्ण जगभर थैमान घातले आहे. साथीच्या आजाराच्या सुरुवातीपासूनच औषध उद्योग वाढीस लागला आहे. विशेषतः जगामध्ये जेनेरिक औषधांचा सर्वात मोठा उत्पादक भारत आहे. सुरुवातीच्या काळात बाजारामध्ये 55 अब्ज डॉलर्स 2020 हे भारतमध्ये हायड्रोक्सीस्लोरोक्विन निर्यात करत आहे. युएस, युके, कॅनडा आणि मध्य–पूर्व पर्यंत साथीच्या आजारामूळे चीनमधून आयात केलेल्या कच्चा मालाच्या किंमतीमध्ये नुकतीच वाढ झाली आहे. सामाजिक दुरवस्थेमुळे होणारी आयात, पुरवठा साखळीत व्यत्यय आणि उद्योगातील कामगारांच्या अनुपलब्धतेवर मोठ्या प्रमाणात अवलंबून असल्यामूळे जेनेरिक औषधांचा सर्वाधिक परिणाम होतो. त्याच बरोबर, देशाला पुरेशा प्रमाणात रक्कम मिळावी यासाठी गंभीर औषध, उपकरणे आणि पीपीई किटच्या निर्यातीवर सरकारने घातलेली बंदी असल्याने औषधी उद्योग धडपडत आहे. या औषधांची वाढती मागणी, अडथळा असलेल्या प्रवेशयोग्यतेसह गोष्टी अधिक कठीण करत आहेत. फार्मास्युटिकल कंपन्यावरील आर्थिक ताण कमी करणे, करात सवलत देणे आणि कामगार शक्तीची कमतरता दूर करणे अशा निराशेच्या वेळी वेगळे घटक असू शकतात.

तेल आणि गॅस

भारतीय तेल आणि वायू उद्योग जागतिक संदर्भात लक्षणीय आहे. फक्त युएसए आणि चिनच्या मागे हा तिसरा सर्वात मोठा ऊर्जा ग्राहक आहे. आणि तेलाच्या जागतिक मागणीत 2.2 टक्के आहे. वाहन व औद्योगिक उत्पादन घटल्याने वस्तू व प्रवासी हालचाली (मोठ्या प्रमाणात व वैयक्तिकरित्या) कमी झाल्याने देशभरात संपूर्ण बंद पडल्याने परिवहन इंधनाची मागणी (तेल व वायू क्षेत्रातील 2/3 मागणी आहे) कमी केली. या काळात कच्चा किंमतीत घट झाली असली तरी, महसुली तोटा पूर्ण करण्यासाठी सरकारने उत्पादन शुल्क व विशेष उत्पादन शुल्क वाढविले, त्याव्यतिरिक्त रस्तेही वाढविण्यात आले. धोरणात्मक शिफारस म्हणून मागणी वाढविण्यासाठी किरकोळ दुकानातील ग्राहकांना संपवण्यासाठी कच्चा किंमती कमी झाल्याने होणारे फायदे मंजूर करण्याचा सरकार विचार करु शकेल.

कोविड–19 या साथीच्या आजारामूळे होणाऱ्या परिणामामूळे विस्कळीचे प्रमाण लक्षात घेता, हे दिसून येते की सध्याची मंदी मंदीपेक्षा मूलभूतपणे भिन्न आहे. मागणी आणि अचानक वाढलेली बेरोजगारी व्यवसायाच्या लॅंडस्केपमध्ये बदल घडवून आणणार आहे. 'लोकलायझेशनकडे वळविणे, रोख संवर्धन पुरवठा साखळीची लचक आणि नाविन्य' या सारख्या नवीन तत्वांचा अवलंब व्यवसायांना या अनिश्चित वातावरणात नवीनमार्गावर चालण्यास मदत होईल.

संदर्भ

- संकेतस्थळ
- व्यवसाय जागतिक वेबसाईट
- विकिपीडिया
- शोधगंगा

Peer Reviewed Refereed and UGC
Listed Journal (Journal No. 47037)

ISSN 2278 - 8158
AN INTERNATIONAL
MULTIDISCIPLINARY HALF YEARLY
RESEARCH JOURNAL

ROYAL

Volume - X, Issue - I
June - November - 2021
English / Marathi Part - I

Impact Factor / Indexing
2019 - 5.756
www.sjifactor.com

Ajanta Prakashan

ISSN 2278-8158

AN INTERNATIONAL MULTIDISCIPLINARY
HALF YEARLY RESEARCH JOURNAL

ROYAL

Volume - X Issue - I June - November - 2021

English / Marathi Part - I

Peer Reviewed Refereed
and UGC Listed Journal
Journal No. 47037

ज्ञान-विज्ञान विमुक्तये

IMPACT FACTOR / INDEXING
2019 - 5.756
www.sjifactor.com

❖ EDITOR ❖

Assit. Prof. Vinay Shankarrao Hatole
M.Sc (Math's), M.B.A. (Mkt), M.B.A (H.R),
M.Drama (Acting), M.Drama (Prod & Dirt), M.Ed.

❖ PUBLISHED BY ❖

Ajanta Prakashan
Aurangabad. (M.S.)

VOLUME - X, ISSUE - I - JUNE - NOVEMBER - 2021
ROYAL - ISSN 2278 - 8158 - IMPACT FACTOR - 5.756 (www.sjifactor.com)

CONTENTS OF ENGLISH PART - I

6. Place of Agriculture in National Economy

Prof. Dr. K. V. Dhawale
HOD of Commerce Dept. Mungasaji Maharaj Mahavidyalaya, Darwha.

Conclusion

Thus agriculture occupies a position of outstand importance in the Indian economy having a high emloyment potential; it is important in its contribution to national income as a source of food and raw metrials, as being vital to international trade, as a yielder of state revenue and as countributing to social and political stability. But too much dependence on agriculture makes the Indian economic unstable and unbalance and is a major cause of india's appalling poverty.

The importance of Agriculture to India can hardly be exaggerated. It is the very backbone ot her economic system and is her premier, national, key industry. In fact, the prosperity of agriculture is synonymous with the properity of India. Also, agriculture is assuming even greater importance with the passage ot time. Internal demand for food is on the increase as a result of growing population and rising standard of living. Indian agriculture will have to meet the need of more raw materials of a better quality as the economy grows under the Five-Year Plans. Agriculture is important from several point of view.

As a Source of Liveli Hood

Millions of people in India draw their livehood from agriculture. Some draw their sustenance fromdirect cultivation, others from the movement of crops and still others from trade in the agriculture products. About 75% of the people depand for living on agriculture, directly and indirectly. Whereas in the West and other developed countries, the percentage of the people dependent on agriculture has been going down and is 10 to 20 %, in India it has remained remarkably stable.

As a Coutributor to Nationl Income

Out of a total national income the share of agriculture in the national income is bound to go down as the Indian economy grows, as it has happened in the developed countries of the west, yet for a long time to come, it seems the pre-dominance of agriculture is likely to continue.

As a Supplier of Food: - The inhabitants of the country obtain their food from agriculture in various forms, e.g., cereals, fruit, vegetables, etc. What would have happened to the teeming millions without this source of food can be easily imagined. But we cannot help adding that it is a sorry state of affairs when India has to depend on foreign food in spite of three –fourths of its people engaged in agriculture.

As a support for Industrial Development

It goes without saying that industrialisation of India draws its supports and sustenance from Indian agriculture. It supplies the industrial raw materials like cotton, jute, and sugar cane. Prosperous agriculture will provide the necessary purchasing power to the rural masses for the absorption of manufactured goods. It will lay the foundation of many agro-industries, e.g., food processing industries.

Improtance in Trade

Agriculture products constitute the mainstaples of our internal external trade. Indian agriculture thus determines the volume andcomposition of trade.

As a Foreign Exchange Eraner :- Indian tea, oil seeds, spices, tobacco, etc., find ready market abroad and earn for the country valuable foreign exchange which is an important wherewithal of economic development. Bymeans of it India is able to obtain from abroad plant and machinery, accessories, industrial raw materials and technical know-how.

Financial Stability :- Agriculture is very foundation of financial stability of the Government. Agriculture prosperity enables the Finance Ministers to balance the budgets. A bad year for agriculture is a bad year all round, for it brings down the railway earnings, yield from land revenue and many other taxes.

Social and Political Importance

Agriculture has also great social and political significance for the country. Agriculture are a sturdy self – reliant class a people who are the backbone of the stste. They are the best soldiers.With there fixed out look and attitudes; they exercise a great stabilizing influence in the social and political spheres.

Reference

- Indian Economics - K.K. Devett
- Indian Economics - Gurucharan singh
- Indian Economics - J. D. Varma
- News Papers

Modern Physics Letters A
2050316 (18 pages)

DOI: 10.1142/S0217732320503162

Study of cosmic models in $f(R,T)$ gravity with tilted observers

V. J. Dagwal[*,§], D. D. Pawar[†,¶] and Y. S. Solanke[‡,‖]

[*] *Department of Mathematics, Government College of Engineering, Nagpur 441 108, India*
[†] *School of Mathematical Sciences, Swami Ramanand Teerth Marathwada University, Vishnupuri Nanded 431606, India*
[‡] *Mungsaji Maharaj Mahavidyalaya, Darwha, Yavatmal 445202, India*
[§] *vdagwal@gmail.com*
[¶] *dypawar@yahoo.com*
[‖] *yadaosolanke@gmail.com*

Received 1 May 2020
Revised 30 August 2020
Accepted 11 September 2020
Published 3 November 2020

In this work, we have studied LRS Bianchi type I cosmological models in $f(R,T)$ gravity with tilted observers, where R is the Ricci scalar and T is the trace of the stress energy tensor. We have explored a tilted model and determined the solutions of the field equations by assuming special law of variation of Hubble's parameter, proposed by Berman (1983) that yields constant deceleration parameter. In this scenario, we have used the equation of state $p = (\gamma - 1)\rho$ and power law of velocity to describe the different anisotropic physical models such as Dust Universe, Radiation Universe, Hard Universe and Zedovich Universe. We have discussed graphical presentation of all parameters of the derived models with the help of MATLAB. Some physical and geometrical aspects of the models are also discussed.

Keywords: Tilted models; $f(R,T)$ theory; equation of state.

1. Introduction

Modern astrophysical observations show that the expansion of the Universe is currently in an accelerated era. The observational data of supernovae type Ia[1,2] and cosmic microwave background (CMB) have investigated that our Universe is expanding at an increasing rate. The $f(R,T)$ modified theory of gravity can be used to investigate some problems of recent interest and may lead to some major variances. In $f(R,T)$ modified theory of gravity, the result of cosmic acceleration not only depends on the geometrical contribution but also depends on matter contents. This

[§]Corresponding author.

theory is extension of $f(R)$ theory of gravity including trace of energy-momentum tensor T. $f(R,T)$ modified theory of gravity is investigated by Harko *et al.*[3] Different aspects of $f(R)$ modified theory of gravity that are studied by Houndjo and Houndjo *et al.*,[4,5] Myrzakulov,[6] Pacif *et al.*[7,8] presented irregularity factors in $f(R,T)$ theory of gravity. Sahoo *et al.*[9] calculated anisotropic models in modified theory of gravity. Tilted model and two fluid models in modified theory of gravity are discussed by Pawar and Dagwal,[10] Dagwal,[11] Dagwal *et al.*[12] Aygün *et al.*[13] examined geometrical and physical properties of $f(R,T)$ gravity. Aktaş[14,15] studied higher dimension with dark energy model in $f(R,T)$ theory of gravity. Aktaş *et al.*[16] obtained magnetic field in modified theory of gravity. Pawar and Solanke[17] developed LRS Bianchi type I cosmological Universe in $f(R,T)$ modified theory of gravity. Dagwal and Pawar[18,46] investigated two-fluid sources in $f(T)$ theory of gravity. Yousuf[40] examined the study of electromagnetic field in $f(R,T)$ gravity. Yousuf[41] has investigated self-gravitating system in modified theory of gravity. Some dynamical properties of $f(G,T)$ gravity studied by Yousuf.[42]

In the tilted model, the fluid velocity vector is not orthogonal to the group orbits and also its spatially homogeneous, otherwise the Universe is said to be non-tilted. Tilted cosmological models have been explored by King and Ellis[19]; Ellis and King.[20] Pawar and Dagwal[21]; Pawar *et al.*[22,23] presented tilted models for different gravitational theories. Dagwal and Pawar[24,25] discussed the properties of tilted two fluids models with G and Λ in General Relativity and tilted dark energy. Tilted models in Brans Dicke theory of gravitation are obtained by Pawar *et al.*[26] Tilted Universe in tensor theory of gravitation is obtained by Sahu.[27] Tilted plane symmetric space-time is expressed by Sharif and Tahir.[28] Sharif and Majid[29] discussed the physical properties of tilted model in electromagnetic field. Nilsson *et al.*[30] examined co-moving models radiation fluid. In tilted model the properties of thermodynamics and hydrodynamics have formulated by Herrera *et al.*[31] Yousaf *et al.*[32,33] presented tilted model in modified theory of gravity. Dagwal and Pawar[34] investigated tilted congruence Universe. Yousuf[43] discussed the hydrodynamics properties of non-comoving model.

The observational data show that our current Universe is accelerating and expanding. By Einstein general theory of relativity, an accelerated expansion of the Universe is due to negative pressure called dark energy and positive energy density and therefore has a negative equation of state parameter. The quantity $\omega(t)$ from expressional data have presented by Sahni and Starobinsky,[35] Sahni *et al.*[36] have calculated the experimental data conducted to determine this parameter as a function of cosmological time. Dark energy has been conventionally characterized by EoS parameter mentioned. The simplest candidate of Dark energy is the vacuum energy ($\omega = -1$), which is mathematically corresponding to the cosmological constant Λ. Yousuf[44,45] presented spherically symmetric geometry in Λ-dominated era and studied the effect of cosmological constant. Ratra and Peebles,[37] Caldwell *et al.*[38] and Feng *et al.*[39] discussed EoS parameter, defined by minimally coupled

scalar fields, are quintessence ($\omega > -1$), phantom energy ($\omega < -1$) and the combination of quintessence and phantom.

By the motivation of the above work, here we have investigated LRS Bianchi type I cosmological models in $f(R,T)$ gravity with tilted observers. We have explored a tilted model and determined the solutions of the field equations by assuming special law of variation of Hubble's parameter, proposed by Berman (1983) that yields constant deceleration parameter. In this scenario, we have used the equation of state $p = (\gamma - 1)\rho$ and power law of velocity to describe the different anisotropic physical models such as Dust Universe, Radiation Universe, Hard Universe and Zedovich Universe. We have discussed graphical presentation of all parameters of the derived models with the help of MATLAB. Some physical and geometrical aspects of the models are also discussed.

This paper is organized as follows. Section 2 deals with metric and field equations. Section 3 deals with some physical and geometrical properties. Section 4 deals with the types of Universe by using equation of state. Section 5 deals with results and discussion and concludes in Sec. 6.

2. Metric and Field Equations

We consider the metric in the form

$$ds^2 = dt^2 - R^2 \left\{ dx^2 + dy^2 + \left(1 + \beta \int \frac{dt}{R^3}\right)^2 dz^2 \right\}, \tag{1}$$

where R is functions of t alone.

The field equation in $f(R,T)$ theory of gravity for the function is given by

$$f(R,T) = R + 2f(T), \tag{2}$$

as

$$R_{ij} - \frac{1}{2} R g_{ij} = T_{ij} + 2f'T_{ij} + [2pf'(T) + f(T)]g_{ij}, \tag{3}$$

The energy–momentum tensor as

$$T_{ij} = (p + \rho)u_i u_j - p g_{ij} + q_i u_j + q_j u_i \tag{4}$$

with

$$g^{ij} u_i u_j = 1, \tag{5}$$

$$q_i q^i > 0, \quad q_i u^j = 0, \tag{6}$$

where q_i is the heat conduction vector orthogonal to u_i, ρ is the energy density, p is the pressure. The fluid vector u_i has the components $(R\sinh\alpha,\ 0,\ 0,\ \cosh\alpha)$ satisfying Eq. (5) and α is the tilt angle.

The prime denotes differentiation with respect to the argument.

We choose the function $f(T)$ as the trace of the stress energy tensor of the matter so that

$$f(T) = \lambda T, \tag{7}$$

where λ is constant.

The field equations are

$$\frac{R_4^2}{R^2} + 2\frac{R_{44}}{R} = (1+2\lambda)\left[(\rho+p)\sinh^2\alpha + p + 2q_1\frac{\sinh\alpha}{R}\right] - (\rho-p)\lambda, \tag{8}$$

$$\frac{R_4^2}{R^2} + 2\frac{R_{44}}{R} = (1+2\lambda)p - (\rho-p)\lambda, \tag{9}$$

$$3\frac{R_4^2}{R^2} + \frac{2\beta R_4}{R^4\left(1+\beta\int\frac{dt}{R^3}\right)} = -(1+2\lambda)\left[(\rho+p)\cosh^2\alpha - p + 2q_1\frac{\sinh\alpha}{R}\right] - (\rho-p)\lambda, \tag{10}$$

$$(1+2\lambda)\left[(\rho+p)R\sinh\alpha\cosh\alpha + q_1\cosh\alpha + q_1\frac{\sinh^2\alpha}{\cosh\alpha}\right] = 0. \tag{11}$$

Here, the index 4 after a field variable denotes the difference with resp. to cosmic time.

We take equation of state (Eos), which gives

$$p = (\gamma-1)\rho, \quad 1 \le \gamma \le 2. \tag{12}$$

We have calculated the above set of nonlinear equation with the assistance of special law of variation of Hubble's parameter, presented by Berman (1983) that yields constant deceleration parameter model of Universe. We assumed only constant deceleration parameter model defined as

$$q = -\left[\frac{vv_{44}}{v_4^2}\right], \tag{13}$$

where

$$v = \left[R^3\left(1+\beta\int\frac{dt}{R^3}\right)\right]^{\frac{1}{3}} \tag{14}$$

is the overall scalar factor.

The solution of (13) is given by

$$v = (Kt+L)^{\frac{1}{1+q}} \tag{15}$$

where K and L are integration constants.

From Eqs. (14) and (15), we get

$$\left[R^3\left(1+\beta\int\frac{dt}{R^3}\right)\right]^{\frac{1}{3}}=(Kt+L)^{\frac{1}{1+q}}. \tag{16}$$

Solving above equation we get

$$R=(Kt+L)^{\frac{1}{1+q}}\,e^{\frac{\beta(1+q)}{3K(2-q)}(Kt+L)^{\frac{q-2}{1+q}}}. \tag{17}$$

Metric (1) reduces to the following form:

$$\begin{aligned}ds^2=dt^2-(Kt+L)^{\frac{2}{1+q}}e^{2\left[\frac{\beta(1+q)}{3K(2-q)}\right](Kt+L)^{\frac{q-2}{1+q}}}(dx^2+dy^2)\\-(Kt+L)^{\frac{2}{1+q}}e^{-4\left[\frac{\beta(1+q)}{3K(2-q)}\right](Kt+L)^{\frac{q-2}{1+q}}}dz^2,\end{aligned} \tag{18}$$

where $K=1$.

3. Some Physical and Geometrical Properties

Solving Eqs. (9), (12) and (16), we get

$$\begin{aligned}\rho=\frac{1}{[(1+3\lambda)(\gamma-1)-\lambda]}\Bigg\{\frac{3}{(1+q)^2(Kt+L)^2}+\frac{\beta^2}{3(Kt+L)^{\frac{6}{1+q}}}\\-\frac{2}{(1+q)(Kt+L)^2}-\frac{4\beta}{3(1+q)(Kt+L)^{\frac{4+q}{1+q}}}\Bigg\}.\end{aligned} \tag{19}$$

From Eqs. (12) and (19), we get

$$\begin{aligned}p=\frac{(\gamma-1)}{[(1+3\lambda)(\gamma-1)-\lambda]}\Bigg\{\frac{3}{(1+q)^2(Kt+L)^2}+\frac{\beta^2}{3(Kt+L)^{\frac{6}{1+q}}}\\-\frac{2}{(1+q)(Kt+L)^2}-\frac{4\beta}{3(1+q)(Kt+L)^{\frac{4+q}{1+q}}}\Bigg\}.\end{aligned} \tag{20}$$

The tilt angle α, heat conduction vectors q_i and flow vectors $u_i$for the Universe (18) are

$$\cosh\alpha=\left\{\frac{(1+2\lambda)\gamma\left[\begin{array}{c}\frac{3}{(1+q)^2(Kt+L)^2}+\frac{\beta^2}{3(Kt+L)^{\frac{6}{1+q}}}-\frac{2}{(1+q)(Kt+L)^2}\\-\frac{4\beta}{3(1+q)(Kt+L)^{\frac{4+q}{1+q}}}\end{array}\right]}{\left[\frac{\beta^2}{3(Kt+L)^{\frac{6}{1+q}}}-\frac{1}{(1+q)(Kt+L)^2}\right]}+\frac{1}{2}\right\}^{\frac{1}{2}} \tag{21}$$

$$\sinh\alpha = \left\{ \frac{2(1+2\lambda)\gamma \left[\frac{3}{(1+q)^2(Kt+L)^2} + \frac{\beta^2}{3(Kt+L)^{\frac{6}{1+q}}} - \frac{2}{(1+q)(Kt+L)^2} - \frac{4\beta}{3(1+q)(Kt+L)^{\frac{4+q}{1+q}}} \right] + \left[\frac{1}{(1+q)(Kt+L)^2} - \frac{\beta^2}{3(Kt+L)^{\frac{6}{1+q}}} \right]}{2\left[\frac{\beta^2}{3(Kt+L)^{\frac{6}{1+q}}} - \frac{1}{(1+q)(Kt+L)^2} \right]} \right\}^{\frac{1}{2}}, \tag{22}$$

$$u_1 = (Kt+L)^{\frac{1}{1+q}} e^{\frac{\beta(1+q)}{3K(2-q)}(Kt+L)^{\frac{q-2}{1+q}}} \sinh\alpha, \tag{23}$$

$$u_4 = \cosh\alpha, \tag{24}$$

$$q_1 = \frac{e^{\frac{\beta(1+q)}{3K(2-q)}(Kt+L)^{\frac{q-2}{1+q}}} \sinh\alpha \cosh^2\alpha}{[(1+3\lambda)(\gamma-1)-\lambda](1+2\lambda)} \times \left[\frac{2}{(1+q)(Kt+L)^2} - \frac{2\beta^2}{3(Kt+L)^{\frac{6}{1+q}}} \right]. \tag{25}$$

The scalar expansion, shear scalar, Hubble parameter and spatial volume are, respectively, given by

$$\theta = \frac{18}{(1+q)(Kt+L)}, \tag{26}$$

$$\sigma^2 = \frac{2\beta^2}{3(Kt+L)^{\frac{1}{1+q}}}, \tag{27}$$

$$H = \frac{6}{(1+q)(Kt+L)}, \tag{28}$$

$$V = (Kt+L)^{\frac{3}{(1+q)}}. \tag{29}$$

The Hubble parameter, scalar expansion, shear scalar and spatial volume are presented by 2D and 3D graph in Fig. 1. The shear scalar raises monotonous in the context of the cosmic time and the Hubble parameter and scalar expansion parameters are vanishing as $t \to \infty$. In 3D graph, Fig. 1 specifies that the shear scalar is higher than Hubble parameter and scalar expansion.

The density parameter is given by

$$\Omega = \frac{(1+q)^2(Kt+L)^2}{108[(1+3\lambda)(\gamma-1)-\lambda]} \left\{ \frac{3}{(1+q)^2(Kt+L)^2} + \frac{\beta^2}{3(Kt+L)^{\frac{6}{1+q}}} - \frac{2}{(1+q)(Kt+L)^2} - \frac{4\beta}{3(1+q)(Kt+L)^{\frac{4+q}{1+q}}} \right\}. \tag{30}$$

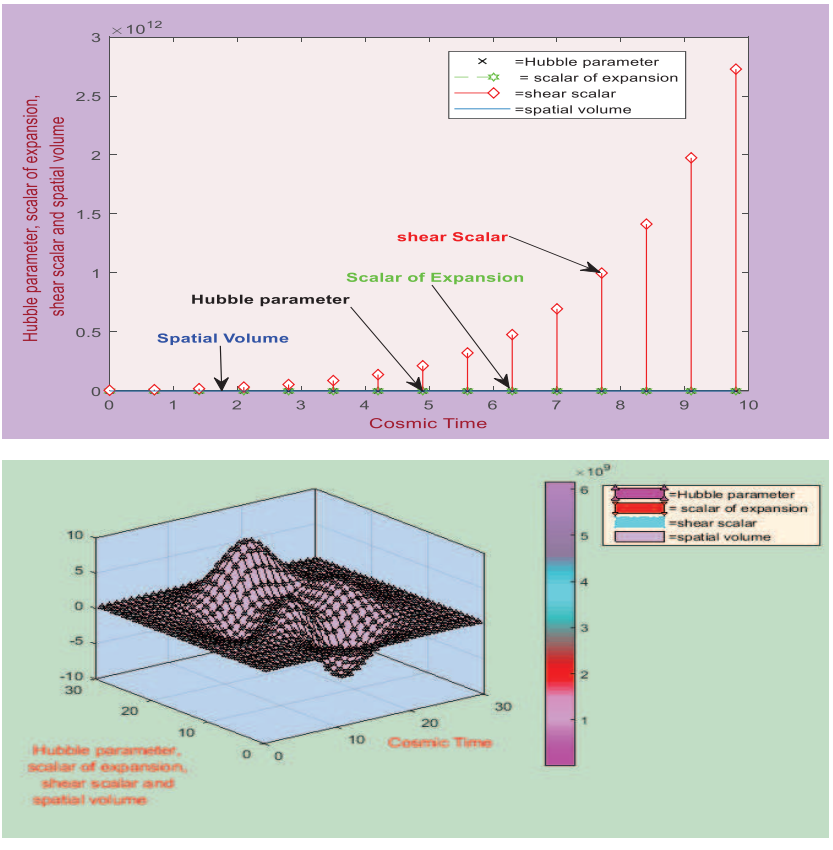

Fig. 1. Variation of Hubble parameter, scalar of expansion, shear scalar and spatial volume vs. cosmic time for $q = -0.33$, $A = 0.4$, $B = 9$, $\beta = 0.5$.

4. Types of Universe by using Equation of State

(a) Dust Universe: When $\gamma = 1$

The pressure and energy density for the model are, respectively, given by

$$\rho = \frac{1}{\lambda}\left\{\frac{2}{(1+q)(Kt+L)^2} + \frac{4\beta}{3(1+q)(Kt+L)^{\frac{4+q}{1+q}}} - \frac{3}{(1+q)^2(Kt+L)^2} - \frac{\beta^2}{3(Kt+L)^{\frac{6}{1+q}}}\right\}, \tag{31}$$

$$p = 0. \tag{32}$$

The energy density and pressure are as shown in Fig. 2. The energy density rises monotonically in the context of the cosmic time and the pressure is vanishing as $t \to \infty$.

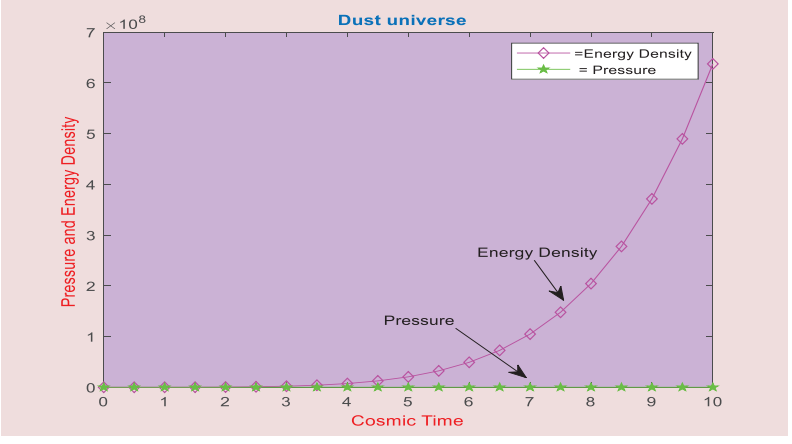

Fig. 2. Variation of energy density, pressure for $q = -0.33$, $A = -10$, $B = -10$, $\beta = 0.2$, $\lambda = -4$, $\gamma = 1$.

The tilt angle α, heat conduction vectors q_i and flow vectors u_i for the Dust Universe are given by

$$\cosh\alpha = \left\{ \frac{(1+2\lambda)\left[\frac{3}{(1+q)^2(Kt+L)^2} + \frac{\beta^2}{3(Kt+L)^{\frac{6}{1+q}}} - \frac{2}{(1+q)(Kt+L)^2} - \frac{4\beta}{3(1+q)(Kt+L)^{\frac{4+q}{1+q}}}\right]}{\left[\frac{\beta^2}{3(Kt+L)^{\frac{6}{1+q}}} - \frac{1}{(1+q)(Kt+L)^2}\right]} + \frac{1}{2} \right\}^{\frac{1}{2}}, \tag{33}$$

$$\sinh\alpha = \left\{ \frac{2(1+2\lambda)\left[\frac{3}{(1+q)^2(Kt+L)^2} + \frac{\beta^2}{3(Kt+L)^{\frac{6}{1+q}}} - \frac{2}{(1+q)(Kt+L)^2} - \frac{4\beta}{3(1+q)(Kt+L)^{\frac{4+q}{1+q}}}\right] + \left[\frac{1}{(1+q)(Kt+L)^2} - \frac{\beta^2}{3(Kt+L)^{\frac{6}{1+q}}}\right]}{2\left[\frac{\beta^2}{3(Kt+L)^{\frac{6}{1+q}}} - \frac{1}{(1+q)(Kt+L)^2}\right]} \right\}^{\frac{1}{2}}, \tag{34}$$

$$u_1 = (Kt+L)^{\frac{1}{1+q}} e^{\frac{\beta(1+q)}{3K(2-q)}(Kt+L)^{\frac{q-2}{1+q}}} \sinh\alpha, \tag{35}$$

$$u_4 = \cosh\alpha, \tag{36}$$

$$q_1 = \frac{e^{\frac{\beta(1+q)}{3K(2-q)}(Kt+L)^{\frac{q-2}{1+q}}} \sinh\alpha\cosh^2\alpha}{\lambda(1+2\lambda)}\left[\frac{2\beta^2}{3(Kt+L)^{\frac{6}{1+q}}} - \frac{2}{(1+q)(Kt+L)^2}\right]. \tag{37}$$

The scalar expansion, shear scalar, Hubble parameter and spatial volume are, respectively, given by

$$\theta = \frac{18}{(1+q)(Kt+L)}, \tag{38}$$

$$\sigma^2 = \frac{2\beta^2}{3(Kt+L)^{\frac{1}{1+q}}}, \tag{39}$$

$$H = \frac{6}{(1+q)(Kt+L)}, \tag{40}$$

$$V = (Kt+L)^{\frac{3}{(1+q)}}. \tag{41}$$

The density parameters

$$\Omega = \frac{-(1+q)^2(Kt+L)^2}{108\lambda}\left\{\frac{3}{(1+q)^2(Kt+L)^2} + \frac{\beta^2}{3(Kt+L)^{\frac{6}{1+q}}} - \frac{2}{(1+q)(Kt+L)^2} - \frac{4\beta}{3(1+q)(Kt+L)^{\frac{4+q}{1+q}}}\right\}. \tag{42}$$

The density parameters, as shown in Fig. 3, rises monotonically in the context of the cosmic time for positive value of λ. The pressure and energy density are relatively short in terms of cosmic time for negative value of λ.

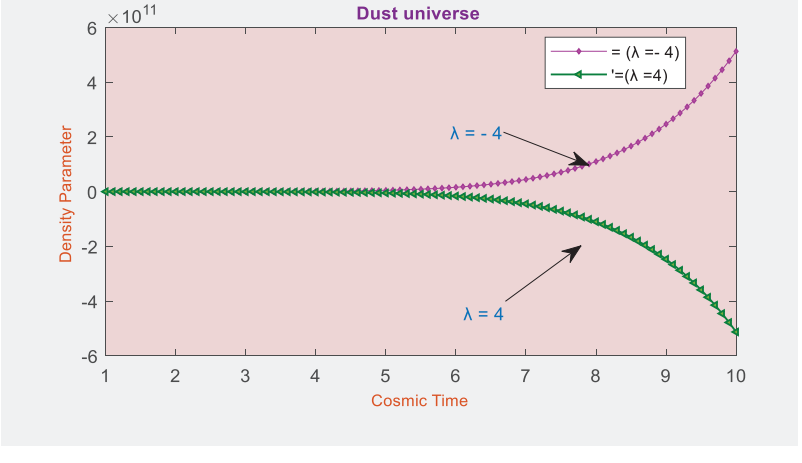

Fig. 3. Variation of density parameters vs. cosmic time for $q = -0.33$, $A = -10$, $B = -10$, $\beta = 0.2$, $\lambda = 4$, $\lambda = -4r$, $\gamma = 1$.

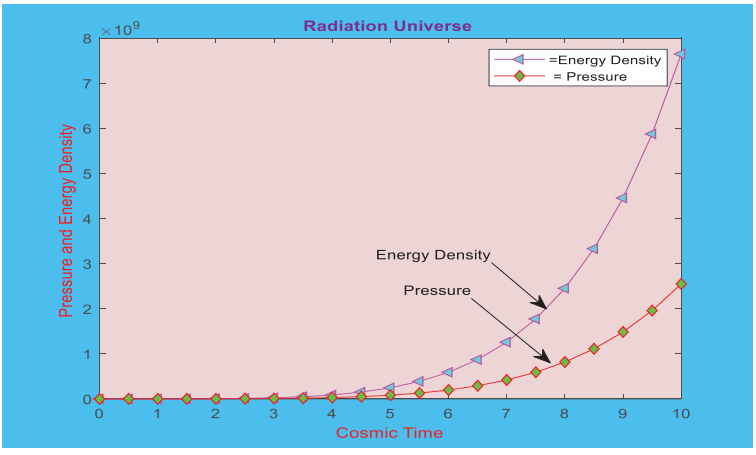

Fig. 4. Variation of energy density, pressure for $q = -0.33$, $A = -10$, $B = -10$, $\beta = 0.2$, $\lambda = -4$, $\gamma = \frac{4}{3}$.

(b) Radiation Universe: When $\gamma = \frac{4}{3}$

The energy density and pressure are, respectively, given by

$$\rho = 3\left\{\frac{3}{(1+q)^2(Kt+L)^2} + \frac{\beta^2}{3(Kt+L)^{\frac{6}{1+q}}} - \frac{2}{(1+q)(Kt+L)^2} - \frac{4\beta}{3(1+q)(Kt+L)^{\frac{4+q}{1+q}}}\right\}, \tag{43}$$

$$p = \left\{\frac{3}{(1+q)^2(Kt+L)^2} + \frac{\beta^2}{3(Kt+L)^{\frac{6}{1+q}}} - \frac{2}{(1+q)(Kt+L)^2} - \frac{4\beta}{3(1+q)(Kt+L)^{\frac{4+q}{1+q}}}\right\}. \tag{44}$$

The energy density, pressure presented in Fig. 4, increases monotonically with respect to time.

The tilt angle α, heat conduction vectors q_i and flow vectors u_i for the Radiation Universe are, respectively, given by

$$\cosh\alpha = \left\{(1+2\lambda)\frac{\left[\frac{12}{(1+q)^2(Kt+L)^2} + \frac{4\beta^2}{3(Kt+L)^{\frac{6}{1+q}}} - \frac{8}{(1+q)(Kt+L)^2} - \frac{16\beta}{3(1+q)(Kt+L)^{\frac{4+q}{1+q}}}\right]}{\left[\frac{\beta^2}{(Kt+L)^{\frac{6}{1+q}}} - \frac{3}{(1+q)(Kt+L)^2}\right]} + \frac{1}{2}\right\}^{\frac{1}{2}}, \tag{45}$$

$$\sinh\alpha = \left\{ \frac{8(1+2\lambda)\left[\begin{array}{c}\frac{3}{(1+q)^2(Kt+L)^2}+\frac{\beta^2}{3(Kt+L)^{\frac{6}{1+q}}}\\ -\frac{2}{(1+q)(Kt+L)^2}-\frac{4\beta}{3(1+q)(Kt+L)^{\frac{4+q}{1+q}}}\end{array}\right]+3\left[\begin{array}{c}\frac{1}{(1+q)(Kt+L)^2}\\ -\frac{\beta^2}{3(Kt+L)^{\frac{6}{1+q}}}\end{array}\right]}{6\left[\frac{\beta^2}{3(Kt+L)^{\frac{6}{1+q}}}-\frac{1}{(1+q)(Kt+L)^2}\right]} \right\}^{\frac{1}{2}}, \tag{46}$$

$$u_1 = (Kt+L)^{\frac{1}{1+q}} e^{\frac{\beta(1+q)}{3K(2-q)}(Kt+L)^{\frac{q-2}{1+q}}} \sinh\alpha, \tag{47}$$

$$u_4 = \cosh\alpha, \tag{48}$$

$$q_1 = \frac{3e^{\frac{\beta(1+q)}{3K(2-q)}(Kt+L)^{\frac{q-2}{1+q}}} \sinh\alpha\cosh^2\alpha}{(1+2\lambda)} \times\left[\frac{2}{(1+q)(Kt+L)^2}-\frac{2\beta^2}{3(Kt+L)^{\frac{6}{1+q}}}\right]. \tag{49}$$

The scalar expansion, shear scalar, Hubble parameter and spatial volume are, respectively, given by

$$\theta = \frac{18}{(1+q)(Kt+L)}, \tag{50}$$

$$\sigma^2 = \frac{2\beta^2}{3(Kt+L)^{\frac{1}{1+q}}}, \tag{51}$$

$$H = \frac{6}{(1+q)(Kt+L)}, \tag{52}$$

$$V = (Kt+L)^{\frac{3}{(1+q)}}. \tag{53}$$

The density parameter is given by

$$\Omega = \frac{(1+q)^2(Kt+L)^2}{36}\left\{\frac{3}{(1+q)^2(Kt+L)^2}+\frac{\beta^2}{3(Kt+L)^{\frac{6}{1+q}}} -\frac{2}{(1+q)(Kt+L)^2}-\frac{4\beta}{3(1+q)(Kt+L)^{\frac{4+q}{1+q}}}\right\}. \tag{54}$$

(c) Hard Universe: When $\left[\gamma \in \left(\frac{4}{3}, 2\right)\right]$, let $\gamma = \frac{5}{3}$

The energy density and pressure are, respectively, given by

$$\rho = \frac{3}{(2+3\lambda)}\left\{\frac{3}{(1+q)^2(Kt+L)^2}+\frac{\beta^2}{3(Kt+L)^{\frac{6}{1+q}}} -\frac{2}{(1+q)(Kt+L)^2}-\frac{4\beta}{3(1+q)(Kt+L)^{\frac{4+q}{1+q}}}\right\}, \tag{55}$$

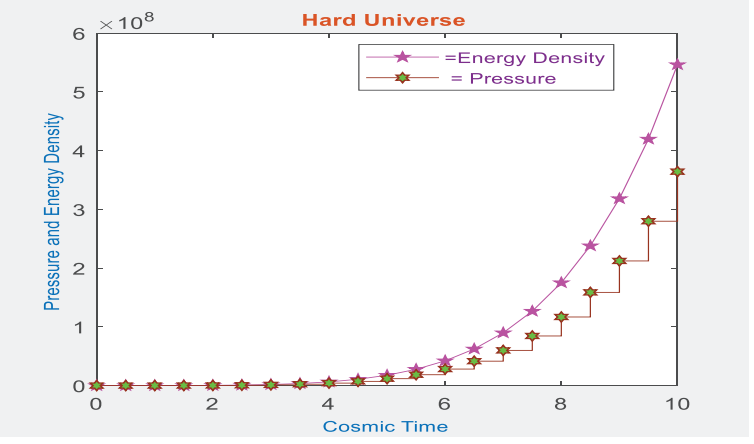

Fig. 5. Variation of energy density, pressure for $q = -0.33$, $A = -10$, $B = -10$, $\beta = 0.2$, $\lambda = 4$, $\gamma = \frac{5}{3}$.

$$p = \frac{2}{(2+3\lambda)}\left\{\frac{3}{(1+q)^2(Kt+L)^2} + \frac{\beta^2}{3(Kt+L)^{\frac{6}{1+q}}} - \frac{2}{(1+q)(Kt+L)^2} - \frac{4\beta}{3(1+q)(Kt+L)^{\frac{4+q}{1+q}}}\right\}. \tag{56}$$

The energy density, pressure presented in Fig. 5, rises monotonically in the context of the cosmic time for positive value of λ. The pressure and energy density are relatively short in terms of cosmic time negative value of λ.

The tilt angle α, heat conduction vectors q_i and flow vectors u_i for Hard Universe are, respectively, given as

$$\cosh\alpha = \left\{\frac{5(1+2\lambda)\left[\frac{3}{(1+q)^2(Kt+L)^2} + \frac{\beta^2}{3(Kt+L)^{\frac{6}{1+q}}} - \frac{2}{(1+q)(Kt+L)^2} - \frac{4\beta}{3(1+q)(Kt+L)^{\frac{4+q}{1+q}}}\right]}{\left[\frac{3\beta^2}{(Kt+L)^{\frac{6}{1+q}}} - \frac{3}{(1+q)(Kt+L)^2}\right]} + \frac{1}{2}\right\}^{\frac{1}{2}}, \tag{57}$$

$$\sinh\alpha = \left\{\frac{10(1+2\lambda)\left[\frac{3}{(1+q)^2(Kt+L)^2} + \frac{\beta^2}{3(Kt+L)^{\frac{6}{1+q}}} - \frac{2}{(1+q)(Kt+L)^2} - \frac{4\beta}{3(1+q)(Kt+L)^{\frac{4+q}{1+q}}}\right] + 3\left[\frac{1}{(1+q)(Kt+L)^2} - \frac{\beta^2}{3(Kt+L)^{\frac{6}{1+q}}}\right]}{6\left[\frac{\beta^2}{3(Kt+L)^{\frac{6}{1+q}}} - \frac{1}{(1+q)(Kt+L)^2}\right]} + \frac{1}{2}\right\}^{\frac{1}{2}}, \tag{58}$$

$$u_1 = (Kt+L)^{\frac{1}{1+q}} e^{\frac{\beta(1+q)}{3K(2-q)}(Kt+L)^{\frac{q-2}{1+q}}} \sinh\alpha, \tag{59}$$

$$u_4 = \cosh\alpha, \tag{60}$$

$$q_1 = \frac{e^{\frac{\beta(1+q)}{3K(2-q)}}(Kt+L)^{\frac{q-2}{1+q}} \sinh\alpha\cosh^2\alpha}{(2+7\lambda+6\lambda^2)} \times \left[\frac{2}{(1+q)(Kt+L)^2} - \frac{2\beta^2}{3(Kt+L)^{\frac{6}{1+q}}}\right]. \tag{61}$$

The scalar expansion, shear scalar, Hubble parameter and spatial volume are, respectively, given by

$$\theta = \frac{18}{(1+q)(Kt+L)}, \tag{62}$$

$$\sigma^2 = \frac{2\beta^2}{3(Kt+L)^{\frac{1}{1+q}}}, \tag{63}$$

$$H = \frac{6}{(1+q)(Kt+L)}, \tag{64}$$

$$V = (Kt+L)^{\frac{3}{(1+q)}}. \tag{65}$$

The density parameter is given by

$$\Omega = \frac{(1+q)^2(Kt+L)^2}{36(2+3\lambda)}\left\{\frac{3}{(1+q)^2(Kt+L)^2} + \frac{\beta^2}{3(Kt+L)^{\frac{6}{1+q}}} - \frac{2}{(1+q)(Kt+L)^2} - \frac{4\beta}{3(1+q)(Kt+L)^{\frac{4+q}{1+q}}}\right\}. \tag{66}$$

(d) Zeldovich Universe: When $\gamma = 2$

The pressure and energy density are given by

$$\rho = p = \frac{1}{(1+2\lambda)}\left\{\frac{3}{(1+q)^2(Kt+L)^2} + \frac{\beta^2}{3(Kt+L)^{\frac{6}{1+q}}} - \frac{2}{(1+q)(Kt+L)^2} - \frac{4\beta}{3(1+q)(Kt+L)^{\frac{4+q}{1+q}}}\right\}. \tag{67}$$

The energy density, pressure presented in Fig. 6, rises monotonically in the context of the cosmic time for positive value of λ. The pressure and energy density are relatively short in terms of cosmic time for negative value of λ.

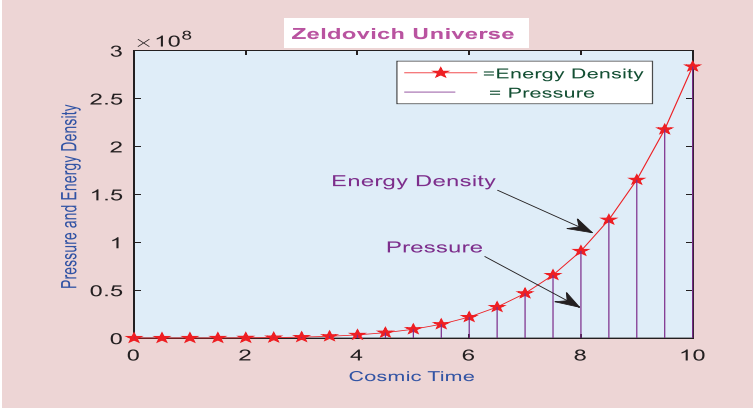

Fig. 6. Variation energy density, pressure for $q = -0.33$, $A = -10$, $B = -10$, $\beta = 0.2$, $\lambda = 4$, $\gamma = 2$.

The tilt angle α, flow vectors u_i and heat conduction vectors q_i for Zeldovich Universe are, respectively, given by

$$\cosh\alpha = \left\{ \frac{(1+2\lambda)2\left[\frac{3}{(1+q)^2(Kt+L)^2} + \frac{\beta^2}{3(Kt+L)^{\frac{6}{1+q}}} - \frac{2}{(1+q)(Kt+L)^2} - \frac{4\beta}{3(1+q)(Kt+L)^{\frac{4+q}{1+q}}}\right]}{\left[\frac{\beta^2}{3(Kt+L)^{\frac{6}{1+q}}} - \frac{1}{(1+q)(Kt+L)^2}\right]} + \frac{1}{2} \right\}^{\frac{1}{2}}, \tag{68}$$

$$\sinh\alpha = \left\{ \frac{4(1+2\lambda)\left[\frac{3}{(1+q)^2(Kt+L)^2} + \frac{\beta^2}{3(Kt+L)^{\frac{6}{1+q}}} - \frac{2}{(1+q)(Kt+L)^2} - \frac{4\beta}{3(1+q)(Kt+L)^{\frac{4+q}{1+q}}}\right] + \left[\frac{1}{(1+q)(Kt+L)^2} - \frac{\beta^2}{3(Kt+L)^{\frac{6}{1+q}}}\right]}{2\left[\frac{\beta^2}{3(Kt+L)^{\frac{6}{1+q}}} - \frac{1}{(1+q)(Kt+L)^2}\right]} \right\}^{\frac{1}{2}}, \tag{69}$$

$$u_1 = (Kt+L)^{\frac{1}{1+q}} e^{\frac{\beta(1+q)}{3K(2-q)}(Kt+L)^{\frac{q-2}{1+q}}} \sinh\alpha, \tag{70}$$

$$u_4 = \cosh\alpha, \tag{71}$$

$$q_1 = \frac{e^{\frac{\beta(1+q)}{3K(2-q)}(Kt+L)^{\frac{q-2}{1+q}}} \sinh\alpha\cosh^2\alpha}{(1+2\lambda)^2}\left[\frac{2}{(1+q)(Kt+L)^2} - \frac{2\beta^2}{3(Kt+L)^{\frac{6}{1+q}}}\right]. \tag{72}$$

The scalar expansion, shear scalar, Hubble parameter and spatial volume are, respectively, given by

$$\theta = \frac{18}{(1+q)(Kt+L)}, \tag{73}$$

$$\sigma^2 = \frac{2\beta^2}{3(Kt+L)^{\frac{1}{1+q}}}, \tag{74}$$

$$H = \frac{6}{(1+q)(Kt+L)}, \tag{75}$$

$$V = (Kt+L)^{\frac{3}{(1+q)}}. \tag{76}$$

The density parameter is given by

$$\Omega = \frac{(1+q)^2(Kt+L)^2}{108(1+2\lambda)}\left\{\frac{3}{(1+q)^2(Kt+L)^2} + \frac{\beta^2}{3(Kt+L)^{\frac{6}{1+q}}} - \frac{2}{(1+q)(Kt+L)^2} - \frac{4\beta}{3(1+q)(Kt+L)^{\frac{4+q}{1+q}}}\right\}. \tag{77}$$

The density parameters for all Universes are presented in Fig. 7. Dust Universe rises monotonically in the context of the cosmic time; Radiation Universe is vanishing as $t \to \infty$ whereas Hard Universe and Zeldovich Universe decrease monotonically with respect time.

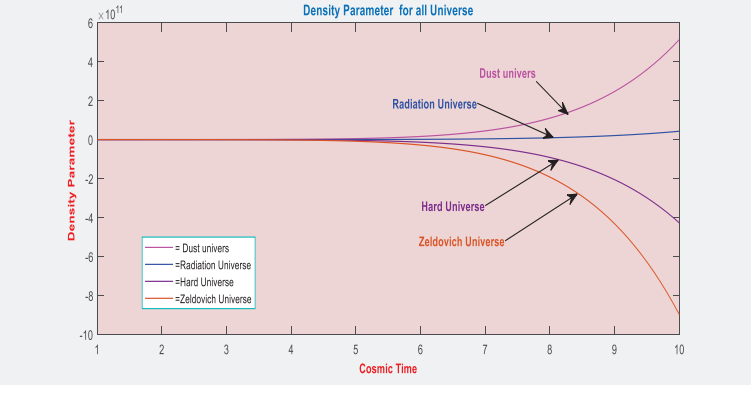

Fig. 7. Variation of density parameters vs. cosmic time for $q = -0.33$, $A = -10$, $B = -10$, $\beta = 0.2$, $\lambda = -4$, $\gamma = 1$.

The tilt angle for all Universe is presented in Fig. 8. From the Table 1 it is observed that the value of tilt angle is low in Dust Universe and high in Zeldovich Universe.

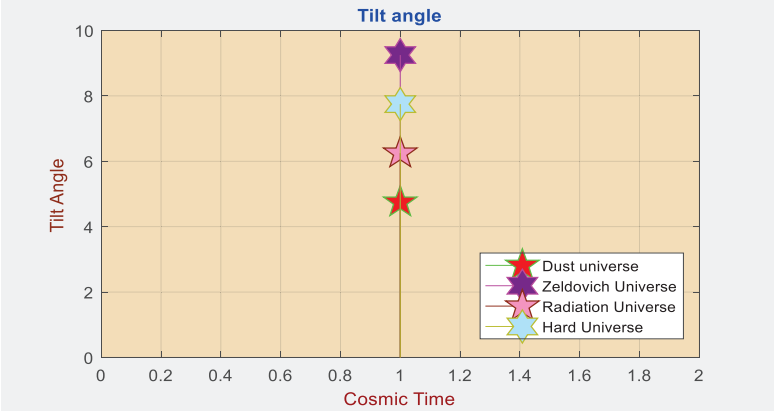

Fig. 8. Variation of tilt angle vs. cosmic time for $q = -0.33$, $A = 10$, $B = 10$, $\beta = 0.2$, $\lambda = 4$, $\gamma = 1, \frac{4}{3}, \frac{5}{3}, 2$.

Table 1. Tilt angle vs. cosmic time for $q = -0.33$, $A = 10$, $B = 10$, $\beta = 0.2$, $\lambda = 4$.

Type of Universes	Equation of State $p = (\gamma - 1)\rho$, $1 \leq \gamma \leq 2$	Tilt angle
Dust	$\gamma = 1 \rightarrow p = 0$	4.7488
Radiation	$\gamma = \frac{4}{3} \rightarrow p = \frac{\rho}{3}$	6.2484
Hard	$\gamma = \frac{5}{3} \rightarrow \frac{2\rho}{3}$	7.7480
Zeldovich	$\gamma = 2 \rightarrow p = \rho$	9.2484

5. Result and Discussion

Dust Universe: For this model, the energy density and pressure are as shown in Fig. 2. The energy density rises monotonically in the context of the cosmic time and the pressure is vanishing as $t \rightarrow \infty$.

The density parameters, as shown in Fig. 3, rise monotonically in the context of the cosmic time for positive value of λ. The pressure and energy density are relatively short in terms of cosmic time for negative value of λ.

Radiation Universe: For this model, the energy density and pressure presented in Fig. 4 increase monotonically with respect to time.

Hard Universe: For this model, the energy density and pressure presented in Fig. 5 rise monotonically in the context of the cosmic time for positive value of λ. The pressure and energy density are relatively short in terms of cosmic time negative value of λ.

Zeldovich Universe: For this model, the energy density and pressure presented in Fig. 6 rise monotonically in the context of the cosmic time for positive value of λ. The pressure and energy density are relatively short in terms of cosmic time for negative value of λ.

6. Conclusion

We have presented the tilted cosmological model by using equation of state parameter in $f(R,T)$ theory of gravity. We have concluded new idea of $f(R,T)$ theory of gravity by using tilted model. We have investigated different types of Universe with equation of state $p = (\gamma - 1)\rho$. We have discussed graphical presentation of all parameters with the help of MATLAB. In Zeldovich Universe, the value of tilt angle is higher than the other Universe. Model is accelerating in Dust Universe, Radiation Universe and Hard Universe, Zeldovich Universe at $\lambda = -4$ and $\lambda = 4$. This is a better result of tilted model in $f(R,T)$ theory of gravity than general theory of relativity for this spacetime. The value of tilt angle is constant in General theory of relativity whereas the value of tilt angle is non-constant in $f(R,T)$ theory of gravity. So, we conclude that there is no singularity of tilted Universe for this space time in $f(R,T)$ theory of gravity.

References

1. A. G. Riess *et al.*, *Astrom. J.* **116**, 1009 (1998).
2. S. Perlmutter *et al.*, *Astrophys. J.* **517**, 565 (1999).
3. T. Harko, F. S. N. Lobo, S. D. Nojiri and S. D. Odintsov, *Phys. Rev. D* **84**, 024020 (2011).
4. M. J. S. Houndjo, *Int. J. Mod. Phys. D* **21**, 1250003 (2012).
5. M. J. S. Houndjo and O. F. Piattella, *Int. J. Mod. Phys. D* **21**, 1250024 (2012).
6. R. Myrzakulov, *Eur. Phys. J. C* **72**, 2203 (2012).
7. S. K. J. Pacif, Md. S. Khan, L. K. Paikroy and S. Singh, *Mod. Phys. Lett. A* **35**, 2050011 (2020).
8. S. K. J. Pacif and B. Mishra, *Res. Astron. Astrophys.* **15**, 2141 (2015).
9. P. K. Sahoo, S. K. Sahu and A. Nath, *Eur. Phys. J. Plus* **131**, 18 (2016).
10. D. D. Pawar and V. J. Dagwal, *Aryabhatta J. Math. Inf.* **7**, 17 (2015).
11. V. J. Dagwal, *Can. J. Phys.*, doi:10.1139/cjp-2019-0226.
12. V. J. Dagwal, D. D. Pawar, Y. S. Solanke and H. R. Shaikh, *Mod. Phys. Lett. A* **35**, 2050196 (2020).
13. S. Aygün, C. Aktaş and B. Mishra, *Indian J. Phys.* **93**, 407 (2019).
14. C. Aktaş, *Mod. Phys. Lett. A* **34**, 1950098 (2019).
15. C. Aktaş, *Mod. Phys. Lett. A* **34**, 1950066 (2019).
16. C. Aktaş, S. Aygün and P. K. Sahoo, *Mod. Phys. Lett. A* **33**, 1850135 (2018).
17. D. D. Pawar and Y. S. Solanke, *Turkish J. Phys.* **39**, 54 (2015).
18. V. J. Dagwal and D. D. Pawar, *Mod. Phys. Lett. A* **34**, 1950357 (2019), doi:10.1142/S0217732319503577.
19. R. King and G. G. R. Ellis, *Commun. Math. Phys.* **31**, 209 (1973).
20. G. G. R. Ellis and A. R. King, *Commun. Math. Phys.* **38**, 119 (1974).
21. D. D. Pawar and V. J. Dagwal, *Int. J. Theor. Phys.* **53**, 2441 (2014).
22. D. D. Pawar, V. J. Dagwal and Y. S. Solanke, *Int. J. Theor. Phys.* **54**, 1926 (2014).

23. D. D. Pawar, V. J. Dagwal and S. P. Shahare, arXiv:1602.05223v1.
24. V. J. Dagwal and D. D. Pawar, *Int. J. Math Archive.* **9**, 120 (2018).
25. V. J. Dagwal and D. D. Pawar, *Mod. Phys. Lett. A* **33**, 1850213 (2018).
26. D. D. Pawar, S. P. Shahare and V. J. Dagwal, *Mod. Phys. Lett. A* **33**, 1850011 (2018).
27. S. K. Sahu, *J. Mod. Phys.* **1**, 67 (2010).
28. M. Sharif and H. Tahir, *Eur. Phys. J. Plus* **128**, 146 (2013).
29. M. Sharif and H. Majid, *Astrophys. Space Sci.* **348**, 583 (2013).
30. U. S. Nilsson, M. J. Hancock and J. Wainwright, arXiv:gr-qc/991201v1.
31. L. Herrera, A. Di Prisco and J. Ibáñez, *Phys. Rev. D* **84**, 064036 (2011).
32. Z. Yousaf, M. Z. H. Bhatti and A. Rafaqat, *Astrophys. Space Sci.* **362**, 68 (2017), doi:10.1007/s10509-017-3045-8.
33. Z. Yousaf, M. Z. H. Bhatti and A. Rafaqat, *Int. J. Mod. Phys. D* **26**, 1750099 (2017).
34. V. J. Dagwal and D. D. Pawar, *Indian J. Phys.*, doi:10.1007/s12648-019-01625-1.
35. V. Sahni and A. Starobinsky, *Int. J. Mod. Phys. D* **15**, 2105 (2006).
36. V. Sahni, A. Shafielooa and A. Starobinsky, *Phys. Rev. D* **78**, 103502 (2008).
37. B. Ratra and P. J. E. Peebles, *Phys. Rev. D* **37**, 3406 (1988).
38. R. R. Caldwell, *Phys. Lett. B* **23**, 545 (2002).
39. B. Feng, *Phys. Lett. B* **35**, 607 (2005).
40. Z. Yousuf, *Dark Universe Phys.* **28**, 100509 (2020).
41. Z. Yousuf, *Phys. Scripta* **95**, 075307 (2020).
42. Z. Yousuf, *Eur. Phys. J. Plus* **134**, 245 (2019).
43. Z. Yousuf, *Mod. Phys. Lett. A* **34**, 1950333 (2019).
44. Z. Yousuf, *Eur. Phys. J. Plus* **132**, 71 (2017).
45. Z. Yousuf, *Eur. Phys. J. Plus* **132**, 276 (2017).
46. V. J. Dagwal and D. D. Pawar, *Indian J. Phys.*, doi:10.1007/s12648-020-01691-w.